Proliferation and autophagic degradation of peroxisomes in Hansenula polymorpha

Zutphen, Tim van

Proliferation and autophagic degradation of peroxisomes in *Hansenula polymorpha*

The studies presented in this thesis were carried out in the research unit Molecular Cell Biology of the Groningen Biomolecular Sciences and Biotechnology Institute (GBB) of the University of Groningen in the Netherlands. Funding was provided by the Netherlands organisation for Scientific Research (NWO).

Printed by Ipskamp, Enschede, the Netherlands

Rijksuniversiteit Groningen

Proliferation and autophagic degradation of peroxisomes in *Hansenula polymorpha*

Proefschrift

ter verkrijging van het doctoraat in de
Wiskunde en Natuurwetenschappen
aan de Rijksuniversiteit Groningen
op gezag van de
Rector Magnificus, dr. F. Zwarts,
in het openbaar te verdedigen op
vrijdag 12 november 2010
om 13.15 uur

door

Tim van Zutphen

geboren op 26 juli 1980

te Utrecht

Promotor:	Prof. dr. I.J. van der Klei
Beoordelingscommissie:	Prof. dr. E.J. Boekema
	Prof. dr. J. Kok
	Prof. dr. D.J. Slotboom

Preface

Wow, I never thought time could fly by so fast! Driving into haren with all my belongings in my car and the ink on my masters diploma still wet, 4 years felt like an infinite amount of time to do research. That turned out to be a little misconception, but still before you lies the proof that my thesis been completed.

For sure this would not have been possible without the help of many people. First of all I would like to thank my promoter Ida and supervisor Marten, for offering me the opportunity to work in the Eukaryotic Microbiology and later Molceular Cell Biology group, and for giving me space to pursuit my own path, combined with the necessary guidance at the right times. You have tought me a lot about how scientific research should be performed and gave me the little push I needed to pursue a new challenge in Graz, Austria.

Many thanks to my paranimfs André & Rinse, my students Astrid & Roelof and of course Selva, all great teamplayers and a big help.

Thanks to all the other members of the department that make it a great place to work; Bart, Eda & Virginia were there in the for a good start and Arjen, Jan, Marleen & Richard, were always there with a helping hand. Ron & Rinse helped me immensly with EM. Annemarie, Daphne, Malgosia, Kim & Wieb were all very cheerful roommates and Loknath, Ruchi, Sandra, Shirisha & Susan saved me from many nightly trips. Also thanks to Bea, Elena, Frank, Jikke, Kasinath, Klaas, Laura, Łukasz, Magda & Roel. I'm grateful to you all, it was a pleasure working amongst you. I'll for sure miss the coffee breaks, dinners & trips; even all the way to India.

Thanks also to all my friends, with funny refreshing questions about e.g. my "chromosome-counting" activities.
Finally I would like to thank my parents for all their support.

Contents

Aim and Outline

One of the most striking features of an eukaryotic cell is the presence of subcompartments termed organelles, each dedicated to specific cellular processes. A particular dynamic organelle, with respect to size, abundance and protein content, is the peroxisome. In this organelle an array of metabolic processes takes place, of which β-oxidation of fatty acids is the most common one. Proper peroxisome biogenesis and function are vital for human health. The aim of this research is to better understand processes involved in the regulation of peroxisome proliferation and selective degradation by autophagy (termed pexophagy).

In **chapter 1** the current knowledge on peroxisome homeostasis (the regulation and molecular mechanisms involved in peroxisome proliferation and degradation by autophagy) is reviewed. Peroxisomes can be formed by fission of pre-existing ones, but – at specific conditions – they can also be formed from the endoplasmic reticulum. The sorting and insertion of peroxisomal membrane proteins involves the function of Pex3 and Pex19. Interestingly, the peroxisomal membrane protein Pex3 has also been implicated in pexophagy. Matrix proteins are post-translationally imported in pre-existing organelles. An important peroxin in this process is Pex14, a peroxisomal membrane protein that is a component of the receptor docking site and has also been implicated in peroxisome degradation.

Chapter 2 describes a transcriptome analysis in which glucose-grown *H. polymorpha* cells were compared with cells shifted to medium containing methanol as sole carbon source for 2 hours. Of the ~1200 upregulated genes, the peroxisomal transciption factor Mpp1 was upregulated most.

Other strongly upregulated genes included those encoding enzymes involved in methanol metabolism, β-oxidation of fatty acids, redox control and proteins involved in autophagy. Of the ~1200 downregulated genes many were related to transcription and translation. *PEX* genes involved in peroxisome biogenesis were only moderately upregulated. The highest upregulated gene was *PEX32*, which encodes a peroxisomal membrane protein of unknown function.

Chapter 3 describes the involvement of the repressors Mig1 and Mig2 in repression of the gene encoding alcohol oxidase a key enzyme in methanol metabolism. Cells devoid of *MIG1 and MIG2* also display impaired macropexophagy, but showed constitutive microautophagy.

Chapter 4 describes methods to study pexophagy in *H. polymorpha*.

In **Chapter 5** a detailed study is described in which the possible role of other members of the Pex14-containing peroxisomal importomer in pexophagy was analysed. This study indicated that Pex14 is the sole member of this complex involved in pexophagy.

Upon induction of pexophagy by a shift of methanol grown *H. polymorpha* cells to glucose, removal of Pex3 - most likely via the ubiquitin-proteasome system – is an initial and essential step. In **Chapter 6** data are presented on the fate of peroxisomes after artificial removal of Pex3 from peroxisomes during peroxisome-inducing conditions. At these conditions an alternative Atg1-dependent pexophagy pathway was observed. This process also occurs in wild type cells when methanol-grown cells were exposed to excess methanol. Probably the alternative mechanism represents a mode to rapidly remove dysfunctional organelles.

Chapter 1

The peroxisome life-cycle

Tim van Zutphen and Ida J. van der Klei

Molecular Cell Biology, Groningen Biomolecular Sciences and Biotechnology Institute, University of Groningen, Haren, The Netherlands

Introduction

One of the most striking features of an eukaryotic cell is its compartmentalized makeup. Each of the membrane-enclosed compartments or organelles is devoted to specific cellular processes. Microbodies represent the most recently identified class of organelles, comprising glycosomes, glyoxysomes and peroxisomes, which all consist of a proteinaceous matrix surrounded by a single membrane (De Duve & Baudhuin, 1966; van der Klei *et al.,* 2006).

Peroxisomes are defined by the presence of H_2O_2-producing oxidases as well as catalase and are almost universally present among eukaryotes. The most common function is β-oxidation of fatty acids, however dependent on the organism, peroxisomes can harbour a range of additional functions. These include catabolic processes like α-oxidation of branched-chain fatty acids and polyamine metabolism in man and methanol oxidation in methylotrophic yeast species (Wanders & Waterham, 2006; van der Klei *et al.,* 2006). Examples of biosynthetic pathways are ether phospholipid and bile acid biosynthesis in man and penicillin production in *Penicillium chrysogenum*.

Several inherited peroxisomal disorders have been identified, which are caused by defects in the biogenesis of the organelle, or in specific peroxisomal enzymes or transporters of the peroxisomal membrane (Wanders, 2004). These disorders are often very severe and in many cases lethal, therefore functional peroxisomes are vital for human health.

This review summarizes the current knowledge on the different aspects of the peroxisome life-cycle; starting with the transcriptional network that regulates peroxisome proliferation, followed by the molecular mechanisms involved in organelle biogenesis. Next, peroxisomal quality control mechanisms are described, finally coming full circle with a description of peroxisome turnover by autophagy.

Regulation of peroxisome proliferation

Peroxisome size and number depends on cell type and environmental conditions. In yeast and filamentous fungi peroxisome proliferation can easily be induced by changing the medium composition. Especially carbon sources influence proliferation of peroxisomes.

When yeast cells are grown on glucose, peroxisomes are not required for growth. Glucose represses many genes, including a large number of genes involved in peroxisomal metabolism and proliferation (Rolland *et al.,* 2002).

As a consequence only a few small organelles are present per cell. Upon depletion of glucose a large number of genes is expressed as a consequence of derepression, leading to proliferation of peroxisomes. This phenomenon has also been observed in mammalian cells (Jansen *et al.,* 2009).

In yeast these, as well as additional genes involved in peroxisome biogenesis and function, are induced to a much higher level by peroxisome inducing substrates.

Peroxisome induction is most prominent upon a shift of glucose grown yeast cells to media containing oleic acid or methanol (Smith *et al.,* 2002; van Zutphen *et al.,* 2010).
In other organisms also peroxisome proliferators (e.g. clofibrate in mammals), hormones, oxidative stress and even light in plants can induce proliferation of peroxisomes (Chen *et al.,* 1995; Hu & Desai, 2008).
In the presence of glucose Mig1 represses many yeast genes involved in the utilization of non-fermentable carbon sources as well as gluconeogenesis (Nehlin & Ronne, 1990; Mercado *et al.,* 1991). Mig1 may recruit the central negative regulators Cyc8 and Tup1 to glucose-repressed genes (Vallier & Carlson, 1994). Upon depletion of glucose, Mig1 is phosphorylated and transported from the nucleus to the cytosol in a Snf1-dependent manner (Treitel *et al.,* 1998). Yeast Snf1, an AMP-activated protein kinase, senses energy depletion and has a central role in glucose derepression (Hardie, 2007). Snf1 acts on several regulators including Adr1, a regulator of genes involved in ethanol, glycerol and fatty acid utilization (Ratnakumar & Young, 2010). Adr1 binds to type 1 upstream activating sequences in the promoter regions of target genes, while Pip2-Oaf1 bind to oleate responsive elements and together regulate genes involved in fatty acid degradation and peroxisome proliferation in yeast (Gurvitz & Rottensteiner, 2006).

Binding of the fatty acid ligand to Oaf1 resembles ligand binding to peroxisome proliferator activated receptor alpha (PPARα), a key regulator of peroxisome proliferation in mammalian cells (Isseman *et al.,* 1990).

The family of PPARs regulate the transcription of many genes involved in a wide array of processes and are therefore extensively studied. Upon ligand binding, PPARα dimerizes with RXRα and binds to peroxisome proliferator response elements in the promoters of target genes (reviewed in Mandard *et al.,* 2004). Induction of peroxisomes by methanol in methylotrophic yeasts is also regulated by Adr1 (Lin-Cereghino *et al.,* 2006). Induction by methanol however, requires several other regulators like Mpp1, Trm1, Trm2, Swi1 and Snf2 (Leao-Helder *et al.,* 2003; Ozimek *et al.,* 2004; Sasano *et al.,* 2008, 2010).
Deletion of *MPP1*, the most highly upregulated gene in *Hansenula polymorpha* upon a shift of cells from glucose to methanol, results in a block in the induction of peroxisome proliferation (Leao-Helder *et al.,* 2003; van Zutphen *et al.,* 2010).

Peroxisome proliferation

Currently, two important models exist for the formation of peroxisomes. The first model states that peroxisomes, like mitochondria and chloroplasts, are autonomous organelles and multiply by growth and division of pre-existing organelles, as illustrated in figure 1 (Motley & Hettema, 2007; Nagotu *et al.,* 2008). In this model the endoplasmatic reticulum (ER) merely acts as a supplier of lipids. In the second model peroxisomes originate *de novo* from specialized regions of the ER (Hoepfner *et al.,* 2005). Both processes have been demonstrated to exist in various organisms. However, it is debated what the contribution of fission and formation from the ER is in wild type cells.

The peroxisomal membrane proteins Pex3 and Pex16 (absent in most yeast species) as well as the soluble protein Pex19 have fundamental roles in peroxisomal membrane formation, since in the absence of these proteins peroxisomal membranes remnants are absent.

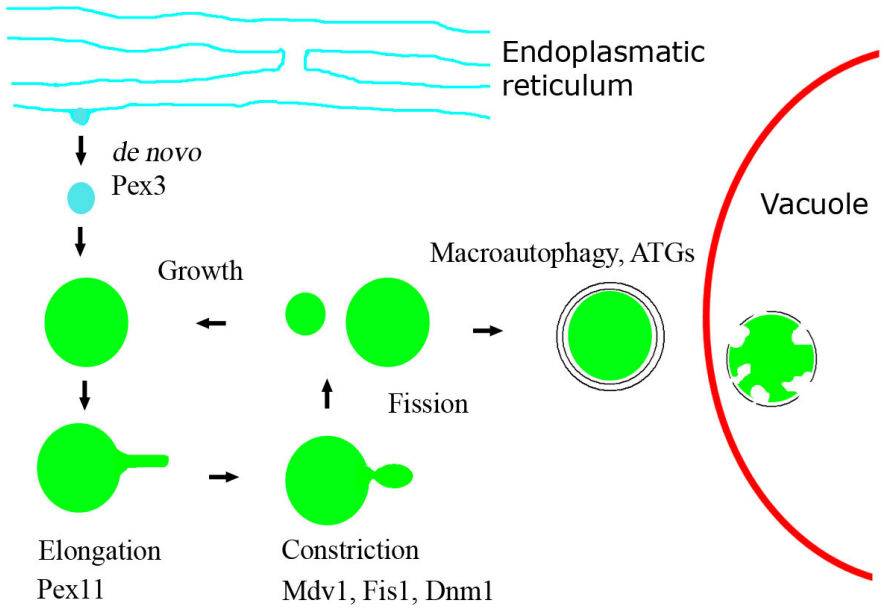

Figure 1. Peroxisome biogensis. Peroxisomes can be formed from specialized regions of the ER in a Pex3-dependent manner that also involves Pex16 in higher eukaryotes. In yeast peroxisomes are predominantly formed by fission from pre-existing organelles. Fission depends on Pex11-mediated elongation and subsequent constriction by the fission machinery; Dnm1, Mdv1 and Fis1 that is also involved in mitochondrial fission. In *S. cerevisiae*, fission also involves Vps1. Mature peroxisomes may be degraded via macroautophagy, termed macropexophagy, leading to sequestration of a single peroxisome and uptake in the vacuole.

Pex3 has been proposed to be the docking site for Pex19 that functions as a peroxisomal membrane protein (PMP) chaperone and receptor, delivering newly synthesized PMPs (the class I PMPs) to the peroxisome (Jones *et al.*, 2004: Fang *et al.*, 2004).

Pex3 itself belongs to the class II PMPs and is sorted to peroxisomes independent of Pex19 (Jones *et al.,* 2004). Recently Pex22 was also added to the class II PMPs, since the regions in Pex3 and Pex22 that contain peroxisomal targeting information are interchangeable and do not interact with Pex19 (Halbach *et al.,* 2008).

Upon re-introduction of full-length Pex3 in *pex3Δ* cells, the protein first colocalizes with the ER and subsequently concentrates in a spot that transforms into a new peroxisome (Hoepfner *et al.,* 2005). Based on this result d*e novo* formation of peroxisomes from the ER has been suggested to depend on Pex3. However there is still controversy whether newly synthesized Pex3 first traffics to the ER invariably (i.e. also in WT cells). The observation that *PEX3* transcripts preferentially localizes close to the ER suggest that Pex3 may be first inserted into the ER (Zipor *et al.,* 2009). However, other studies using cells containing pre-existing peroxisomes indicated that Pex3 may also travel directly to peroxisomes. Transiently expressed myc-tagged Pex3 solely co-localized with peroxisomes in *Arabidopsis thaliana* (Hunt *et al.,* 2004). Moreover, in human cells Pex3 was shown to be sorted directly to peroxisomes in a Pex16-dependent manner (Matsuzaki & Fujiki, 2008).

Finally, the Pex13 C-terminus containing class I PMP targeting information, fused to either Pex3 or Pex22 lacking their endogenous targeting signal, could complement *PEX3* and *PEX22* deletion strains, respectively. This indicates that the direct route of Pex13 to peroxisomes is also sufficient in yeast for Pex3 function.

In contrast to these data, a recent report proposed that most PMPs travel via the ER (van der Zand *et al.,* 2010).At steady state conditions most PMPs localize to peroxisomes, however some exceptions exist. Pex30 and Pex31 in the methylotrophic yeast *Pichia pastoris* localize to both ER and peroxisomes, phosphorylated Pex11 was shown to localize to the ER in *Saccharomyces cerevisiae*, in plants Pex10, ascorbate peroxidase and also plant and mammalian Pex16 localize to ER and peroxisomes (Flynn *et al.,* 2005; Nagotu *et al.,* 2010; Knoblach & Rachubinski, 2010).

Targeting of Pex3 to a specific subdomain of the ER depends on Pex16 in mammalian cells, which seems to be the dominant site of peroxisome formation (Kim *et al.,* 2006). Most yeast species however lack *PEX16.* Also, data in both *S. cerevisiae* and *H. polymorpha* indicate that peroxisomes are primarily formed by fission from pre-existing organelles (Motley & Hettema, 2007; Nagotu *et al.,* 2008).

Fission of peroxisomes requires the same machinery as mitochondrial fission; a Dynamin-like protein (DLP), the membrane anchor Fis1 and in yeast species also the adaptor Mdv1 (Motley *et al.,* 2008). Recently also a third factor for fission in mammalian cells was identified; Mff (Gandre-babbe & van der Bliek, 2008). Although this protein is also supposed to act as an adaptor, its function seems to be independent of Fis1 and DLP. In *S. cerevisiae* also two different routes depending on either the DLP Dnm1 or Vps1 exist (Kuravi *et al.,* 2006).

DLP's are GTPases thought to regulate the final constriction of membranes that leads to division (Shpetner & Vallee, 1989). Prior to the actual fission, tubulation and constriction of the organelle occurs, which requires the peroxisomal membrane protein Pex11 (Nagotu *et al.,* 2010).
In *S. cerevisiae* also Pex28, Pex29, Pex30, Pex31 and Pex32 regulate peroxisome size and number, yet how these peroxins of the proposed Pex23 family function, remains largely unclear (Kiel *et al.,* 2006). In *P. pastoris* Pex30 and Pex31 also regulate size and number during oleate induction, yet induction of peroxisomes by methanol is not affected in strains lacking these proteins (Yan *et al.,* 2008).
Studies in yeast showed that fission is the dominant form of peroxisome proliferation, whereas *de novo* formation from the ER might be dominant in higher eukaryotes, nevertheless vesicular trafficking between both organelles has been proposed for both pathways (Schekman, 2005; Nagotu *et al.,* 2010).
Data supporting this came from studies with Brefeldin A, an inhibitor of coated vesicle formation that disrupted sorting of peroxisomal proteins (Salomons *et al.,* 1997). Also several ER-Golgi anterograde and retrograde trafficking components localize to peroxisomes and disruption of these components affects peroxisome number (Kurbatova *et al.,* 2009; Perry *et al.,* 2009).
In yeast most of the enzymes involved in phospholipid biosynthesis are localized to the ER, therefore phospholipids may be transferred by vesicular trafficking to peroxisomes.

However, also non-vesicular transfer of phospholipids to peroxisomes has been described (Raychaudhuri & Prinz, 2008). Next to the ER, also mitochondria-derived vesicles were recently proposed to fuse with a subset of peroxisomes (Neuspiel *et al.,* 2008).

These observations challenge the model of peroxisomes being autonomous organelles. Indeed for plant a semi-autonomous model was proposed in which vesicular trafficking from the ER to peroxisomes occurs via an intermediate compartment that may also serve as pre-peroxisomal structure for *de novo* organelle formation, next to fission of peroxisomes (Mullen & Trelease, 2006).

Protein import

Matrix proteins are imported into peroxisomes in a folded state. Most matrix protein contain a peroxisomal targeting signal (PTS) 1, consisting of a C-terminal tripeptide with –SKL as consensus that is recognized by the cycling receptor Pex5 (Girzalsky *et al.,* 2009). Pex5 contains a C-terminal tetratricopeptide domain involved in binding of the PTS1. In addition Pex5 has a WxxxF/Y motif which is important for association of the receptor to the peroxisomal membrane (Otera *et al.,* 2002). At the peroxisomal membrane Pex5 interacts with both Pex13 and Pex14 that form the docking subcomplex, together with Pex17 (only in yeast; Agne *et al.,* 2003). The Pex14 N-terminus binds the WxxxF/Y motif of Pex5.

Interestingly the cargo-loaded form of Pex5 has a stronger affinity for Pex14 as compared to Pex5 lacking cargo, which has a stronger affinity for Pex13 (Otera *et al.,* 2002). Pex14 also binds Pex13. In *S. cerevisiae* Pex14 binds with a PxxP motif to the SH3 domain of Pex13, a domain that is also involved in binding to Pex5. In mammalian cells the Pex13 SH3 domain also interacts with the N-terminus of Pex14 (Itoh & Fujiki, 2006). Recently Pex5 and Pex14 were shown to be capable of forming a large transient pore in vitro, suggesting that these two proteins form the minimal translocation machinery (Meinecke *et al.,* 2010). In addition to Pex5 and in mammals Pex13, also Pex19 binds with a similar motif as Pex5 to the N-terminus of Pex14, yet this motif has a ~100-fold less affinity then Pex5 (Neufeld *et al.,* 2009). Whether this interaction is involved in targeting of Pex14 to the peroxisome or blocks the binding site of Pex14 in the absence of proteins with a higher affinity, like cargo-loaded Pex5, remains unclear.

In *H. polymorpha*, *P. pastoris* and mouse cells Pex14 was shown to be present in a non-phosphorylated and phosphorylated form (Komori *et al.,* 1999; Johnson *et al.,* 2001; Villén *et al.,* 2007). In *H. polymorpha* glucose-grown cells only the non-phosphorylated form is detectable, whereas during the mid-exponential growth phase of methanol-grown cells, phosphorylated Pex14 becomes more abundant. Upon a shift of these cells to glucose medium, the amount of phosphorylated Pex14 decreases more rapidly compared to the non-phosphorylated form. However, the function of this protein modification is still unclear (de Vries *et al.,* 2006).

The docking subcomplex is linked via Pex8 and perhaps also Pex3 to the Ring finger subcomplex consisting of the zinc-finger containing proteins Pex2, Pex10 and Pex12, allogether forming the peroxisomal importomer (Hazra *et al.,* 2002; Agne *et al.,* 2003). After cargo release Pex5 is removed from the importomer, which involves either monoubiquitination or polyubiquitination. Ubiquitination is a three-step process, starting with ubiquitin (Ub) activation by the Ub-activating enzyme E1, of which only a single member is present in yeast.

Ub is next transferred to the E2 Ub-conjugating enzyme, that attaches the Ub peptide to a lysine or cysteine residue in the target protein, together with the E3 ligase, that confers specificity (Schwartz & Ciechanover, 2009). A subsequent Ub can be ligated to Lys48 of the first Ub and so forth, resulting in polyubiquitination which serves as a signal for proteasomal degradation of the protein.

Pex4 is the E2 enzyme for monoubiquitination of Pex5 and is anchored to the peroxisomal membrane by Pex22. Pex12 was shown to be the E3 ligase in Pex5 recycling by monoubiquitination (Platta *et al.,* 2009). Ubc4-dependent polyubiquitination depends on Pex2 as E3 ligase and is thought to remove Pex5 from the import complex followed by proteasomal degradation as a quality control mechanism when proper Pex5 recycling is affected (Platta *et al.,* 2009). In addition Pex10 may also function in this process (Williams *et al.,* 2008).

Pex15 in yeast species or its homolog Pex26 in higher eukaryotes anchor the AAA ATPases Pex1 and Pex6 to the membrane, which associate with the importomer (Thoms & Erdmann, 2006). This complex is involved in the final phase of protein translocation, namely recycling of Pex5 back to the cytosol.
The Pex1/Pex6-complex as well as the importomer are highly dynamic complexes, that probably come together transiently in an ordered manner to accommodate translocation and disconnect again, as suggested by the different higher order complexes isolated from peroxisomal membranes (Agne *et al.,* 2003).
Few proteins contain a PTS2 recognized by the receptor Pex7, which also binds to the docking complex for translocation via co-receptors (Lazarow, 2006). The co-receptor Pex20 is required for delivery of PTS2 proteins in most yeast and fungal species, whereas the redundant proteins Pex18 and Pex21 perform this function in *S. cerevisiae*. In plants and mammalian cells both import systems are linked, since Pex5 in plants and the large isoform Pex5L in mammals function as co-receptor (Schliebs & Kunau, 2006).

Quality control

Because of their oxidative metabolism, peroxisomes are an intracellular source of reactive oxygen species (ROS), that may damage the proteins and lipids of the organelle and leak into the cytosol. To prevent damage, peroxisomes contain the antioxidant enzyme catalase that mainly neutralizes H_2O_2 (Loew, 1900; de Duve & Baudhuin, 1966).

Hypocatalesemic patients only have a single functional *CAT* allele and therefore have reduced levels of the enzyme. As a consequence H_2O_2 levels are higher, resulting in accelerated age-related diseases (Wood *et al.,* 2006).

Next to catalase, yeast peroxisomes also contain a peroxiredoxin, a thioredoxin-dependent peroxidase, also designated Pmp20. Deletion of the *PMP20* gene results in oxidation of phospholipids in the peroxisomal membrane in *Candida boidinii* and *H. polymorpha* (Aksam *et al.,* 2009). Plants also contain an ascorbate-glutathione cycle localized to several organelles, including peroxisomes. H_2O_2 is reduced by ascorbate peroxidase at the membrane, while the formed monodehydroascorbate is subsequently regenerated by a glutathione pathway in the peroxisomal matrix (reviewed by del Rio *et al.,* 2002).

Next to enzymes acting on ROS, peroxisomes were also shown to contain proteases which may process damaged proteins within the matrix. Several of these enzymes are also implicated in processing of peroxisomal enzymes; for instance the mouse protease Tysnd1, the plant serine protease DEG15 and human insulin degrading enzyme, however the latter enzyme was also proposed to degrade oxidized proteins (Kurochkin *et al.,* 2007; Schumann *et al.,* 2008). In addition most organisms were shown to contain a peroxisomal Lon protease, which most likely degrades oxidized proteins (Aksam *et al.,* 2007, 2009).

Peroxisome degradation by autophagy

General introduction

The autophagy pathway is capable of degrading virtually any component of the cell, including organelles, protein aggregates and even invading pathogens. Degradation takes place by translocation of cargo into the mammalian lysosome or plant/fungal vacuole and subsequent degradation by hydrolases. Because of this fundamental role in cellular housekeeping, autophagy is involved in many physiological processes like development, ageing, survival during starvation and programmed cell death (Mizushima *et al.,* 2008). As a consequence autophagy is also linked to severe human disorders such as myopathies, neurodegenerative diseases, and cancer (Todde *et al.,* 2009).

Autophagy can occur via three main modes: microautophagy, macroautophagy and chaperone-mediated autophagy (CMA; only in mammals), illustrated in figure 2. Microautophagy involves the direct uptake of particles/cytoplasm via invaginations of the lysosome/vacuole (for simplicity termed vacuole from now on), leading to direct sequestration. Macroautophagy initiates by formation of a double-membrane structure, the autophagosome, that sequesters cargo from the cytosol (Mizushima *et al.,* 2008). The outer layer of the autophagosome next fuses with the vacuole, leading to degradation of the content. CMA involves the uptake of soluble proteins containing the pentapeptide "KFERQ" via LAMP2A-dependent translocation, only present in higher eukaryotes and will not be described further (recently reviewed by Kon & Cuervo, 2010).

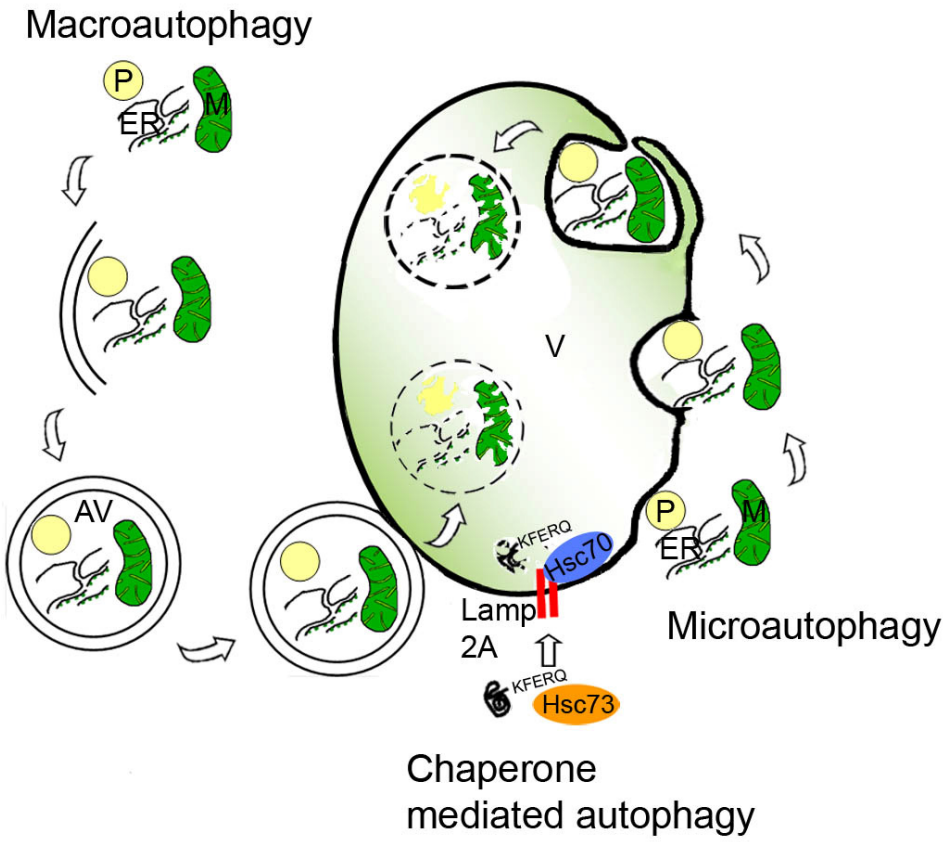

Figure 2 Main modes of autophagy. Cytoplasmic material can be degraded by 3 main mechanisms of autophagy. During Macroautophagy cytoplasm is sequestered by a newly formed double membrane called the autophagsome (AV). This includes organelles like peroxisomes (P), mitochondria (M) and pieces of the endoplasmatic reticulum (ER). After completion, the outer layer fuses with the vacuole/lysosome (V), leading to degradation of its content. Microautophagy involves the uptake of cytoplasm by direct invagination of the vacuole, fusion of the opposing ends of the vacuolar arms and degradation in the lumen. Chaperone mediated autophagy degrades soluble proteins with the signal sequence KFERQ, which are recognized by the chaperone Hsc73 and translocated by the lysosomal membrane protein LAMP2a in conjunction with the lysosomal chaperone Hsc70.

Both micro- and macroautophagy can be selective or non-selective, depending on the activating signal, in addition to constitutive degradation at a basal level (Tuttle & Dunn, 1995; Hara *et al.*, 2006).

These signals can come from the environment; like starvation, hypoxia or growth factors, but also from within the cell for instance when protein aggregates, intracellular pathogens, or dysfunctional/redundant organelles are present.

Non-specific degradation of non-essential components and subsequent recycling of their degradation products (e.g. amino acids) occurs during nutrient starvation in order to survive (Kristensen *et al.,* 2008). In most organisms macroautophagy is responsible for starvation-induced autophagy, yet in some organisms and cell types microautophagy is induced during starvation (de Waal *et al.,* 1986; Bellu *et al.,* 2001). Selective degradation is observed when superfluous organelles like peroxisomes and mitochondria are cleared from the cytoplasm, which also may occur via micro- or macroautophagy (Tuttle & Dunn, 1995).

Regulation of autophagy

Upon induction of autophagy, distinct steps can be defined, which are highly-regulated. Both selective micro- and macroautophagy initiate with recognition of a target, followed by sequestration from the cytoplasm, translocation into the vacuole lumen and finally degradation. How non-selective autophagy initiates remains to be established.

Although each specific type of micro- and macroautophagy requires a subset of specific proteins, genetic screens and analysis of genome databases have identified a core machinery consisting of autophagy-related (Atg) proteins (Xie & Klionsky, 2007), which is remarkably conserved from yeast to man (Meijer *et al.*, 2007). Autophagy is regulated by many signalling pathways that transduce an activating signal via several core complexes (Fig. 3).

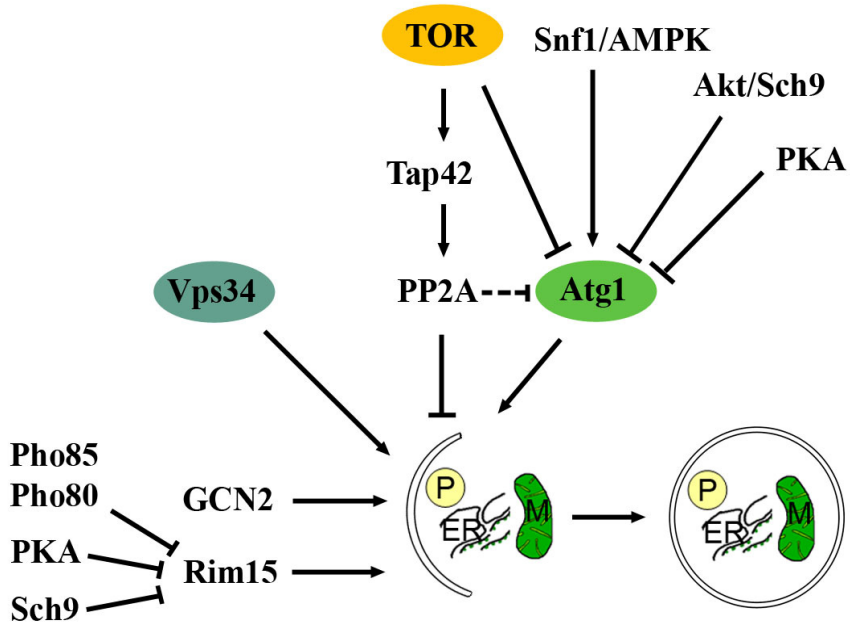

Figure 3 Regulation of macroautophagy in yeast. Tor inhibits autophagy by phosphorylation of the Atg1-complex during nutrient availability and also by activating the suppresors Tap42 and PP2A. TOR activity is paralleled by the PKA and AKT/Sch9 pathways, whereas the nutritional sensor Snf1 positively regulates autophagy, by acting on Atg1. PKA also inactivates the kinase Rim15, together with Sch9 and the cyclin-dependent kinase Pho85, in conjunction with several cyclins. The PI3p-kinase VPS34 is an additional essential regulator of autophagy. Upon starvation, the regulator Gcn2 is also required for autophagy, yet perhaps indirectly by acting on general protein synthesis.

TOR-kinase (Target Of Rapamycin) is the catalytic subunit of the TOR complex 1 (TORC1), which functions as a central regulator in fundamental processes like protein synthesis, ribosome biogenensis, cell-cycle progression and autophagy (Wullschleger *et al.,* 2006). In the presence of abundant nutrients, TORC1 inhibits autophagy, by phosphorylating Atg13 in yeast, an effector of the second key regulator, the serine/threonine kinase Atg1.
In mammalian cells both Atg13 and mammalian Atg1 (named Ulk1) are phosphorylated by TORC1 (Kamada *et al.,* 2010). Starvation inactivates TORC1, leading to dephosphorylation of the Atg1-complex, inactivation of the suppressors Tap42 and protein phosphatase 2A and activation of GCN2 that may act indirectly by modulating general protein synthesis (He & Klionsky, 2009). The PKA and AKT pathways may act in parallel to the TORC1, whereas Snf1 stimulates autophagy upon activation.
The induction also leads to a G_0 growth arrest in which the cyclin-dependent kinase Pho85 in conjunction with several cyclins affects autophagy by downregulating the kinase Rim15 (Yang et *al.,* 2010).
In yeast, starvation next leads to formation of a complex consisting of Atg1, Atg13, Atg17, Atg29 and Atg31, that recruits the majority of the Atg proteins to the phagophore assembly site (PAS), in conjunction with a second essential complex for autophagy the phosphatidylinositol-3 kinase complex (PtdIns3K). In mammals Ulk1, interacts with Atg13 , FIP200 (Atg17 ortholog) and Atg101. So far the PAS structure has only been described based on fluorescence microscopy (Mizushima, 2010).

The PtdIns3K-complex contains as catalytic unit the PtdIns-3 kinase Vps34, a regulator of multiple vacuole sorting pathways. Vps34 forms a complex with Vps15, Vps30, Atg6 and either Atg14 or Vps38 in yeast, resulting in complex I or complex II respectively (Kihara *et al.,* 2001). In mammals Beclin-1 (Bcl-1) is the homolog of Atg6, UVRAG is the homolog of Vps38 and the complex contains an additional component the negative regulator Rubiscon (Zhong *et al.,* 2009). Complex I is involved in autophagy processes, via the generation of the signal lipid PtdIns-3P at the PAS in yeast and at the ER or trans-Golgi network (TGN) in mammals, leading to recruitment of Atg proteins.

Binding of the anti-apoptotic factor Beclin-2 (Bcl-2) to Bcl-1 disrupts the association of Bcl-1 with the Vps34 complex and therefore inhibits autophagy (Pattingre *et al.,* 2005). There is an intimate but complex connection between autophagy and apoptosis in which Bcl-2 functions at the crossroads. Recently also two negative regulators of autophagy were identified in mammalian cell lines; Jumpy and MTMR3, which both dephosphorylate PtdIns-3P and associate with the isolation membrane and early autophagosomes, therefore a complex interplay between phosphatases and kinases is involved in regulation of autophagy (Taguchi-Atarashi *et al.,* 2010).
For the initial nucleation step of autophagosome formation, the Vps34- and Atg1-complexes are required, as well as the cargo, whereas the subsequent expansion step requires the Atg8- and Atg9-complexes (discussed below; Xie & Klionsky, 2007).

Recognition of cargo

In yeast Atg11 is involved in the recognition of specific targets and possibly also delivery of the cargo to the PAS via actin cables (Reggiori *et al.,* 2005). Atg11 binds for instance to Atg19 (involved in the Cvt pathway), the peroxisomal membrane protein Atg30 and the mitochondrial membrane protein Atg32 (Scott *et al.,* 2001; Farre *et al.,* 2008; Kanki *et al.,* 2009). Delivery of cargo may also form the signal for assembly of the PAS and initiation of sequestration (Shintani & Klionsky, 2004). Next to Atg11, Atg8 also binds to receptors like Atg32 and the receptor for ubiquitinated protein aggregates P62/SQSTM1, which all contain a WxxL-like "Atg8-family interacting motif", however no interaction with the peroxisomal receptor Atg30 has been identified so far (Bjørkøy *et al.,* 2005; Noda *et al.,* 2010). The mammalian counterpart of Atg8, microtububle associated protein light chain (LC3, Meijer *et al.,* 2007) and its homologs, seems to be the only receptor-binding protein in higher eukaryotes.
Atg8/LC3 is activated by a ubiquitin-like conjugation system. Atg8/LC3 also has a prominent role in all forms of autophagy and is one of few proteins that ends up in the vacuole together with the cargo, therefore Atg8/LC3 structure, function and trafficking has drawn much attention (Kirisako *et al.,* 1999; Geng *et al.,* 2008a).

The Atg12 and Atg8/LC3-conjugation system

Two systems reminiscent of the ubiquitination pathway are involved in the expansion of the autophagosome during macroautophagy and for closure of the expanding vacuolar arms during microautophagy of peroxisomes.

These systems include Atg8 and Atg12, which are both structurally very similar to ubiquitin (Sugawara *et al.,* 2004, Suzuki *et al.,* 2005). Atg8 is first cleaved by Atg4 to enable activation by the E1-like Atg7 and transfer to the E2-like Atg3, that subsequently conjugates Atg8 to the phospholipid phosphatidylethanolamine (PE), stimulated by the E3-like function of the Atg5-Atg12-Atg16 complex (Ichimura *et al.,* 2000; Hanada *et al.,* 2007). The formation of this complex involves a second ubiquitin-like pathway. There Atg7 activates and transfers Atg12 to the E2-like enzyme Atg10, which conjugates Atg12 to Atg5 (Mizushima *et al.,* 1998). Next Atg5 interacts with Atg16 and together form a large multimeric complex, that forms the E3-like enzyme for Atg8 conjugation (Hanada *et al.,* 2007). Lipidation of Atg8 is reversible. In addition to activation of Atg8, Atg4 can also cleave the membrane-bound Atg8-PE to recycle Atg8, which is necessary to complete the autophagosome, nevertheless a portion of Atg8 becomes trapped inside the vesicle and is ultimately degraded (Kirisako *et al.,* 1999).

The ratio of the conjugated Atg8-II form compared to Atg8-I has been used often as a measure for induction of autophagy; at nutrient rich conditions most Atg8 is soluble, whereas upon starvation most Atg8 becomes membrane-bound (Ichimura *et al.,* 2000). Similar findings were made for lipid conjugation of the mammalian Atg8 homologs LC3, GATE16, GABARAP and Atg8L (Kabeya *et al.,* 2004).

Since Atg8 controls autophagosome size while residing on the expanding membrane, it is removed prior to autophagosome completion and is also the most abundant Atg protein at the site of autophagosome formation, a coat adaptor function was recently proposed (Xie *et al.,* 2009; Geng *et al.,* 2008b). Yet the Atg8-PE conjugate was also demonstrated to have liposome tethering and hemifusion properties, which was claimed to be consistent with a role in autophagosome expansion (Nakatogawa *et al.,* 2007).
In addition *H. polymorpha atg8*Δ cells displayed a defect in closure of the autophagosome rather then expansion, similar to data in mammalian cells in which LC3 processing was hampered, both suggesting a function in autophagosome completion rather then expansion (Monastyrska *et al.,* 2005a; Fujita *et al.,* 2008).
Altogether these observations make the function of the most well-studied autophagy protein Atg8 still puzzling, yet its localisation and lipidation state are generally accepted markers for autophagy.

Origin of the autophagosomal membrane

Although autophagy has been studied for almost half a century, still the membrane source of the autophagosome has remained enigmatic (Juhasz & Neufeld, 2006).
In yeast the localisation of most Atg's to the perivacuolar PAS upon induction of autophagy and the cycling between the cell periphery and the PAS of the Atg9-complex, favours the assembly model, which states that autophagosomes are formed *de novo*.

This complex containing the 2 transmembrane proteins Atg9 and Atg27 as well as Atg23, cycles between the cell periphery and the PAS in an Atg1-complex dependent manner and is therefore believed to deliver membrane components to the site of autophagosome formation (Webber & Tooze, 2010a). This is supported by the finding that several components of the ER, exit from the Golgi and early secretory pathway are also required (van der Vaart *et al.,* 2010; Geng *et al.,* 2010).

However, there is also accumulating evidence for the maturation model that proposes formation of an autophagosome from pre-existing organelles, for which the ER is the most obvious candidate, especially in mammalian cells (Juhasz & Neufeld, 2006). Here Atg9 localizes to the TGN and endosomes, whereas upon starvation it redistributes to a peripheral pool that co-localizes with LC3, in a P38IP-dependent manner (Webber & Tooze, 2010b). Mammalian autophagosomes also do not form at one distinct location in the cell, like in yeast (Jahreiss *et al.,* 2008).

Recent findings elegantly showed the translocation of PtdIns-3P binding proteins to the periphery of the ER upon starvation, in close association with Vps34-containing particles (Axe *et al.,* 2008). Here a ring-like particle was formed, termed an omegasome, in which the autophagome formed, in close association with the ER (Axe *et al.,* 2008).
Consistent with the ER as source for the autophagosome are electron tomography studies, which showed a direct connection of the expanding autophagosome with the ER (Hayashi-Nishino *et al.,* 2009).

Similar observations were made in yeast upon induction of selective ER degradation (Bernales *et al.,* 2006). However, also mitochondria have been suggested to contribute to the autophagosomal membrane formation, therefore formation may very well rely on the contribution of multiple membrane sources (Hailey *et al.,* 2010).

Vacuole/Lysosome fusion

The autophagosome, next fuses with the vacuole, which largely depends on proteins also involved in the homotypic vacuole fusion machinery. A small Rab-GTPase, regulatory lipids, three Q- and one R-SNARE, N-ethylmaleimide-sensitive factor (NSF), soluble NSF attachment protein (SNAP) and the homotypic fusion and vacuole protein sorting complex (HOPS), form this fusion machinery (Wickner & Schekman, 2008).

Ultimately the SNAREs on each opposing membrane form a 4-helical bundle and drive fusion. In mammalian cells lysosome fusion is often preceded by fusion of the autophagosome with endosomes in a Rab7-dependent manner, leading to formation of an amphisome (Jäger *et al.,* 2004).

After vacuole uptake, degradation of cargo as well as the inner autophagosomal membrane in case of macroautophagy and the vacuolar membrane that separates cargo from the lumen during microautophagy, takes place by vacuolar hydrolases (Wang *et al.,* 2002; Sarry *et al.,* 2007). How these membranes as part of the autophagosome or vacuole are resistant towards hydrolases, whereas, upon release into the vacuole lumen become degraded, is currently unknown.

In yeast so far only one putative vacuolar lipase has been identified, Atg15. Atg15 was shown to be involved in breakdown of intravacuolar vesicles (Epple *et al.,* 2001). This glycosylated integral membrane protein first localizes to the ER and is subsequently targeted to the vacuole via the multivesicular body pathway. Atg22 was reported to be a permease involved in recycling amino acids back into the cytosol (Yang *et al.,* 2006).

Nutrient starvation is considered an inducer of non-specific autophagy. Yet analysis of the type of cargo revealed an ordered uptake in yeast, suggesting that even under harsh starvation conditions a certain level of selectivity exits (Kristensen *et al.,* 2008). Also for uptake of ribosomes during starvation, the Ubp3/Bre5 uniquitin protease needs to be present, whereas other cellular components are still degraded in strains lacking the activity of this protease (Kraft *et al.,* 2008).

Selective degradation of various organelles like peroxisomes, mitochondria and the ER has been observed, as well as of harmful constituents like protein aggregates (Bjørkøy *et al.,* 2005; Klionsky *et al.,* 2007). Selective turnover becomes most evident when the organelle becomes redundant for growth. Perhaps this is the reason that most research on selective organelle turnover has been dedicated to peroxisomes (Dunn *et al.,* 2005).

Pexophagy

Selective turnover of peroxisomes, or pexophagy, has been studied to a limited extend in mammals and plants, however in several yeast species much more is known about the molecular mechanisms involved (Dunn *et al.,* 2005; Iwata *et al.,* 2006). Although *S. cerevisiae* is a commonly used model organism in cell biology, morphological details on pexophagy are very limited and conflicting results exist on the exact mechanism responsible for pexophagy (Hutchins *et al.,* 1999). Nevertheless macroautophagy is held responsible for pexophagy in *S. cerevisiae* (Hutchins *et al.,* 1999; Reggiori *et al.,* 2005). In contrast much more is known on pexophagy in methylotrophic yeasts like *H. polymorpha* and *P. pastoris* (Manjithaya *et al.,* 2010). In *H. polymorpha* a shift of methanol-grown cells to media containing glucose or ethanol induces macropexophagy, whereas in *P. pastoris* a shift to glucose media induces micropexophagy and to ethanol macropexophagy (Veenhuis *et al.,* 1983; Tuttle & Dunn, 1995). The divergent modes of pexophagy in *P. pastoris* seem to depend rather on ATP-levels then on the change in substrate, since similar to *H. polymorpha*, a shift to media containing relatively low glucose concentrations also induces macropexophagy (Ano *et al.,* 2005b). Upon induction of macropexophagy in *H. polymorpha*, Pex3 needs to be removed from the organelle as was concluded from several lines of evidence; complementation of *pex3Δ* cells with *S. cerevisiae PEX3* resulted in cells that grow on methanol and form peroxisomes, yet upon a shift to glucose, Pex3 levels remained stable and sequestration of peroxisomes was not observed.

In addition a C-terminal tagged Pex3 variant has no effect on peroxisome biogenesis, whereas pexophagy is severely inhibited. Inhibition of the proteasome also blocks pexophagy. Probably ubiquitination of Pex3 followed by proteasomal degradation is responable for Pex3 removal. Finally in *pdd* mutants blocked in macropexophagy Pex3 levels decreases upon induction of macropexophagy, whereas the organelles remained intact (Bellu *et al.,* 2002).

Pex3 degradation may lead to the exposure of the N-terminus of Pex14, which is required to initiate sequential sequestration of individual organelles, preferentially the large mature peroxisomes, whereas one or vew nascent small organelles escape the proces (Veenhuis *et al.,* 1983; Bellu *et al.,* 2001). Starvation induced non-specific microautophagy of peroxisomes does not require Pex14 in *H. polymorpha*, yet, unlike macropexophagy, does require protein synthesis (de Vries *et al.,* 2006; Monastyrska *et al.,* 2005b).
In *P. pastoris* the peroxisomal membrane protein Atg30, essential for both modes of pexophagy, binds to Pex3 and phosphorylated Pex14 as well as to Atg11 and requires to be phosphorylated during pexophagy (Farre *et al.,* 2008).

These observations have led to a model of the initial steps of macropexophagy on the peroxisomal membrane prior to sequestration (Fig. 4, Kiel *et al.,* 2003).

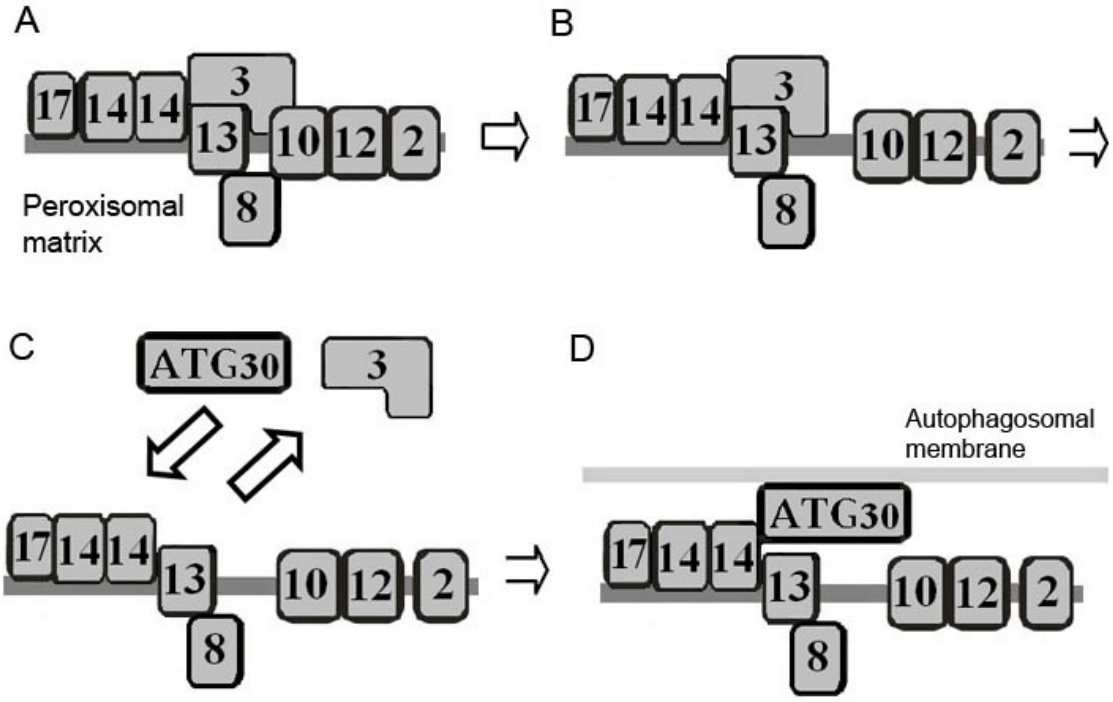

Figure 4 Hypothetical model of the function of peroxisomal membrane proteins during macropexophagy in methylotrophic yeasts. In nascent actively importing peroxisomes the docking subcomplex (Pex13, Pex14 and Pex17) is connected to the Ring finger subcomplex (Pex2, Pex10, Pex12) via Pex8 and Pex3 to form the active importomer (A). In mature peroxisomes that do not import matrix proteins anymore, the components of the complex may be dissociated, rendering Pex3 susceptible to removal. Upon an activating signal, i.e. a shift of methanol grown cells to glucose, Pex3 is removed from the membrane, thereby exposing Pex14 to the autophagic machinery (C). Pex14 next interacts with phosphorylated Atg30, leading to binding of Atg11 and sequestration of the organelle (D). Model is adapted from Kiel *et al.* (2003).

Sequestration next proceeds as described for general macroautophagy, although in addition Atg25 was identified in *H. polymorpha* as a factor that resides on autophagosomes next to Atg8.

Deletion of *ATG25*, which is only present in a few yeast species, blocks macropexophagy at a late stage, yet induces constitutive degradation of peroxisomes by microautophagy (Monastyrska *et al.,* 2005b; Meijer *et al.,* 2007).
Deletion of *ATG28* also disrupts both modes of pexophagy at a late stage without inhibiting other autophagy pathways (Stasyk *et al.,* 2006). Analysis of the final stage of macropexophagy, namely fusion of the autophagosome with the vacuole, indicated that deletion of SNAREs indeed inhibits macropexophagy (Ano *et al.,* 2005a; Stevens *et al.,* 2006). Degradation of mammalian peroxisomes by autophagy also requires Pex14 (Hara-Kuge & Fujiki, 2008).

Micropexophagy in *P. pastoris* initiates with the selective engulfment of the whole peroxisome cluster (Sakai *et al.,* 1998). For complete sequestration however, an additional membrane structure is formed termed the micropexophagy specific membrane apparatus (MIPA), that results in full sequestration of the organelles by fusing to the tips of the vacuole extensions that engulf the organelles (Mukaiyama *et al.,* 2004). Since this isolation membrane also contains Atg8 and requires most Atg-proteins to form, it may resemble autophagosome formation, however there are also differences (Manjithaya *et al.,* 2010).

The UDPglucose:sterol glucosyltransferase Atg26 was shown to be required for micropexophagy and only for macropexophagy in case of methanol-grown *P. pastoris* cells that contain large peroxisomes and not for oleate- or amine-grown cells that harbour smaller ones (Oku *et al.,* 2003; Nazarko *et al.,* 2007). Atg26 binds with its GRAM domain to PI4P at the MIPA and promotes elongation of the isolation membrane (Yamashita *et al.,* 2006). Yet in *Yarrowia lipolytica* and *S. cerevisiae*, *atg26Δ* cells normally degrade peroxisomes (Cao & Klionsky, 2007; Nazarko *et al.,* 2007). Only micropexophagy requires Vac8, possibly because micropexophagy often involves fragmentation of the vacuole and Vac8 also functions in homotypic vacuole fusion (Fry *et al.,* 2006).

Concluding remarks & Perspectives

Peroxisome homeostasis is maintained by a delicate balance between proliferation and turnover that can be rapidly shifted by environmental cues. To ensure this balance, these two processes are converged at the molecular level; Pex3 and Pex14 fulfill pivotal roles in both biogenesis and degradation by macroautophagy (Bellu *et al.,* 2001, 2002; de Vries *et al.,* 2006). In addition factors involved in vacuole fusion that mediate the final delivery of cargo to the vacuole lumen, also may affect peroxisome formation (Ano *et al.,* 2005a; Stevens *et al.,* 2006).

Lipids synthesized in the ER or mitochondria are incorporated into both the peroxisome as well as the autophagosome. Still it is obscure how these molecules are transported to the target organelles (Neuspiel *et al.,* 2008; Hayashi-Nishino *et al.,* 2009 Nagotu *et al.,* 2010; Hailey *et al.,* 2010).

The autophagic degradation of cellular constituents shows the existence of a general theme consisting of a specific receptor for each target of autophagy, that forms the connection to the core machinery that is always active at a basal level, but can also be induced when required. In addition a posttranslational modification of these receptors often precedes induction of turnover, as observed for ribosomes, mitochondria and peroxisomes (Kraft *et al.,* 2008; Farre *et al.,* 2008; Geisler *et al.,* 2010).

Among the Atg proteins several kinases are present, yet which kinase phosphorylates Atg30 and Pex14 prior to pexophagy, remains to be established.

Screens for mutants disturbed in peroxisome degradation mostly identified genes required for both micro- and macropexophagy, which may be the result of a shared core machinery, or related to the fact that both mechanisms are able to compensate for malfunction of the other.

One should keep in mind however, that these two classical forms of autophagy responsible for organelle turnover, may not be all there is to it, as for instance in mammalian cells superfluous peroxisomes could also be degraded by 15-lipoxygenase-dependent disruption of the membrane and degradation by cytosolic proteases (van Leyen *et al.,* 1998).

Since peroxisomes have a limited life-span, constitutive degradation occurs during peroxisome-inducing conditions (Aksam *et al.,* 2007), which may be the most relevant form of pexophagy for human health, however the mechanism responsible still needs to be uncovered.

References

Agne B, Meindl NM, Niederhoff K, Einwächter H, Rehling P, Sickmann A, Meyer HE, Girzalsky W, Kunau WH. Pex8p: an intraperoxisomal organizer of the peroxisomal import machinery. Mol Cell 2003; 11:635-46.

Aksam EB, Koek A, Kiel JAKW, Jourdan S, Veenhuis M & van der Klei IJ. A peroxisomal lon protease and peroxisome degradation by autophagy play key roles in vitality of *Hansenula polymorpha* cells. Autophagy 2007; 3:96-105.

Aksam EB, de Vries B, van der Klei IJ, Kiel JA. Preserving organelle vitality: peroxisomal quality control mechanisms in yeast. FEMS Yeast Res 2009; 9:808-20.

Ano Y, Hattori T, Kato N, Sakai Y. Intracellular ATP correlates with mode of pexophagy in *Pichia pastoris*. Biosci Biotechnol Biochem 2005a; 69:1527-33.

Ano Y, Hattori T, Oku M, Mukaiyama H, Baba M, Ohsumi Y, Kato N, Sakai Y. A sorting nexin PpAtg24 regulates vacuolar membrane dynamics during pexophagy via binding to phosphatidylinositol-3-phosphate. Mol Biol Cell 2005b; 16:446-57.

Axe EL, Walker SA, Manifava M, Chandra P, Roderick HL, Habermann A, Griffiths G, Ktistakis NT. Autophagosome formation from membrane compartments enriched in phosphatidylinositol 3-phosphate and dynamically connected to the endoplasmic reticulum. J Cell Biol 2008; 182:685-701.

Bellu AR, Komori M, van der Klei IJ, Kiel JA, Veenhuis M. Peroxisome biogenesis and selective degradation converge at Pex14p. J Biol Chem 2001; 276:44570-4.

Bellu AR, Salomons FA, Kiel JA, Veenhuis M, Van Der Klei IJ. Removal of Pex3p is an important initial stage in selective peroxisome degradation in *Hansenula polymorpha*. J Biol Chem 2002; 277:42875-80.

Bernales S, McDonald KL, Walter P. Autophagy counterbalances endoplasmic reticulum expansion during the unfolded protein response. PLoS Biol 2006; 4:e423.

Bjørkøy T, Lamark A, Brech H, Outzen M, Perander A, Overvatn H, Stenmark, Johansen T. P62/SQSTM1 forms protein aggregates degraded by autophagy and has a protective effect on huntingtin-induced cell death. J Cell Biol 2002; 171:603–614.

Cao Y, Klionsky DJ. Atg26 is not involved in autophagy-related pathways in *Saccharomyces cerevisiae*. Autophagy 2007; 3:17-20.

Chen T, Li W, Schulz PJ, Furst A, Chien PK. Induction of peroxisome proliferation and increase of catalase activity in yeast, Candida albicans, by cadmium. Biol Trace Elem Res 1995; 50:125-33.

Cherry JR, Johnson TR, Dollard C, Shuster JR, Denis CL. Cyclic AMP-dependent protein kinase phosphorylates and inactivates the yeast transcriptional activator ADR1. Cell 1989; 56:409-19.

De Duve C, Baudhuin P. Peroxisomes (microbodies and related artcles). Physiol Rev 1966; 46:323.

Del Río LA, Corpas FJ, Sandalio LM, Palma JM, Gómez M, Barroso JB. Reactive oxygen species, antioxidant systems and nitric oxide in peroxisomes. J Exp Bot 2002; 53372:1255-72.

De Vries B, Todde V, Stevens P, Salomons F, van der Klei IJ, Veenhuis M. Pex14p is not required for N-starvation induced microautophagy and in catalytic amounts for macropexophagy in *Hansenula polymorpha*. Autophagy 2006; 2:183-8.

Dunn WA Jr, Cregg JM, Kiel JA, van der Klei IJ, Oku M, Sakai Y, Sibirny AA, Stasyk OV, Veenhuis M. Pexophagy: the selective autophagy of peroxisomes. Autophagy 2005; 1:75-83.

Epple UD, Suriapranata I, Eskelinen EL, Thumm M. Aut5/Cvt17p, a putative lipase essential for disintegration of autophagic bodies inside the vacuole. J Bacteriol 2001; 183:5942-5955.

Fang Y, Morrell JC, Jones JM, Gould SJ. PEX3 functions as a PEX19 docking factor in the import of class I peroxisomal membrane proteins. J Cell Biol 2004; 164:863-75.

Farré JC, Manjithaya R, Mathewson RD, Subramani S. PpAtg30 tags peroxisomes for turnover by selective autophagy. Dev Cell 2008;14:365-76.

Flynn CR, Schumann MHU, Gietl C, Trelease RN. Compartmentalization of the plant peroxin, AtPex10p, within subdomain(s) of ER, Plant Sci 2005; 168:635–652.

Fry MR, Thomson JM, Tomasini AJ, Dunn WA Jr. Early and late molecular events of glucose-induced pexophagy in *Pichia pastoris* require Vac8. Autophagy 2006; 2:280-8.

Fujita N, Hayashi-Nishino M, Fukumoto H, Omori H, Yamamoto A, Noda T, Yoshimori T. An Atg4B mutant hampers the lipidation of LC3 paralogues and causes defects in autophagosome closure. Mol Biol Cell 2008;19:4651-9.

Gandre-Babbe S, van der Bliek AM. The novel tail-anchored membrane protein Mff controls mitochondrial and peroxisomal fission in mammalian cells. Mol Biol Cell 2008; 19:2402-12.

Geisler S, Holmström KM, Skujat D, Fiesel FC, Rothfuss OC, Kahle PJ, Springer W. PINK1/Parkin-mediated mitophagy is dependent on VDAC1 and p62/SQSTM1. Nat Cell Biol 2010; 12:119-31.

Geng J, Baba M, Nair U, Klionsky DJ. Quantitative analysis of autophagy-related protein stoichiometry by fluorescence microscopy. J Cell Biol 2008a; 182:129-40.

Geng J, Klionsky DJ. Quantitative regulation of vesicle formation in yeast nonspecific autophagy. Autophagy 2008b; 4:955-7.

Geng J, Nair U, Yasumura-Yorimitsu K, Klionsky DJ. Post-Golgi Sec Proteins Are Required for Autophagy in *Saccharomyces cerevisiae*. Mol Biol Cell 2010. Epub ahead of print.

Girzalsky W, Platta HW, Erdmann R. Protein transport across the peroxisomal membrane. Biol Chem 2009; 390:745-51.

Gurvitz A, Rottensteiner H. The biochemistry of oleate induction: transcriptional upregulation and peroxisome proliferation. Biochim Biophys Acta 2006;1763:1392-402.

Hailey DW, Rambold AS, Satpute-Krishnan P, Mitra K, Sougrat R, Kim PK, Lippincott-Schwartz J. Mitochondria supply membranes for autophagosome biogenesis during starvation. Cell 2010;141:656-67.

Halbach A, Rucktäschel R, Rottensteiner H, Erdmann R. The N-domain of Pex22p can functionally replace the Pex3p N-domain in targeting and peroxisome formation. J Biol Chem 2009; 284:3906-16.

Hanada T, Noda NN, Satomi Y, Ichimura Y, Fujioka Y, Takao T, Inagaki F, Ohusmi Y. The Atg12–Atg5 conjugate has a novel E3-like activity for protein lipidation in autophagy. J Biol Chem 2007; 282:37298–37302.

Hara T, Nakamura K, Matsui M, Yamamoto A, Nakahara Y, Suzuki-Migishima R, Yokoyama M, Mishima K, Saito I, Okano H, Mizushima N. Suppression of basal autophagy in neural cells causes neurodegenerative disease in mice. Nature 2006; 441:885-889.

Hara-Kuge S, Fujiki Y. The peroxin Pex14p is involved in LC3-dependent degradation of peroxisomes. Exp Cell Res 2008; 314:3531-3541.

Hardie DG. AMP-activated/SNF1 protein kinases: conserved guardians of cellular energy. Nat Rev Mol Cell Biol 2007; 8:774-785.

Hayashi-Nishino M, Fujita N, Noda T, Yamaguchi A, Yoshimori T, Yamamoto A. A subdomain of the endoplasmic reticulum forms a cradle for autophagosome formation. Nat Cell Biol 2009;11:1433-7.

Hazra PP, Suriapranata I, Snyder WB, Subramani S. Peroxisome remnants in pex3delta cells and the requirement of Pex3p for interactions between the peroxisomal docking and translocation subcomplexes. Traffic 2002; 3:560-74.

He C, Klionsky DJ. Regulation mechanisms and signaling pathways of autophagy. Annu Rev Genet 2009; 43:67-93.

Hoepfner D, Schildknegt D, Braakman I, Philippsen P, Tabak HF. Contribution of the endoplasmic reticulum to peroxisome formation, Cell 2005; 122;85–95.

Hu J, Desai M. Light control of peroxisome proliferation during Arabidopsis photomorphogenesis. Plant Signal Behav 2008; 3:801-3.

Hunt JE, Trelease RN. Sorting pathway and molecular targeting signals for the Arabidopsis peroxin 3. Biochem Biophys Res Commun 2004; 314:586-96.

Hutchins MU, Veenhuis M, Klionsky DJ. Peroxisome degradation in *Saccharomyces cerevisiae* is dependent on machinery of macroautophagy and the Cvt pathway. J Cell Sci 1999; 112:4079–4087.

Ichimura Y, Kirisako T, Takao T, Satomi Y, Shimonishi Y, Ishihara N, Mizushima N, Tanida I, Kominami E, Ohsumi M, Noda T, Ohsumi Y. A ubiquitin-like system mediates protein lipidation. Nature 2000; 408:488–492.

Issemann I, Green S. Activation of a member of the steroid hormone receptor superfamily by peroxisome proliferators. Nature 1990; 347: 645–50.

Itoh R, Fujiki Y. Functional domains and dynamic assembly of the peroxin Pex14p, the entry site of matrix proteins. J Biol Chem 2006; 281:10196-10205.

Iwata J, Ezaki J, Komatsu M, Yokota S, Ueno T, Tanida I, Chiba T, Tanaka K, Kominami E. Excess peroxisomes are degraded by autophagic machinery in mammals. J Biol Chem 2006; 281:4035-41.

Jäger S, Bucci C, Tanida I, Ueno T, Kominami E, Saftig P, Eskelinen EL. Role for Rab7 in maturation of late autophagic vacuoles. J Cell Sci 2004; 117:4837-48.

Jahreiss L, Menzies FM, Rubinsztein DC. The itinerary of autophagosomes: from peripheral formation to kiss-and-run fusion with lysosomes. Traffic 2008; 9:574-87.

Jansen S, Cashman K, Thompson JG, Pantaleon M, Kaye PL. Glucose deprivation, oxidative stress and peroxisome proliferator-activated receptor-alpha (PPARA) cause peroxisome proliferation in preimplantation mouse embryos. Reproduction 2009; 138:493-505.

Johnson MA, Snyder WB, Cereghino JL, Veenhuis M, Subramani S, Cregg JM. *Pichia pastoris* Pex14p, a phosphorylated peroxisomal membrane protein, is part of a PTS-receptor docking complex and interacts with many peroxins. Yeast. 2001; 18:621-641.

Jones JM, Morrell JC, Gould SJ. PEX19 is a predominantly cytosolic chaperone and import receptor for class 1 peroxisomal membrane proteins. J Cell Biol 2004;164:57-67.

Juhasz G, Neufeld TP. Autophagy: a forty-year search for a missing membrane source. PLoS Biol 2006; 4:e36.

Kabeya Y, Mizushima N, Yamamoto A, Oshitani-Okamoto S, Ohsumi Y, Yoshimori T. LC3, GABARAP and GATE16 localize to autophagosomal membrane depending on form-II formation. J Cell Sci 2004; 117:2805–2812.

Kamada Y, Yoshino K, Kondo C, Kawamata T, Oshiro N, Yonezawa K, Ohsumi Y. Tor directly controls the Atg1 kinase complex to regulate autophagy. Mol Cell Biol 2010; 30:1049-58.

Kanki T, Klionsky DJ. Atg32 is a tag for mitochondria degradation in yeast. Autophagy 2009; 5:1201-2.

Kiel JA, Komduur JA, van der Klei IJ, Veenhuis M. Macropexophagy in *Hansenula polymorpha*: facts and views. FEBS Lett 2003; 549:1-6.

Kiel JA, Veenhuis M, van der Klei IJ. *PEX* genes in fungal genomes: common, rare or redundant. Traffic 2006; 7:1291-303.

Kihara A, Noda T, Ishihara N, Ohsumi Y. Two distinct Vps34 phosphatidylinositol 3-kinase complexes function in autophagy and carboxypeptidase Y sorting in *Saccharomyces cerevisiae*. J Cell Biol 2001; 152:519-30.

Kim PK, Mullen RT, Schumann U, Lippincott-Schwartz J. The origin and maintenance of mammalian peroxisomes involves a de novo PEX16-dependent pathway from the ER. J Cell Biol 2006;173:521-532.

Kirisako T, Baba M, Ishihara N, Miyazawa K, Ohsumi M, Yoshimori T, Noda T, Ohsumi Y. Formation process of autophagosome is traced with Apg8/Aut7p in yeast. J Cell Biol 1999; 147:435-46.

Klionsky DJ, Cuervo AM, Dunn WA Jr, Levine B, van der Klei I, Seglen PO. How shall I eat thee? Autophagy 2007; 3:413-6.

Knoblach B, Rachubinski RA. Phosphorylation-dependent activation of peroxisome proliferator protein PEX11 controls peroxisome abundance. J Biol Chem 2010; 285:6670-6680.

Koek A, Komori M, Veenhuis M, van der Klei IJ. A comparative study of peroxisomal structures in *Hansenula polymorpha pex* mutants. FEMS Yeast Res 2007; 7:1126-1133.

Komori M, Kiel JA, Veenhuis M. The peroxisomal membrane protein Pex14p of *Hansenula polymorpha* is phosphorylated in vivo. FEBS Lett 1999; 457:397-399.

Kon M, Cuervo AM. Chaperone-mediated autophagy in health and disease. FEBS Lett 2010; 584:1399-404.

Kraft C, Deplazes A, Sohrmann M, Peter M. Mature ribosomes are selectively degraded upon starvation by an autophagy pathway requiring the Ubp3p/Bre5p ubiquitin protease. Nat Cell Biol 2008; 10:602-10.

Kristensen AR, Schandorff S, Høyer-Hansen M, Nielsen MO, Jäättelä M, Dengjel J, Andersen JS. Ordered organelle degradation during starvation-induced autophagy. Mol Cell Prot 2008; 7:2419-28.

Kuravi K, Nagotu S, Krikken AM, Sjollema K, Deckers M, Erdmann R, Veenhuis M, van der Klei IJ. Dynamin-related proteins Vps1p and Dnm1p control peroxisome abundance in Saccharomyces cerevisiae. J Cell Sci 2006;119:3994-4001.

Kurbatova E, Otzen M, van der Klei IJ. p24 proteins play a role in peroxisome proliferation in yeast. FEBS Lett 2009; 583:3175-80.

Kurochkin IV, Mizuno Y, Konagaya A, Sakaki Y, Schönbach C, Okazaki Y. Novel peroxisomal protease Tysnd1 processes PTS1- and PTS2-containing enzymes involved in beta-oxidation of fatty acids. EMBO J 2007; 26:835-45.

Leao-Helder AN, Krikken AM, van der Klei IJ, Kiel JA, Veenhuis M. Transcriptional down-regulation of peroxisome numbers affects selective peroxisome degradation in *Hansenula polymorpha*. J Biol Chem 2003; 278:40749-56.

Lin-Cereghino GP, Godfrey L, de la Cruz BJ, Johnson S, Khuongsathiene S, Tolstorukov I, Yan M, Lin-Cereghino J, Veenhuis M, Subramani S, Cregg JM. Mxr1p, a key regulator of the methanol utilization pathway and peroxisomal genes in *Pichia pastoris*. Mol Cell Biol 2006; 26:883-97.

Loew O. A New Enzyme of General Occurrence in Organisms. Science 1900; 279:701–2.

Mandard S, Müller M, Kersten S. Peroxisome proliferator-activated receptor α target genes. Cell Mol Life Sci 2004; 61:393-416.

Manjithaya R, Nazarko TY, Farré JC, Subramani S. Molecular mechanism and physiological role of pexophagy. FEBS Lett 2010; 584:1367-73.

Matsuzaki T, Fujiki Y. The peroxisomal membrane protein import receptor Pex3p is directly transported to peroxisomes by a novel Pex19p- and Pex16p-dependent pathway. J Cell Biol 2008; 183:1275-86.

Meijer WH, van der Klei IJ, Veenhuis M, Kiel JA. ATG genes involved in non-selective autophagy are conserved from yeast to man, but the selective Cvt and pexophagy pathways also require organism-specific genes. Autophagy 2007; 3:106-16.

Meinecke M, Cizmowski C, Schliebs W, Krüger V, Beck S, Wagner R, Erdmann R. The peroxisomal importomer constitutes a large and highly dynamic pore. Nat Cell Biol 2010; 12:273-7.

Mercado JJ, Vincent O, Gancedo JM. Regions in the promoter of the yeast FBP1 gene implicated in catabolite repression may bind the product of the regulatory gene MIG1. FEBS Lett 1991; 291:97–100.

Mizushima N, Noda T, Yoshimori T, Tanaka Y, Ishii T, George MD, Klionsky DJ, Ohsumi M, Ohsumi Y. A protein conjugation system essential for autophagy. Nature 1998; 395:395-8.

Mizushima N, Levine B, Cuervo AM, Klionsky DJ. Autophagy fights disease through cellular self-digestion. Nature. 2008; 451:1069-75.

Mizushima N. The role of the Atg1/ULK1 complex in autophagy regulation. Curr Opin Cell Biol 2010; 22:132-9.

Monastyrska I, van der Heide M, Krikken AM, Kiel JA, van der Klei IJ, Veenhuis M. Atg8 is essential for macropexophagy in *Hansenula polymorpha*. Traffic 2005a;6:66-74.

Monastyrska I, Kiel JA, Krikken AM, Komduur JA, Veenhuis M, van der Klei IJ. The *Hansenula polymorpha ATG25* gene encodes a novel coiled-coil protein that is required for macropexophagy. Autophagy 2005b;1:92-100.

Motley AM, EH Hettema EH. Yeast peroxisomes multiply by growth and division. J Cell Biol 2007; 178:399-410.

Motley AM, Ward GP, Hettema EH. Dnm1p-dependent peroxisome fission requires Caf4p, Mdv1p and Fis1p. J Cell Sci 2008; 121:1633-40.

Mukaiyama H, Baba M, Osumi M, Aoyagi S, Kato N, Ohsumi Y, Sakai Y. Modification of a ubiquitin-like protein Paz2 conducted micropexophagy through formation of a novel membrane structure. Mol Biol Cell 2004; 15:58-70.

Mullen RT, Trelease RN. The ER-peroxisome connection in plants: development of the "ER semi-autonomous peroxisome maturation and replication" model for plant peroxisome biogenesis. Biochim Biophys Acta 2006; 1763:1655-1668.

Nagotu S, Saraya R, Otzen M, Veenhuis M, van der Klei IJ. Peroxisome proliferation in *Hansenula polymorpha* requires Dnm1p which mediates fission but not de novo formation. Biochim Biophys Acta 2008;1783**:**760-9.

Nagotu S, Veenhuis M, van der Klei IJ. Divide et impera: the dictum of peroxisomes. Traffic 2010; 11:175-84.

Nakatogawa H, Ichimura Y, Ohsumi Y. Atg8, a ubiquitin-like protein required for autophagosome formation, mediates membrane tethering and hemifusion. Cell 2007; 130:165-78.

Nazarko TY, Polupanov AS, Manjithaya RR, Subramani S, Sibirny AA. The requirement of sterol glucoside for pexophagy in yeast is dependent on the species and nature of peroxisome inducers. Mol Biol Cell 2007; 18:106-18.

Nehlin JO, Ronne H. Yeast MIG1 repressor is related to the mammalian early growth response and Wilms' tumour finger proteins. EMBO J 1990; 9:2891–2898.

Neufeld C, Filipp FV, Simon B, Neuhaus A, Schüller N, David C, Kooshapur H, Madl T, Erdmann R, Schliebs W, Wilmanns M, Sattler M. Structural basis for competitive interactions of Pex14 with the import receptors Pex5 and Pex19. EMBO J 2009; 28:745-54

Neuspiel M, Schauss AC, Braschi E, Zunino R, Rippstein P, Rachubinski RA, Andrade-Navarro MA, McBride HM. Cargo-Selected Transport from the Mitochondria to Peroxisomes Is Mediated by Vesicular Carriers. Curr Biol 2008; 18:102-108.

Noda NN, Ohsumi Y, Inagaki F. Atg8-family interacting motif crucial for selective autophagy. FEBS Lett 2010; 584:1379-85.

Oku M, Warnecke D, Noda T, Müller F, Heinz E, Mukaiyama H, Kato N, Sakai Y. Peroxisome degradation requires catalytically active sterol glucosyltransferase with a GRAM domain. EMBO J 2003; 22:3231-41.

Otera H, Setoguchi K, Hamasaki M, Kumashiro T, Shimizu N, Fujiki Y. Peroxisomal targeting signal receptor Pex5p interacts with cargoes and import machinery components in a spatiotemporally differentiated manner: conserved Pex5p WXXXF/Y motifs are critical for matrix protein import. Mol Cell Biol 2002; 22:1639–1655.

Ozimek P, Lahtchev K, Kiel JAKW, Veenhuis M, Klei IJ: *Hansenula polymorpha* Swi1 and Snf2 are essential for methanol utilisation. FEMS Yeast Res 2004; 4:673-682.

Pattingre S, Tassa A, Qu X, Garuti R, Liang XH, Mizushima N, Packer M, Schneider MD, Levine B. Bcl-2 antiapoptotic proteins inhibit Beclin 1-dependent autophagy. Cell 2005; 122:927-939.

Perry RJ, Mast FD, Rachubinski RA. Endoplasmic reticulum-associated secretory proteins Sec20p, Sec39p, and Dsl1p are involved in peroxisome biogenesis. Eukaryot Cell 2009; 8:830-843.

Platta HW, El Magraoui F, Bäumer BE, Schlee D, Girzalsky W, Erdmann R. Pex2 and pex12 function as protein-ubiquitin ligases in peroxisomal protein import. Mol Cell Biol 2009; 29:5505-16.

Raychaudhuri S, Prinz WA. Nonvesicular phospholipid transfer between peroxisomes and the endoplasmic reticulum. Proc Natl Acad Sci 2008; 105:15785-15790.

Ratnakumar S, Young ET. Snf1 dependence of peroxisomal gene expression is mediated by Adr1. J Biol Chem 2010; 285:10703-14.

Reggiori F, Monastyrska I, Shintani T, Klionsky DJ. The actin cytoskeleton is required for selective types of autophagy, but not nonspecific autophagy, in the yeast *Saccharomyces cerevisiae*. Mol Biol Cell 2005; 16:5843-56.

Rolland F, Winderickx J, Thevelein JM. Glucose-sensing and –signalling mechanisms in yeast. FEMS Yeast Res 2002; 2:183-201.

Sakai Y, Koller A, Rangell LK, Keller GA, Subramani S. Peroxisome degradation by microautophagy in *Pichia pastoris*: identification of specific steps and morphological intermediates. J Cell Biol 1998; 141:625-36.

Sarry J-E, Chen S, Collum RP, Liang S, Mingsheng Peng, Lang A, Naumann B, Dzierszinski F, Yuan C-X, Hippler M, Rea PA. Analysis of the vacuolar luminal proteome of *Saccharomyces cerevisiae*. FEBS J 2007; 274:4287-4305.

Sasano Y, Yurimoto H, Yanaka M, Sakai Y. Trm1p, a Zn(II)2Cys6-type transcription factor, is a master regulator of methanol-specific gene activation in the methylotrophic yeast *Candida boidinii*. Eukaryot Cell 2008;7:527-36.

Sasano Y, Yurimoto H, Kuriyama M, Sakai Y. Trm2p-dependent derepression is essential for methanol-specific gene activation in the methylotrophic yeast *Candida boidinii*. FEMS Yeast Res 2010 Apr 29. Epub ahead of print.

Schekman R. Peroxisomes: another branch of the secretory pathway? Cell 2005;122:1-2.

Schwartz AL, Ciechanover A. Targeting proteins for destruction by the ubiquitin system: implications for human pathobiology. Annu Rev Pharmacol Toxicol. 2009; 49:73-96.

Scott SV, Guan J, Hutchins MU, Kim J, Klionsky DJ. Cvt19 is a receptor for the cytoplasm-to-vacuole targeting pathway. Mol Cell 2001; 7:1131-1141.

Shintani T, Klionsky DJ. Cargo proteins facilitate the formation of transport vesicles in the cytoplasm to vacuole targeting pathway. J Biol Chem 2004; 279:29889–29894.

Shpetner HS, Vallee RB. Identification of dynamin, a novel mechanochemical enzyme that mediates interactions between microtubules. Cell 1989; 59:421-32.

Smith JJ, Marelli M, Christmas RH, Vizeacoumar FJ, Dilworth DJ, Ideker T, Galitski T, Dimitrov K, Rachubinsky RA, Aitchison JD. Transcriptome profiling to identify genes involved in peroxisome assembly and function. J Cell Biol 2002; 158:259-271.

Stasyk OV, Stasyk OG, Mathewson RD, Farré JC, Nazarko VY, Krasovska OS, Subramani S, Cregg JM, Sibirny AA. Atg28, a novel coiled-coil protein involved in autophagic degradation of peroxisomes in the methylotrophic yeast *Pichia pastoris*. Autophagy 2006; 2:30-8.

Stevens P, Monastyrska I, Leão-Helder AN, van der Klei IJ, Veenhuis M, Kiel JA. *Hansenula polymorpha* Vam7p is required for macropexophagy. FEMS Yeast Res 2005; 5:985-97.

Sugawara K, Suzuki NN, Fujioka Y, Mizushima N, Ohsumi Y, Inagaki F. The crystal structure of microtubule-associated protein light chain 3, a mammalian homologue of *Saccharomyces cerevisiae* Atg8. Genes Cells 2004; 9:611-8.

Suzuki NN, Yoshimoto K, Fujioka Y, Ohsumi Y, Inagaki F. The crystal structure of plant ATG12 and its biological implication in autophagy. Autophagy 2005; 1:119–126.

Taguchi-Atarashi N, Hamasaki M, Matsunaga K, Omori H, Ktistakis NT, Yoshimori T, Noda T. Modulation of local PtdIns3P levels by the PI phosphatase MTMR3 regulates constitutive autophagy. Traffic 2010; 11:468-78.

Thoms S, Erdmann R. Peroxisomal matrix protein receptor ubiquitination and recycling. Biochim Biophys Acta 2006; 1763:1620-8.

Todde V, Veenhuis M, van der Klei IJ. Autophagy: principles and significance in health and disease. Biochim Biophys Acta 2009; 1792:3-13.

Treitel MA, Kuchin S, Carlson M. Snf1 protein kinase regulates phosphorylation of the Mig1 repressor in *Saccharomyces cerevisiae*. Mol Cell Biol 1998;18:6273-80.

Tuttle DL, Dunn WA. Divergent modes of autophagy in the methylotrophic yeast *Pichia pastoris*. J Cell Sci 1995; 108:25-35.

Vallier LG, Carlson M. Synergistic release from glucose repression by mig1 and ssn mutations in *Saccharomyces cerevisiae*. Genetics 1994; 137:49-54.

Van der Klei IJ, Yurimoto H, Sakai Y, Veenhuis M. The significance of peroxisomes in methanol methabolism in methylotrophic yeast. Biochem Biophys Act 2006; 1763:1453-1462.

Van der Vaart A, Griffith J, Reggiori F. Exit from the Golgi Is Required for the Expansion of the Autophagosomal Phagophore in Yeast *Saccharomyces cerevisiae*. Mol Biol Cell. 2010 Epub ahead of print.

Van der Zand A, Braakman I, Tabak HF. Peroxisomal membrane proteins insert into the endoplasmic reticulum. Mol Biol Cell 2010; 21:2057-65.

Van Leyen K, Duvoisin RM, Engelhardt H, Wiedmann M. A function for lipoxygenase in programmed organelle degradation. Nature 1998; 395:392-5.

Van Zutphen T, Baerends RJ, Susanna KA, de Jong A, Kuipers OP, Veenhuis M, van der Klei IJ. Adaptation of *Hansenula polymorpha* to methanol: a transcriptome analysis. BMC Genomics 2010; 11:1.

Veenhuis M, Zwart K, Harder W. Degradation of peroxisomes after transfer of methanol-grown *Hansenula polymorpha* into glucose-containing media. Arch Microbiol 1983; 134:193-203.

Villén J, Beausoleil SA, Gerber SA, Gygi SP. Large-scale phosphorylation analysis of mouse liver. Proc Natl Acad Sci 2007; 104:1488-1493.

Wanders RJ. Metabolic and molecular basis of peroxisomal disorders: a review. Am J Med Genet A 2004; 126:355-75.

Wanders RJA, Waterham HR. Biochemistry of mammalian peroxisomes revisited. Annu Rev Biochem 2006; 75:295-332.

Wang L, Seeley ES, Wickner W, Merz AJ. Vacuole fusion at a ring of vertex docking sites leaves membrane fragments within the organelle. Cell 2002; 108:357-369.

Webber JL, Tooze SA. New insights into the function of Atg9. FEBS Lett 2010a; 584:1319-1326.

Webber JL, Tooze SA. Coordinated regulation of autophagy by p38alpha MAPK through mAtg9 and p38IP. EMBO J 2010b; 29:27-40.

Wickner W, Schekman R. Membrane fusion. Nat Struct Mol Biol 2008; 15:658-64.

Williams C, van den Berg M, Geers E, Distel B. Pex10p functions as an E3 ligase for the Ubc4p-dependent ubiquitination of Pex5p. Biochem Biophys Res Commun 2008; 374:620-624.

Wood CS, Koepke JI, Teng H, Boucher KK, Katz S, Chang P, Terlecky LJ, Papanayotou I, Walton PA, Terlecky SR. Hypocatalasemic fibroblasts accumulate hydrogen peroxide and display age-associated pathologies. Traffic 2006; 7:97-107.

Wullschleger S, Loewith R, Hall MN. TOR Signaling in Growth and Metabolism. Cell 2006; 124:471-484.

Xie Z, Klionsky DJ. Autophagosome formation: core machinery and adaptations. Nat Cell Biol 2007; 9:1102-9.

Xie Z, Nair U, Geng J, Szefler MB, Rothman ED, Klionsky DJ. Indirect estimation of the area density of Atg8 on the phagophore. Autophagy 2009; 5:217-20.

Yamashita S, Oku M, Wasada Y, Ano Y, Sakai Y. PI4P-signaling pathway for the synthesis of a nascent membrane structure in selective autophagy. J Cell Biol 2006; 173:709-17.

Yang Z, Huang J, Geng J, Nair U, Klionsky DJ. Atg22 recycles amino acids to link the degradative and recycling functions of autophagy. Mol Biol Cell 2006; 17:5094-5104.

Yang Z, Geng J, Yen W-L, Wang K, Klionsky DJ. Positive or Negative Roles of Different Cyclin-dependent kinase Pho85-cyclin complexes orchestrate induction of autophagy in *Saccharomyces cerevisiae*. Mol Cell 2010; 38:250–264.

Zipor G, Haim-Vilmovsky L, Gelin-Licht R, Gadir N, Brocard C, Gerst JE. Localization of mRNAs coding for peroxisomal proteins in the yeast, *Saccharomyces cerevisiae*. Proc Natl Acad Sci 2009;106:19848-53.

Chapter 2

Adaptation of *Hansenula polymorpha* to methanol: a transcriptome analysis

Tim van Zutphen[1], Richard JS Baerends[1], Kim A Susanna[1], Anne de Jong[2], Oscar P Kuipers[2], Marten Veenhuis[1,3] and Ida J van der Klei[1,3]

[1]Molecular Cell Biology, University of Groningen, Haren, the Netherlands; [2]Molecular Genetics, University of Groningen, Haren, the Netherlands; [3]Kluyver Centre for Genomics of Industrial Fermentation, P.O. Box 5057, 2600 GA Delft, the Netherlands

Published in *BMC GENOMICS 2010; 11:1.*

Abstract

Background

Methylotrophic yeast species (e.g. *Hansenula polymorpha*, *Pichia pastoris*) can grow on methanol as sole source of carbon and energy. These organisms are important cell factories for the production of recombinant proteins, but are also used in fundamental research as model organisms to study peroxisome biology. During exponential growth on glucose, cells of *H. polymorpha* typically contain a single, small peroxisome that is redundant for growth while on methanol multiple, enlarged peroxisomes are present. These organelles are crucial to support growth on methanol, as they contain key enzymes of methanol metabolism.

In this study, changes in the transcriptional profiles during adaptation of *H. polymorpha* cells from glucose- to methanol-containing media were investigated using DNA-microarray analyses.

Results

Two hours after the shift of cells from glucose to methanol nearly 20% (1184 genes) of the approximately 6000 annotated *H. polymorpha* genes were significantly upregulated with at least a two-fold differential expression. Highest upregulation (> 300-fold) was observed for the genes encoding the transcription factor Mpp1 and formate dehydrogenase, an enzyme of the methanol dissimilation pathway.

Upregulated genes also included genes encoding other enzymes of methanol metabolism as well as of peroxisomal β-oxidation.
A moderate increase in transcriptional levels (up to 4-fold) was observed for several *PEX* genes, which are involved in peroxisome biogenesis. Only *PEX11* and *PEX32* were higher upregulated. In addition, an increase was observed in expression of the several *ATG* genes, which encode proteins involved in autophagy and autophagy processes. The strongest upregulation was observed for *ATG8* and *ATG11*. Approximately 20% (1246 genes) of the genes were downregulated. These included glycolytic genes as well as genes involved in transcription and translation.

Conclusion

Transcriptional profiling of *H. polymorpha* cells shifted from glucose to methanol showed the expected downregulation of glycolytic genes together with upregulation of the methanol utilisation pathway. This serves as a confirmation and validation of the array data obtained. Consistent with this, also various *PEX* genes were upregulated. The strong upregulation of *ATG* genes is possibly due to induction of autophagy processes related to remodeling of the cell architecture required to support growth on methanol. These processes may also be responsible for the enhanced peroxisomal β-oxidation, as autophagy leads to recycling of membrane lipids. The prominent downregulation of transcription and translation may be explained by the reduced growth rate on methanol (td glucose 1 h vs td methanol 4.5 h).

Background

Hansenula polymorpha is an important cell factory for the production of pharmaceutical proteins[1]. Moreover, it is extensively used in fundamental research aiming at understanding the molecular principles of peroxisome biology[2].

As cell factory, *H. polymorpha* has several important advantages. First, it contains very strong and inducible promoters derived from the methanol metabolism pathway. Also, the organism is thermotolerant (it can grow at high temperatures up to 48°C),[3] and tolerates various environmental stresses. *H. polymorpha* does not hyperglycosylate secreted proteins, which often is a problem in heterologous protein production in *Saccharomyces cerevisiae*.

In *H. polymorpha* peroxisomes massively develop during growth on methanol as sole source of carbon and energy. Methanol is oxidized by the enzyme alcohol oxidase (AOX), which is localized in peroxisomes together with catalase and dihydroxyacetone synthase (DHAS), the first enzyme of the assimilation pathway. Peroxisomes are not required for primary metabolism when cells are grown on glucose. Moreover, glucose represses the key enzymes of methanol metabolism AOX and DHAS. Therefore, during growth on glucose *H. polymorpha* cells contain only a single, small peroxisome. Upon a shift to methanol media, the enzymes of methanol metabolism are induced paralleled by an increase in peroxisome size and abundance. The initial small peroxisome serves as the target organelle for the enzymes of methanol metabolism and proliferates by fission[4].

Ultimately, in exponentially growing cells, each cell contains several enlarged peroxisomes[5].

A wealth of information is now available of individual genes encoding enzymes of the methanol metabolism as well as on genes involved in peroxisome formation (*PEX* genes). However, genomics approaches in *H. polymorpha* are still rare.

We used genome-wide transcriptional profiling to dissect the initial events accompanying the adaptation of glucose grown *H. polymorpha* cells to methanol metabolism. This will gain information on the induction and repression of metabolic genes as well as on non-metabolic genes, including *PEX* genes.

Results and discussion

All experiments described in this paper were performed in batch cultures. We chose not to grow the cells in carbon-limited chemostats, as glucose-limitation results in derepression of genes involved in methanol metabolism[6].

H. polymorpha cells were extensively pre-cultivated in batch cultures on mineral media supplemented with glucose as sole carbon source in order to fully repress the enzymes of methanol metabolism. Glucose cultures in the late exponential growth phase were transferred to fresh mineral medium containing methanol as sole carbon and energy source. As shown in figure 1, RT-PCR indicated that the inoculum cells (from the glucose batch culture at the late exponential growth phase, OD660 nm 2.3) did not contain transcript of alcohol oxidase (AOX) or dihydroxyacetone synthase (DHAS), key enzymes of methanol metabolism. However, two hours after the shift to medium containing methanol, mRNAs of both genes were readily detected, a time-point which has also been identified as threshold for the detection of first AOX enzyme activity[5]. Therefore, 2 hours incubation on methanol was selected as sampling point of cells for transcriptome analysis.

Replicates were obtained by growing 4 independent cultures on glucose that were independently transferred to fresh media containing methanol. Of each culture, mRNA isolated from the glucose and the methanol sample was labeled (and dye-swapped) and hybridized on two arrays per culture.

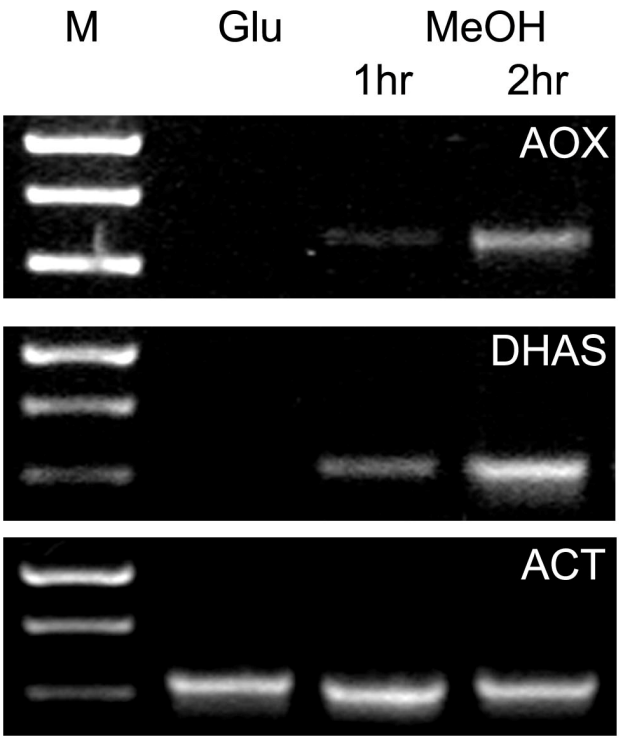

Figure 1. Transcript level of *AOX* and *DHAS*. RT-PCR was performed on RNA samples using *AOX* and *DHAS* primers from glucose containing precultures (OD 2,3), and cultures shifted for 1 or 2 hrs to methanol medium. As loading control transcript levels of actin (ACT) were analysed.

In addition, as a control *AOX* transcript levels of these samples were determined by RT-PCR, confirming the absence of transcript in the glucose-grown pre-cultures and the presence of *AOX* transcript after 2 hours incubation (data not shown).

Overview of the DNA microarray data

The DNA microarray analyses data were analyzed to generate the ratio between the transcripts on methanol and glucose for each gene to identify any differential expression and to determine the p-value to assess the significance and the A-value to check the intensity of the signals. [Additional file 1: Supplemental table S1] presents an overview of the array results.

Of the nearly 6000 annotated *H. polymorpha* genes that are listed, approximately 20% (1184 genes) are upregulated, while another 20% (1246 genes) are downregulated with at least a two-fold differential expression, meeting the significance and signal intensity criteria.

Of the upregulated genes, 13 are more than 100 times upregulated, 192 genes show a 10-100-fold upregulation, 156 genes increase between 5 and 10-fold and the remaining 823 genes are less than 5-fold upregulated. Highest upregulated are the central methanol metabolism regulator *MPP1* (394-fold, Hp27g360, see below) and the gene encoding formate dehydrogenase (347-fold), required in methanol catabolism. Also the other components of the methanol metabolic pathway are highly upregulated. Moreover, *CRC1* is highly induced, encoding a mitochondrial inner membrane carnitine transporter, which is required for the transport of acetyl-CoA from peroxisomes to mitochondria during fatty acid beta-oxidation (111-fold).
In line with *CRC1*, also the genes involved in the beta-oxidation of fatty acids are overrepresented among the highly upregulated genes (for details see below). Furthermore, approximately 13% of the more than 10-fold upregulated genes is involved in transport. The upregulation of hexose transporters may be important for the uptake of the residual glucose that was present in the inoculum.

Of the downregulated genes, the highest fold downregulation (65-fold) is observed for Hp24g956, encoding a protein with strong similarity to Sik1p of *S. cerevisiae*, which is involved in pre-rRNA processing.

This predicted function is consistent with the general trend among the downregulated genes, since of the 179 genes that are over 10-fold downregulated, nearly 50% code for products that function in either transcription or translation processes. Of the other downregulated genes, 269 show a 5- to 10-fold downregulation. Of these, nearly 40% encode proteins involved in transcription and translation. The other 789 genes are less than 5-fold reduced in transcript levels.

Functional overview DNA microarray data - FUNCATS

To obtain an overview of the functions of the differentially expressed genes, these were categorized according to the Functional Catalogue, FUNCAT[7,8]. In this system, each gene is classified in one or more groups, depending on its function.
The number of genes in each category is shown as the percentage of the total number of up- or downregulated genes in the diagrams shown in figure 2.
For comparison, a diagram showing the contribution of each functional category to the total number of genes in *H. polymorpha* is included. To construct this diagram, all known *H. polymorpha* genes are used; both up- and downregulated genes as well as non-regulated genes.

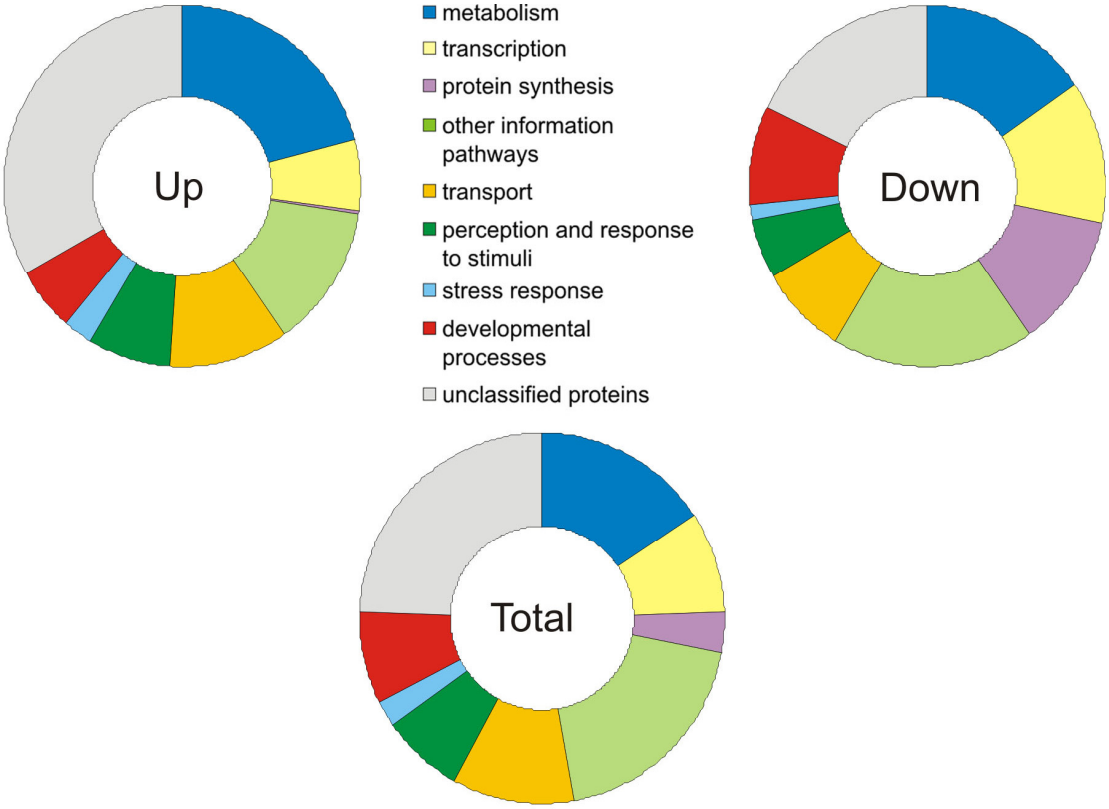

Figure 2. FUNCATS. Representation of functional groups among up- and downregulated genes is shown in a diagram. For comparison, a similar diagram is made for the total number of genes in Hansenula polymorpha (up-, down- and non-regulated genes). Genes are classified in one or multiple groups based on the Functional Catalogue.

As expected, genes involved in metabolic pathways strongly contribute to both the up- and downregulated genes (20% and 15.5%, respectively), reflecting the large-scale adaptations accompanying the shift from glucose to methanol. However, metabolism is a large group also in the total genome and the contribution in percentages does not reflect the nature of the metabolic pathways that are regulated (see below).

In contrast to metabolism, some other functional categories display a difference in contribution to the upregulated compared to the downregulated genes. One such functional category is the group of protein synthesis genes, which is almost absent among upregulated genes (0.25%), while it composes a large portion of the downregulated genes (12.1%). Of the total genome of *H. polymorpha* only approximately 4% is involved in protein synthesis, reflecting the considerable effect of a shift to methanol on protein synthesis. In addition, also the group of genes involved in transcription is more predominant among downregulated genes (12.7% versus 6.3% of the upregulated genes and an intermediate 9% of the total genome). In concurrence with the trend of genes related to transcription and translation, also genes related to nucleotide biosynthesis are mostly downregulated (42 of 51 genes), yet genes involved in amino acid biosynthesis show a less clear trend (30 down-, 9 upregulated, 54 not differentially expressed). The observed downregulation of major anabolic processes most likely is related to the reduction in doubling time (td of cells on methanol relative to growth on glucose (td methanol = 4.5 h, td glucose = 1 h) and may reflect the accompanying decrease in DNA replication, RNA transcription and translation.

Stress response genes form only relatively small categories among both the upregulated genes relative to the downregulated genes (2.9% vs 1.6%). Based on the Functional Catalogue, only 185 of the nearly 6000 annotated *H. polymorpha* genes are indicated as stress response genes.

However, based on several studies by Gasch in *S. cerevisiae*[9-11], many more genes could contribute to the cellular stress response. Hence, most likely also genes classified in other groups play a role in coping with stress accompanying a shift in cultivation conditions. Thus, the contribution of the stress response to the total differential expression in *H. polymorpha* upon transfer to methanol medium is probably larger than the observed 2.9% upregulation and 1.6% downregulation.

A last remarkable group in the Functional Catalogue diagram is the category of unclassified proteins, showing that 33% of the upregulated genes and 17.9% of the downregulated genes are thus far not experimentally characterized, relative to 25% of the genes of the total genome of *H. polymorpha*. This observation suggests that our current knowledge on adaptation to methanol is far from complete.

Metabolic pathways - upregulation of methanol metabolism

As expected, genes involved in methanol metabolism are highly upregulated. In figure 3 an overview of the methanol metabolism, including the microarray data, is presented[2]. In peroxisomes, methanol is oxidized to formaldehyde and hydrogen peroxide by alcohol oxidase (AOX), which is 17.3 times upregulated at the transcriptional level. The hydrogen peroxide is detoxified by catalase (CAT) to water and oxygen (42.8-fold upregulated).

Formaldehyde can be further metabolized via two different routes: 1) dissimilation via formaldehyde dehydrogenase (FLD1, 8.4-fold up), S-formyl glutathione hydrolase (FGH, 2.2-fold up) and formate dehydrogenase (FMD, 347-fold up) to CO2, generating NADH and CO2 or 2) assimilation via the peroxisome-borne enzyme dihydroxyacetone synthase (DHAS, 19,0-fold up) to generate cell constituents. DHAS is part of the xylulose-5-phosphate cycle and catalyzes the formation of two C3-molecules (dihydroxyacetone and glyceraldehyde-3-phosphate) from one C1 (formaldehyde) and one C5 compound (xylulose-5-phosphate) [2].

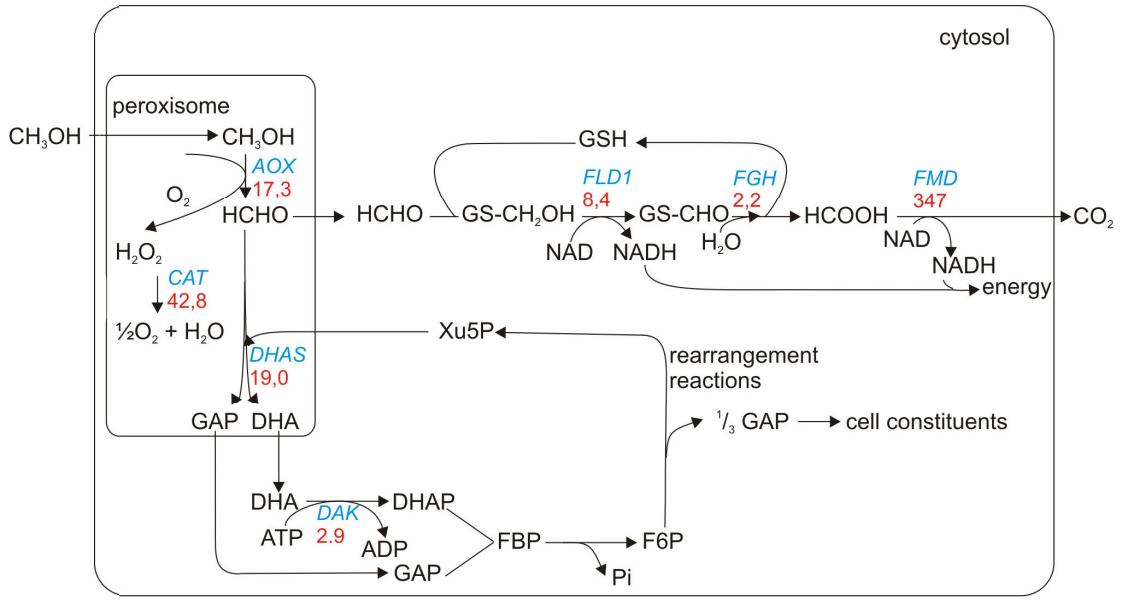

Figure 3. Methanol metabolism. Overview of the methanol metabolism in *H. polymorpha*. The fold upregulation of the indicated genes is shown in red. GAP: glyceraldehyde-3-phosphate; DHA: dihydroxyacetone; DHAP: dihydroxyacetone phosphate; FBP: fructose bisphosphate; F6P: fructose-6-phosphate; XU5P: xylulose-5-phosphate; GSH: reduced glutathione; GS-CH2OH: S-hydroxymethylglutathione; GS-CHO: S-formylglutathione. *AOX*: alcohol oxidase; *CAT*: catalase; *DHAS*: dihydroxyacetone synthase; *DAK*: dihydroxyacetone kinase; *FLD*: formaldehyde dehydrogenase; *FGH*: S-formyl glutathione hydrolase and *FMD*: formate dehydrogenase.

Promoter studies in *Candida boidinii* using phosphatase as a reporter enzyme revealed that upon a shift to methanol medium FMD was induced first, followed by DHAS and even later AOX[12]. The early induction of FMD (347-fold up 2 hours after the shift to methanol medium) relative to AOX and DHAS (17.3-, 19-fold up respectively) suggests that a similar induction pattern may exist in *H. polymorpha*. The differences in induction of the genes 2 hours after the shift to methanol medium does not reflect the ultimate protein levels in the cells, as AOX and DHAS are the major protein bands in extracts prepared from methanol grown *H. polymorpha* cells[12,13].

PEX genes

PEX genes control the development and function of a specialized class of organelles, the peroxisomes. Most of the PEX genes showed a moderate induction upon the shift to methanol (up to 4-fold; Table 1). This is in line with earlier studies of *S. cerevisiae* cells that were shifted from glucose to the peroxisome-inducing carbon source oleate[14,15].

Of the *PEX* genes involved in import of peroxisomal matrix enzymes (AOX, DHAS and CAT), the highest upregulation was observed for *PEX1, PEX4, PEX5, PEX13, PEX14* and *PEX26*, which all encode key components of the PTS1 protein import machinery[16].

Highest upregulation was observed for *PEX11* (4.7-fold) and *PEX32* (4.8-fold). Pex11p, together with Pex25p and Pex11cp, are the three members of the Pex11p protein family in *H. polymorpha*[16].

Table 1. Expression changes of *PEX* genes

***PEX* genes**		**Ratio**
Hp46g103	*PEX1*	2.9
Hp24g603	*PEX2*	1.7
Hp47g896	*PEX3*	1.5
Hp13g30	*PEX4*	3.1
Hp28g69	*PEX5*	3.3
Hp33g316	*PEX6*	1.6
Hp15g912	*PEX7*	1.8
Hp27g144	*PEX8*	1.7
Hp6g229	*PEX10*	1.6
Hp24g562	*PEX11*	4.7
Hp5g555	*PEX11C*	-1.6
Hp39g539	*PEX12*	2.6
Hp32g232	*PEX13*	3.0
Hp24g522	*PEX14*	3.5
Hp14g184	*PEX17*	2.1
Hp9g314	*PEX19*	1.1
Hp11g43	*PEX20*	1.0
Hp37g108	*PEX22*	-1.3
Hp39g248	*PEX23*	1.2
Hp25g249	*PEX23-like*	-1.2
Hp47g626	*PEX24*	2.9
Hp16g88	*PEX25*	2.2
Hp15g17	*PEX26*	3.6
Hp29g7	*PEX29*	-1.2
Hp27g236	*PEX32*	4.8

All genes shown have a p-value below 0.05. Negative values indicate downregulation on methanol, positive values indicate upregulation on methanol.

These proteins are implicated in regulating peroxisome proliferation. Also in bakers' yeast cells shifted from glucose to oleic acid medium *PEX11* increased by far the most[14].
H. polymorpha PEX25 was upregulated 2.2-fold, whereas *PEX11C*, whose function is still unknown, showed a 1.6-fold downregulation[16].

Pex32p is a member of the Pex23 protein family, a group of membrane proteins with unknown function[16]. *Yarrowia lipolytica pex23* mutants cannot grow on oleate and partially mislocalize peroxisomal proteins to the cytosol, suggesting a role in matrix protein import.
In contrast however, *S. cerevisiae* Pex23p, Pex31p and Pex32p are not required for protein import but play a role in peroxisome proliferation. Where ScPex23p appears to be a positive regulator of peroxisome size, ScPex31p and ScPex32p have been suggested to negatively regulate this process. The function of *H. polymorpha* Pex32p is not yet known. Based on our current study this protein may be, together with Pex11p, responsible for the initial increase in size of the peroxisomes, as was observed by detailed ultrastructural analysis (figure 4, below) and in concurrence with earlier findings[5]. The relative high induction of this peroxin makes it an interesting candidate for further study in *H. polymorpha*.

Metabolic pathways - downregulation of glucose utilisation

As depicted in Table 2, the majority of the genes involved in glycolysis are downregulated (-1.2 to -5.7). Since the genes are listed in order of appearance in the pathway, it is evident that the strongest downregulation is observed in the steps before fructose 1,6 bisphosphate aldolase. This corresponds with the fact that the products of methanol metabolism, dihydroxyacetone and glyceraldehyde 3 phosphate, enter the glycolytic pathway directly after this step, so the subsequent enzymes are still required for progression with the pathway towards the TCA cycle.

Table 2 Expression changes of glycolysis and gluconeogenesis genes

Gene	Function	Ratio
Glycolysis		
Hp25g374	Hexokinase	- 5.7
Hp24g239	Glucokinase	- 2.3
Hp33g380	Glucose-6-phosphate isomerase	- 1.7
Hp1g417	Phosphofructokinase alpha subunit	- 2.9
Hp39g214	Phosphofructokinase beta subunit	- 2.0
Hp47g1019	Fructose 1,6-bisphosphate aldolase	+ 2.1
Hp16g222	Triosephosphate isomerase	- 1.5
Hp25g306	Glyceraldehyde-3-phosphate dehydrogenase	- 1.4
Hp26g207	3-phosphoglycerate kinase	- 1.3
Hp37g8	Phosphoglycerate mutase	+ 1.2*
Hp27g405	Phosphopyruvate hydratase (enolase)	- 1.7
Hp39g227	Pyruvate kinase	- 1.2
Hp6g262	Pyruvate dehydrogenase, alpha subunit	- 1.3
Hp37g184	Pyruvate dehydrogenase, beta subunit	- 1.8
Gluconeogenesis		
Hp18g102	Pyruvate carboxylase	+ 1.9
Hp5g547	Phosphoenolpyruvate carboxykinase	+ 8.9
Hp46g88	Fructose 1,6 bisphosphatase	+ 4.4

*With the exception of the one marked with an asterisk, all genes shown have a p-value below 0.05. Negative values indicate downregulation on methanol, positive values indicate upregulation on methanol.

The observed mild decrease in expression of their encoding genes can be attributed to the reduction in the substrate flow, when switching from glucose to methanol utilisation. However, it should be noted that the enzymes of the final part of glycolysis in majority also function in the direction of gluconeogenesis, by catalyzing the reverse reactions.

Finally, the upregulation of the gene encoding fructose 1,6 bisphosphate aldolase which, on methanol, catalyzes the formation of fructose 1,6 bisphosphate from dihydroxyacetone and glyceraldehyde-3-phosphate, reflects an increase of this reaction, which has been shown to be important in the rearrangement reactions to replenish the cell with xylulose-5-phosphate to the downstream reactions in methanol metabolism[2].

Regulatory networks

Accompanying the changes in expression of many metabolic genes, also changes in the underlying regulatory networks are expected. In addition to global changes, the DNA microarray data reflect the initial adaptation to methanol and thus enables analysis of more specific changes resulting in activation of methanol-dependent genes or in repression of glucose-dependent genes. Among the upregulated genes, 49 are involved in regulation of transcription. Most of these encode general transcription factors or transcription factors which have not been linked to a specific process. Regulators involved in stress response (6), glucose sensing/derepression (4), and peroxisome-related pathways (4) are overrepresented, as is expected due to the change in carbon source.

The expression of genes coding for peroxisome assembly and function is controlled by a transcriptional regulatory network, which has been studied extensively in *S. cerevisiae* in response to oleate[17-19]. The Oaf1-Pip2 complex plays a prominent role, although the putative *H. polymorpha* homolog of *PIP2* is only moderately upregulated during adaptation to methanol.

However the homolog of *ADR1* (23.7-fold), a second activator of oleate-responsive genes is strongly upregulated in *H. polymorpha* and is also involved in regulation of the response to both oleate and methanol in *P. pastoris* (named *MXR1*[20]). Virtually all known targets of Adr1 and its co-regulator Cat8 were indeed also upregulated in *H. polymorpha*, suggesting an important role in regulation of methanol metabolism, while most probably also activation by Snf1 is initiated after the shift, since this global regulator is crucial for growth on non-fermentable carbon sources[21,22].

Mpp1, another transcriptional regulator of methanol metabolism in *H. polymorpha*, is encoded by the strongest upregulated gene of this study (Hp27g360, 394-fold up), thus suggesting it is a master regulator of methanol-responsive genes[23].Swi1 and Snf2 also belong to a regulatory complex involved in gene expression of methanol-related genes as well as peroxisomal assembly, however their encoding genes were not induced in the early adaptation phase to methanol[24].

Among the downregulated genes, the decreased transcription of *RAP1* (Hp16g154, -3.1) is remarkable. This transcriptional regulator is known to activate transcription of genes encoding ribosomal proteins[25,26] and its downregulation is consistent with the observed massive decrease in transcripts for ribosomal proteins. Interestingly, this gene is also shown to be repressed during the environmental stress response in *S. cerevisiae* as described by Gasch et al.,[9].

Autophagy

Adaptation of *H. polymorpha* cells to methanol requires a major rearrangement of the cellular architecture. The finding that most *ATG* genes, which are involved in autophagy and autophagy related processes,[27] as well as several proteasomal genes are upregulated (18 up vs 2 down), suggests that cellular reorganisation requires massive degradation of cellular components (Table 3).

Table 3. Expression changes of *autophagy*-related genes

***ATG* genes**		**Ratio**
Hp24g929	*ATG1*	+ 3.7
Hp15g1008	*ATG2*	+ 2.6
Hp42g317	*ATG3*	+ 3.9
Hp24g999	*ATG4*	+ 2.3
Hp47g352	*ATG5*	+ 1.8
Hp24g284	*ATG6*	+ 3.7
Hp19g8	*ATG7*	+ 2.2
Hp48g37bm	*ATG8*	+ 6.2
Hp16g127	*ATG9*	+ 1.6
Hp24g546m	*ATG10*	+ 2.5
Hp25g507	*ATG11*	+ 5.2
Hp33g43	*ATG12*	+ 2.3
Hp19g348	*ATG13*	+ 1.6
Hp47g589	*ATG15*	+ 2.2
Hp24g680m	*ATG16*	+ 1.7
Hp8g289	*ATG17*	+ 1.1*
Hp25g289	*ATG18*	+ 1.9
Hp13g64	*ATG19*-like	+ 6.6
Hp16g331	*ATG20*	- 1.1
Hp44g480	*ATG21*	+ 1.8
Hp18g58	*ATG22*	+ 1.7
Hp33g356	*ATG24*	+ 2.8
Hp39g230	*ATG25*	- 4.3
Hp15g447	*ATG26*	+ 2.1
Hp39g339	*ATG27*	- 1.7
Hp47g741	*ATG28*	+ 1.8
Hp32g359	*ATG30*	+ 4.1

*With the exception of the one marked with an asterisk, all genes shown have a p-value below 0.05. Negative values indicate downregulation on methanol, positive values indicate upregulation.

Interestingly, the highest upregulation is observed for *ATG8* and *ATG11*. Atg8 has a prominent role in various selective and non-selective macroautophagic processes, whereas Atg11 is specifically involved in selective macroautophagy[28,29].

The function of HpAtg19-like, of which the encoding gene is also upregulated, is not known. However, HpAtg19-like is not involved in selective degradation of peroxisomes (unpublished data). Remarkably only *ATG25* is significantly downregulated. Atg25 is involved in selective peroxisome degradation by macropexophagy, but not in microautophagy[29]. Ultrastructural analysis of cells at different time-points after the shift indeed showed strong morphological evidence for increased autophagy, reflected in the massive uptake of cytoplasmic components in the vacuole (figure 4). Recent findings showed the importance of autophagy during methanol adaptation of *P. pastoris*, not only for cell remodeling, but also to provide amino acids[30] [30]. Consistent with these findings, we also observed that *H. polymorpha atg* mutants showed a slight delay in methanol adaptation (data not shown).

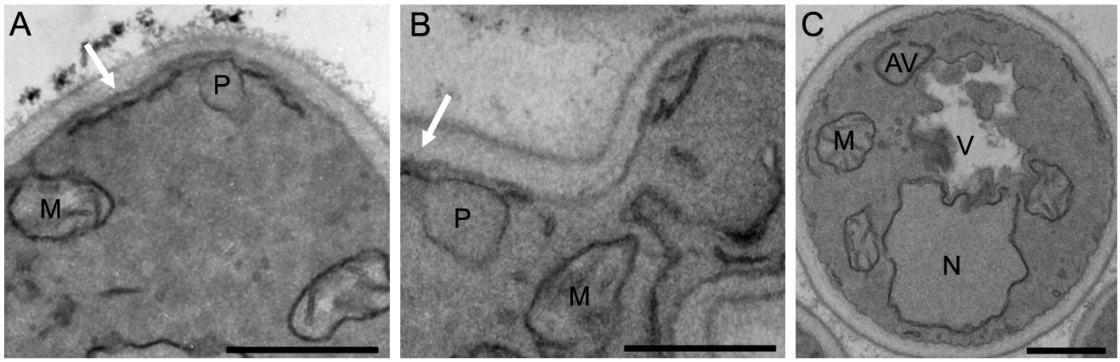

Figure 4. Ultrastructural analysis of the adaptation of cells to methanol. Glucose-grown *H. polymorpha* WT cells were extensively analysed at different time-points after the shift to methanol by electron microscopy of KMnO4-fixed samples. (A) Control glucose-grown cell and (B) after 2 h of incubation in the presence of methanol. A clear increase in peroxisome size was observed, cross-sections of representative cells are depicted. Note the association of the organelles with strands of ER (indicated by arrow). (C) 2 hours after the shift a clear increase was observed in large vacuolar autophagic bodies, indicative of induction of autophagy. N - Nucleus, M - Mitochondrion, V - Vacuole, AV - Autophagosome. Bar represents 0.5 μm.

β-oxidation of fatty acids

A significant upregulation of genes encoding proteins related to β-oxidation of fatty acids was observed[31,32]. This unexpected cluster is listed in Table 4. The regulation of these genes could be merely due to derepression as a result of decreasing glucose levels. However we consider this less likely since the observed ratio's and signals are quite substantial. Another explanation could be co-regulation of multiple peroxisomal pathways by common regulators. A third option is the increase in cellular fatty acid levels, the substrate for peroxisomal β-oxidation. This might originate from the observed autophagy, leading to recycling of intracellular membrane lipids.

Table 4 Expression changes of genes related to fatty acid β-oxidation

Gene	Function	Ratio
Hp8g534	Peroxisomal ABC-transporter sub-unit 1	+8.0
Hp33g390	Peroxisomal ABC-transporter sub-unit 2	+6.4
Hp44g158	Adenine nucleotide transporter	+3.0
Hp33g132	Fatty-acyl coenzyme A oxidase	+14.0
Hp8g261	Multifunctional enzyme	+21.6
Hp24g1381	3-ketoacyl-CoA thiolase	+16.3
Hp27g292	Catalase	+42.8
Hp29g305	Isocitrate lyase	+30.8
Hp43g61	Malate synthase	+8.8
Hp36g14	Isocitrate dehydrogenase	+27.7
Hp47g959	Carnitine acetyl-CoA transferase	+41.6
Hp39g121	Carnitine acetyltransferase, *YAT1*	+47.1
Hp8g466	Carnitine acetyltransferase, *YAT2*	+36.0
Hp15g677	Mitochondrial carnitine/acyl carnitine carrier	+111.3

Mitochondria

Remarkably, the shift of cells from glucose to methanol is associated with a significant increase in mitochondrial volume fractions (figure 5). Several functional links exist between peroxisomes and mitochondria, both for metabolic pathways and for biogenesis of both organelles[4,33]. Of the genes involved in mitochondrial function or assembly 110 are down- and 67 are upregulated.

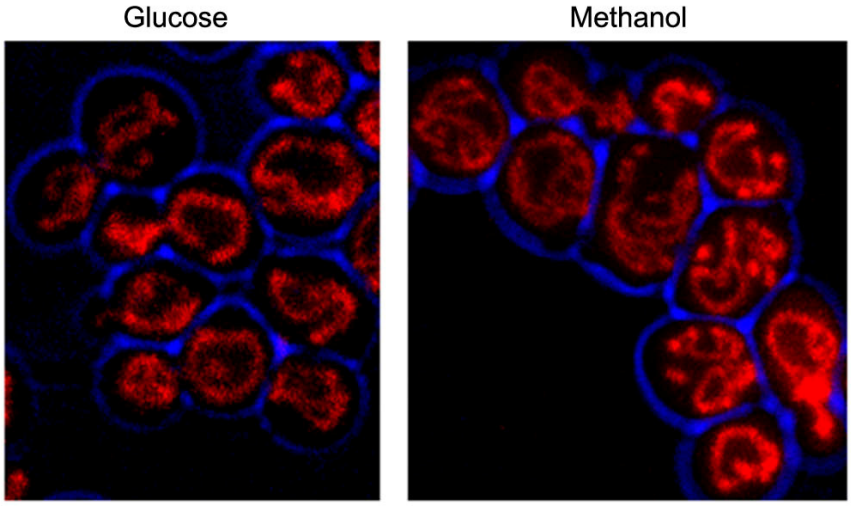

Figure 5. Fluorescence microscopy of mitochondria. Images demonstrating the increase in mitochondrial volume fractions in cells after 2 hours of incubation on methanol, relative to those of the glucose inoculum cells. Mitochondria are marked by MitoTracker Orange.

Genes coding for components of the Dnm1-dependent fission machinery of both organelles are not differentially expressed[4]. Similar to all downregulated genes, of the mitochondrial downregulated genes almost 50% is involved in transcription and translation processes. In addition the genes coding for TOM and TIM protein import complexes are also mostly down-regulated.

Genes involved in FeS cluster, heme biosynthesis and cytochrome c assembly are overrepresented among upregulated mitochondrial genes (9-fold), in agreement with the prominent role for mitochondria as the sole site of ATP generation during methanol-metabolism[2]. Heme is also the co-factor of peroxisomal catalase which is highly induced. FeS cluster formation is also coupled to the glutathione-based redox regulation system via *GRX5*[34].

Reactive oxygen species

Although mitochondria were long considered as the main source of reactive oxygen species (ROS), also peroxisomes actually defined as organelles that harbour H_2O_2-producing enzymes as well as catalase are now recognized as a significant contributor to ROS production[2,35,36]. Besides catalase (42.8-fold up), peroxisomes also contain the peroxiredoxin Pmp20, that is 11-fold upregulated, both indicative of an increase in peroxisomal ROS production[37,38].
We also observed an increase of several pivotal genes involved in cytosolic and mitochondrial ROS detoxification; like the superoxide dismutase *SOD1* (4.3-fold), the glutathione transferase *GTO2* (2.6-fold), the glutathione reductase *GPX3* (8-fold), the glutaredoxin *GRX5* (2.8-fold) and the thioredoxin peroxidase *TSA1* (47.2-fold). The remaining members of the glutathione- and TRX-based system are not differentially expressed (8 other genes found), except for the thioredoxin reductase *TRR1* (10.4-fold). Induction of these key enzymes involved in sustaining the redox balance of the cytosol, suggests that methanol-metabolism also results in enhanced cytosolic ROS levels, which may originate from peroxisomal metabolism.

Comparison with other DNA microarray analyses

Back in 1996, the proof of principle for the use of DNA microarray technology to investigate transcriptional changes was shown for *S. cerevisiae*[39]. Since then, DNA microarray analysis has become a regular, well-established tool, facilitated by the now commercial available array slides. For many other yeast species however, thusfar the usage of DNA microarray analysis is still rather limited. Only recently, species-specific DNA microarray studies have been presented for e.g. *Debaryomyces hansenii*[40] and *P. pastoris*[41]. For *H. polymorpha*, Oh et al.,[42] presented a partial, DNA microarray study, followed by a full DNA microarray analysis describing the transcriptional response of *H. polymorpha* to cadmium exposure[43]. However, this study was not related to the metabolic and architectural alterations associated with a change in cellular metabolism. Smith et al.[15,18] published two studies in which bakers' yeast was shifted to oleate. The first study focused mainly on transcriptional changes of genes encoding peroxisomal proteins and peroxins, the second one on the regulatory network coordinating the response to oleate.

The current study is the first in which arrays were used to study the shift from glucose to methanol in the yeast *H. polymorpha*. Sauer et al.[44] was the first to publish transcriptional profiling of the methylotrophic yeast *P. pastoris*, also upon a shift to methanol. However, in that study, yeast cells were transferred from glycerol to methanol and heterologous hybridisation onto *S. cerevisiae* DNA-microarrays was performed.

Still, the same trend in regulated functional groups was observed. Also, similar effects were reported on carbohydrate metabolism and the regulation of ribosomal genes. Although some of the data obtained for *H. polymorpha* are comparable with those obtained for *P. pastoris*, a significant drawback of the latter study is the absence of *P. pastoris* specific or methylotrophic yeast specific genes on the DNA-microarray slides. There is indeed a substantial amount of methanol-responsive *H. polymorpha* genes found in our study which were not observed in *P. pastoris* using *S. cerevisiae* microarrays (± 450 upregulated, ± 350 downregulated) [Suppl. table S2; open access article: http://www.biomedcentral.com/1471-2164/11/1].

Conclusions

The current DNA microarray study revealed the expected repression of genes involved in glucose metabolism concomitant with the induction of the genes of methanol metabolism in response of a shift of *H. polymorpha* cells from glucose to methanol. Also genes involved in peroxisome biogenesis (*PEX* genes) are upregulated, with *PEX32* being the most strongly upregulated *PEX* gene. A surprising finding was the upregulation of autophagy- and of beta-oxidation-genes. The first can likely be explained by the need for cellular reorganisations and is confirmed by electron microscopy studies showing active uptake of cytoplasmic components in the vacuoles of the cells. The induction of beta-oxidation is thought to be a consequence of the cellular reorganisations and thereby the high turnover of lipids, serving as substrates for beta-oxidation.

A final interesting but not yet uncovered group consists of the 33% of the upregulated genes that have no known function. These genes reflect a large potential of *H. polymorpha* or methylotrophic yeast specific genes with a specialized role in adaptations to growth on methanol as the sole source of carbon and can form interesting targets for future research.

Acknowledgements

TvZ is supported by a grant from the Netherlands Organisation for Scientific Research NWO (Earth and Life Sciences). This project was carried out within the research programme of the Kluyver Centre for Genomics of Industrial Fermentation, which is part of the Netherlands Genomics Initiative/Netherlands Organisation for Scientific Research.
We thank Rhein Biotech GmbH, Düsseldorf, Germany for access to the *H. polymorpha* genome database.

Methods

H. polymorpha microarray probe design

H. polymorpha open reading frame sequences were collected from the *H. polymorpha* genome database (Rhein Biotech[7], unpublished and NCBI[45-47]). For the genes on contigs 1 - 48, the annotation was based on the information from RheinBiotech and Ramezani-Rad et al.[7]. The additional NCBI sequences were listed as Hp50 and Hp51 numbers. The annotation of these genes was as described on NCBI (Hp50s) or by manual blast search (Hp51s). All Hp sequences were applied for design of oligonucleotide probes using OLIGOARRAY v2.1[48] with the following oligonucleotide primer design parameters: a length of 58-60 nucleotides, a melting temperature (Tm) of at least 80°C, a G/C-content of 34-52% and a maximum Tm of secondary structures and cross-hybridisations of 68°C. Oligo's were designed within the 3'-regions of the ORFs (setting: maximum distance between the 5' end of the oligo and the 3' end of the input sequence: 600-nt) to minimize including intron-sequences, since these were not discarded in the input ORF sequences. Paralogous sequences were removed during the final analysis of the design using blastN. Of the 6,248 oligo-probes, 6,002 are from the annotated genes of *H. polymorpha* and 23 probes are from heterologous genes of specific research interest (data not shown). The remaining 223 probes include positive and negative controls. Subsequently, the oligo-set was printed twice in each of the 8 arrays per slide (8-plex format) using Agilent's SurePrint technology (in situ synthesis; via eArray 4.0-website;

Agilent Technologies Netherlands B.V., Amstelveen, the Netherlands).

Organisms & Growth

H. polymorpha strain NCYC 495 leu- was grown in batch cultures on mineral medium containing either 0.5% glucose or 0.5% methanol as carbon source and 0.25% ammonium sulphate as nitrogen source[49,50] . For transcriptome analysis, cells were extensively pre-cultivated in batch cultures on glucose at 37°C prior to a shift to fresh media containing methanol as sole carbon source. Four independent glucose-grown cultures were used to inoculate fresh medium containing methanol as well as for taking samples for RNA isolation. The methanol cultures were grown for two hours, followed by RNA isolation.

RNA isolation

Samples were harvested by freezing them directly in liquid nitrogen, followed by thawing on ice, centrifugation (5.000 G, 4 min, 0°C) and taken up in AE-buffer (50 mM sodium-acetate 10 mM EDTA pH 5.0). 1 volume acid-phenol chloroform isoamylalcohol (125:24:1 pH 4.5, Ambion, Austin USA) and 0.5% SDS was added, and incubated at 65°C for 5 min followed by 15 min at -80°C. After centrifugation (15 min 13.000 G), the upper phase was mixed with 0.5 volume acid phenol/chloroform, centrifuged (4 min 13.000 G) and mixed with 0.5 volume chloroform. The upper phase was used for RNA isolation using column purification according to the manufacturers' instructions (Nucleospin RNA II, Macherey-Nagel, Düren Germany).

The Agilent Bioanalyzer 2100 with RNA 600 Nano chips was used to analyze the quality and integrity of the RNA samples.

Biochemical methods

Transcript levels of methanol-related genes (*AOX* and *DHAS)*, using those of actin as control, were determined by semi-quantitative RT-PCR, using actin as loading control (Ready-to-go RT-PCR beads, GE Healthcare, Little Chalfont UK).

Primers:

AOX-forw: CGTGAGAACAGTGCCAATGAAG
AOX-rev: TCACCGATGGTCAATGCAGTAG
DHAS-forw: GCAGGACGTGTACGACTTCTTC
DHAS-rev: GTAGGACGCCGTAGCGTATCTC
Act1-forw: GGTCATTGATAACGGATCCGG
Act1-rev: CACTTGTGGTGGACAATGGATGG

Cell lysates were essentially obtained as described[51], for subsequent AOX activity measurements as described[52].

DNA microarray analysis - labeling, hybridisation, washing and scanning

Using the Low RNA input linear Amplification kit from Agilent, cDNA was generated based on 500 ng of each isolated mRNA sample. Next, cRNA was made using Cy3-CTP or Cy5-CTP incorporation for labeling purposes. For each original mRNA, a portion of Cy3 and Cy5 labeled cRNA was generated. The concentration and incorporation of the cRNA and the dyes are measured using Nanodrop. For each biological replicate, 300 ng Cy3 labeled glucose culture originating cRNA was used for

hybridisation against 300 ng Cy5 labeled methanol culture originating cRNA and vice versa for the dye-swap, resulting in 8 hybridisations in total. Hybridisation, washing and scanning were performed according to the Agilent 'Two-color Microarray-based gene expression analysis protocol' (version 5.5, February 2007) by ServiceXS (Leiden, The Netherlands).

Data analysis - hybridisation ratio's, A-values and p-values

To extract the data from the scanned DNA-microarray slides, the feature extraction software version 9.5, Protocol GE2-v5_95_Feb07 from Agilent was used. For the background subtraction the option 'No background subtraction and spatial detrend' was used. For each spot, the ratio between the green and red processed signals was calculated, reflecting the ratio of gene expression on methanol overexpression on glucose.

Next, the average ratio per gene was calculated based on the data of 16 spots (8 hybridisations, 2 spots per hybridisation). For reasons of clarity, genes with a ratio of <1 were expressed as -(1 divided by the ratio), thus reflecting the fold downregulation (e.g. -2 instead of 0.5). As a cut-off for differential gene expression, a threshold of (more than) 2-fold up- or downregulation was used, so >2 or <-2. To assess the significance of the data, p-values were computed using the paired-data program at the CyberT interface[53,54]. Genes were considered to be significantly regulated if they had a p-value below 0.05. In addition, average A-values for each gene were calculated as an indication for the intensity of the signals using A = 0.5*(log2Cy3+log2Cy5). An A-value of 6 was used as a lower limit for trustworthy signal intensity.

All data has been deposited to the NCBI Gene expression omnibus and is accessible under accession number GSE19036.

Classification according to the Functional Catalogue

To show the main represented functions among up- and downregulated genes, *H. polymorpha* genes were ordered according to their Functional Catalogue (FunCat) as assigned by RheinBiotech. In the diagrams, the main groups of the hierarchical structure are shown as well as the subgroups 'transcription' and 'protein synthesis'[8]. The group 'subcellular localisation' was omitted, while 'control of cellular organisation', which is not in the FunCat structure, was included under 'developmental processes'. Genes can be present in more than one group.

Analysis of metabolic routes using Biocyc

Changes in expression of metabolic pathway genes were investigated using the omics viewer at the Ecocyc website[55]. Since information on *H. polymorpha* is not included in this database, the genome of *Saccharomyces cerevisiae* S288C was used as a reference.

Microscopy

Ultrathin sections of KMnO4-fixed cells were used for ultrastructural analysis as described[56]. Analysis of mitochondria was performed using confocal microscopy (Zeiss LSM510). Mitochondria were visualized using MitoTracker Orange (CMTMRos, Invitrogen) and visualization with excitation by a 543 nm Neon-laser (Lasos) and detection using a 565-615 band-pass emission filter.

References

1. Gellissen G, Kunze G, Gaillardin C, Cregg JM, Berardi E, Veenhuis M, van der Klei IJ. New yeast expression platforms based on methylotrophic *Hansenula polymorpha* and *Pichia pastoris* and on dimorphic *Arxula Adeninivorans* and *Yarrowia lipolytica* – A comparison. FEMS Yeast Res. 2005; 5:1079-1096.
2. Van der Klei IJ, Yurimoto H, Sakai Y, Veenhuis M. The significance of peroxisomes in methanol metabolism in methylotrophic yeast. Biochim Biophys Acta 2006; 1763:1453-1462.
3. Ischuk OP, Voronovsky AY, Abbas CA, Sibirny AA. Construction of *Hansenula polymorpha* strains with improved thermotolerance. *Biotechnol. Bioeng.* 2009; DOI 10.1002/bit.22457.
4. Nagotu S, Krikken AM, Otzen M, Kiel JAKW, Veenhuis M, van der Klei IJ. Peroxisome fission in *Hansenula polymorpha* requires Mdv1 and Fis1, two proteins also involved in mitochondrial fission. Traffic 2008; 9:1471-1484.
5. Veenhuis M, Keizer I, Harder W. Characterization of peroxisomes in glucose-grown *Hansenula polymorpha* and their development after the transfer of cells into methanol-containing media. Arch Microbiol 1979; 20:167-175.
6. Eggeling L, Sahm H. Derepression and Partial Insensitivity to Carbon Catabolite Regression of the Methanol Dissimilating Enzymes in *Hansenula polymorpha.* Europ J Appl Microbiol Biotechnol 1978; 5:197-202.
7. Ramezani-Rad M, Hollenberg CP, Lauber J, Wedler H, Griess E, Wagner C, Albermann K, Hani J, Piontek M, Dahlems U, Gellissen G. The *Hansenula polymorpha* (strain CBS4732) genome sequencing analysis. FEMS Yeast Res 2003; 4:207-215.
8. Ruepp A, Zollner A, Maier D, Albermann K, Hani J, Mokrejs M, Tetko I, Güldener U, Mannhaupt G, Münsterkötter M, Mewes HW. The FunCat, a functional annotation scheme for systematic classification of proteins from whole genomes. Nucl Acid Res 2004; 32:5539 – 5545.
9. Gasch, AP, Spellman, PT, Kao, CM, Carmel-Harel, O, Eisen, MB, Storz, G, Botstein D, Brown PO. Genomic expression programs in the response of yeast cell to environmental changes. Mol Biol Cell 2000; 11:4241– 4257.
10. Gasch, AP, Werner-Washburne, M. The genomics of yeast responses to environmental stress and starvation. Funct. Integr Genomics 2002; 2:181–192.
11. Gasch, AP. Comparative genomics of the environmental stress response in ascomycete fungi. Yeast 2007; 24:961–976.
12. Yurimoto H, Komeda T, Lim CR, Nakagawa T, Kondo K, Kato N, Sakai Y. Regulation and evaluation of five methanol-inducible promoters in the methylotrophic yeast *Candida boidinii*. Biochim Biophys Act 2000; 1493:56-63.
13. Roa M, Blobel G. Biosynthesis of peroxisomal enzymes in the methylotrophic yeast *Hansenula polymorpha*. Proc Natl Acad Sci 1983; 80:6872-6876.
14. Kal JA, van Zonneveld AJ, Benes V, van den Berg M, Koerkamp MG, Albermann K, Strack N, Ruijter JM, Richter A, Dujon B, Ansorge W, Tabak HF. Dynamics of gene expression revealed by comparison of serial analysis of gene expression transcript profiles from yeast grown on two different carbon sources. Mol Biol Cell 1999, 10:1859-1872.

15. Smith JJ, Marelli M, Christmas, RH, Vizeacoumar FJ, Dilworth DJ, Ideker T, Galitski T, Dimitrov K, Rachubinsky RA, Aitchison JD. Transcriptome profiling to identify genes involved in peroxisome assembly and function. J Cell Biol 2002; 158:259-271.
16. Kiel JAKW, Veenhuis M, van der Klei IJ. *PEX* genes in fungal genomes: common rare or redundant. Traffic 2006; 7:1291-1303.
17. Gurvitz A, Rottensteiner H. The biochemistry of oleate induction: transcriptional upregulation and peroxisome proliferation. Biochim. Biophys. Act 2006; 1763:1392-1402.
18. Smith JJ, Ramsey SA, Marelli M, Marzolf B, Hwang, D, Saleem, RA, Rachubinski RA, Aitchison, JD. Transcriptional responses to fatty acid are coordinated by combinatorial control. Mol Syst Biol 2007; nr 115, doi:10 1038/msb4100157
19. Karpichev IV, Durand-Heredia JM, Luo Y, Small GM. Binding characteristics and regulatory mechanisms of the transcription factors controlling oleate-responsive genes in *Saccharomyces cerevisiae*. J Biol Chem 2008; 283:10264-10275.
20. Lin-Cereghino GP, Godfrey L, de la Cruz BJ, Johnson S, Khuongsathiene S, Tolstorukov I, Yan M, Lin-Cereghino J, Veenhuis M, Subramani S, Cregg JM. Mxr1p, a key regulator of the methanol utilization pathway and peroxisomal genes in *Pichia pastoris*. Mol Cell Biol 2007; 26:883-897.
21. Young ET, Dombek KM, Tachibana C, Ideker T. Multiple pathways are co-regulated by the protein kinase Snf1 and the transcription factors Adr1 and Cat8. J Biol Chem 2003; 278:26146-26158.
22. Tachibana C, Yoo JY, Tagne J-B, Kacherovsky N, Lee TI, Young ET. Combined global localization analysis and transcriptome data identify genes that are directly coregulated by Adr1 and Cat8. Mol Cell Biol 2005; 25:2138-2146.
23. Leão-Helder, AN, Krikken, AM, van der Klei, IJ, Kiel, JAKW, Veenhuis, M. Transcriptional downregulation of peroxisome numbers affects selective peroxisome degradation in *Hansenula polymorpha*. J Biol Chem 2003; 278:40749–40756.
24. Ozimek P, Lahtchev K, Kiel JAKW, Veenhuis M, van der Klei IJ. *Hansenula polymorpha* Swi1 and Snf2 are essential for methanol utilisation. FEMS Yeast Res 2004; 4:673-682.
25. Rotenberg MO, Woolford JL. Tripartite upstream promoter element essential for expression of *Saccharomyces cerevisiae* ribosomal protein genes. Mol Cell Biol 1986; 6:674 – 687.
26. Woudt LP, Smit AB, Mager WH, Planta RJ. Conserved sequence elements upstream of the gene encoding yeast ribosomal protein L25 are involved in transcription activation. EMBO J 1986; 5:1037–1040.
27. Klionsky DJ, Cregg JM, Dunn WA Jr, Emr SD, Sakai Y, Sandoval IV, Sibirny A, Subramani S, Thumm M, Veenhuis M, Ohsumi Y. A unified nomenclature for yeast autophagy-related genes. Dev Cell 2003; 5:539-545.
28. Shintani T, Huang W-P, Stromhaug PE, Klionsky DJ. Mechanism of cargo selection in the cytoplasm to vacuole targeting pathway. Dev Cell 2002; 3:825-837.

29. Monastyrska I, Kiel JAKW, Krikken AM, Komduur JA, Veenhuis M, van der Klei IJ. The *Hansenula polymorpha ATG25* gene encodes a novel coiled-coil protein that is required for macropexophagy. Autophagy 2005; 1:92-100.
30. Yamashita S-I, Yurimoto H, Murakami D, Yoshikawa M, Oku M, Sakai Y. Lag-phase autophagy in the methylotrophic yeast *Pichia pastoris*. Genes Cells 2009; 14:861-870.
31. van Roermund CWT, Waterham HR, Wanders RJH. Fatty acid metabolism in *Saccharomyces cerevisiae*. Cell Mol Life Sci 2003; 60:1838-1851.
32. Zwart KD, Veenhuis M, Plat G, Harder W. Characterization of glyoxysomes in yeasts and their transformation into peroxisomes in response to changes in environmental conditions. Arch Microbiol *1983*; 136:28-38.
33. Wanders RJA, Waterham HR. Biochemistry of mammalian peroxisomes revisited. Annu Rev Biochem 2006; 75:295:332.
34. Rodriguez-Manzaneque MT, Tamarit J, Belli G, Ros J, Herrero E. Grx5 is a mitochondrial glutaredoxin required for the activity of iron/sulfur enzymes. Mol Biol Cell 2002; 13:1109-1121.
35. Herrero E, Ros J, Belli G, Cabiscol G. Redox control and oxidative stress in yeast cells. Biochim Biophys Act 2007; 1780:1217-1235.
36. Bener Aksam E, de Vries B, van der Klei IJ, Kiel JAKW. Preserving organelle vitality: peroxisomal quality control mechanisms in yeast. FEMS Yeast Res 2009; 9:808-20.
37. Goodman JM, Maher J, Silver PA, Pacifico A, Sanders D. The membrane proteins of the methanol-induced peroxisome of *Candida boidinii*. Initial characterization and generation of monoclonal antibodies. J. Biol. Chem 1986; 261: 3464–3468.
38. Bener Aksam E, Jungwirth H, Kohlwein SD, Ring J, Madeo F, Veenhuis M, van der Klei IJ. Absence of the peroxiredoxin Pmp20 causes peroxisomal protein leakage and necrotic cell death. Free Radic Biol Med 2008. 45:1115-1124.
39. Shalon D, Smith SJ, Brown PO. A DNA microarray system for analyzing complex DNA samples using two-color fluorescent probe hybridization. Genome Res 1996; 6:639-645.
40. Gonzalez NA, V'azquez, A, Ortiz Zuazaga HG, Sen A, Olvera HL, Pe"na de Ortiz S, Govind NS. Genome-wide expression profiling of the osmoadaptation response of *Debaryomyces hansenii*. Yeast 2009; 26:111-124.
41. Graf A, Gasser B, Dragosits M, Sauer M, Leparc GG, Tüchler T, Kreil DP, Mattanovich D. Novel insights into the unfolded protein response using *Pichia pastoris* specific DNA microarrays. BMC Genomics 2008; 9:390.
42. Oh KS, Kwon O, Oh, YW, Sohn MJ, Jung S, Kim YK, Kim MG, Rhee SK, Gellissen G, Kang HA. Fabrication of a partial genome microarray of the methylotrophic yeast *Hansenula polymorpha*: optimization and evaluation of transcript profiling. J. Microbiol 2004; 14:1239-1248.
43. Park JN, Sohn MJ, Oh DB, Kwon O, Rhee SK, Hur CG, Lee SY Gelissen G Kang HA. Identification of the Cadmium-inducible *Hansenula polymorpha SEO1* gene promoter by transcriptome analysis and its application to whole-cell heavy-metal detection systems. Appl Env Microbiol 2007; 73:5990-6000.

44. Sauer M, Branduardi P, Gasser B, Valli M, Maurer M, Porro D, Mattanovich D. Differential gene expression in recombinant *Pichia pastoris* analysed by heterologous DNA microarray hybridisation. Microb Cell Fact 2004; 3:17.
45. Blandin G, Llorente B, Malpertuy A, Wincker P, Artiguenave F, Dujon B. Genomic exploration of the hemiascomycetous yeasts: 13 *Pichia angusta*. FEBS Lett 2000; 487: 76-81.
46. Garcia-Lugo P, Gonzalez C, Perdomo G, Brito N, Avila J, de la Rosa JM, Siverio JM. Cloning, sequencing and expression of H.a. YNR1 and H.a. YNI1, encoding nitrate and nitrite reductases in the yeast *Hansenula anomala*. Yeast 2000; 16:1099-1105.
47. Avila J, Gonzalez C, Brito N, Siverio JM. Clustering of the YNA1 gene encoding a Zn(II)2Cys6 transcriptional factor in the yeast *Hansenula polymorpha* with the nitrate assimilation gene YNT1, YNI1 and YNR1, and its involvement in their transcriptional activation. Biochem J 1998; 335:647-652
48. Rouillard JM, Zuker M Gulari E. OligoArray 2.0: design of oligonucleotide probes for DNA microarrays using a thermodynamic approach. Nucl Acid Res 2003; 31:3057-3062.
49. Gleeson MAG, Sudbery PE. Genetic analysis in the methylotrophic yeast *Hansenula polymorpha*. Yeast 1988; 4:293-303.
50. Van Dijken JP, Otto R, Harder W. Growth of *Hansenula polymorpha* in a methanol-limited chemostat. Physiological responses due to the involvement of methanol oxidase as a key enzyme in methanol metabolism. Arch Microbiol 1976; 111:137-144.
51. Waterham HR, Keizer-Gunnink I, Goodman JM, Harder W, Veenhuis M. Development of multipurpose peroxisomes in Candida Boidinii grown in oleic acid-methanol limited continuous cultures. J Bacteriol 1992; 174:4057-4063.
52. Verduyn C, van Dijken JP, Scheffers WA. Colorimetric alcohol assays with alcohol oxidase. J Microbiol Methods 1984; 2:15-25.
53. Cyber-T [http://cybert.microarray.ics.uci.edu]
54. Baldi P, Long AD. A Bayesian Framework for the analysis of microarray expression data: regularized t-Test and statistical interferences of gene changes. Bioinformatics 2001; 17:509–519.
55. Ecocyc database [http://ecocyc.org/]
56. Van Zutphen T, van der Klei IJ, Kiel JAKW. Pexophagy in *Hansenula polymorpha*. Methods Enzymol 2008; 451:197-215.

Chapter 3

The role of *Hansenula polymorpha MIG1* homologues in catabolite repression and pexophagy

Olena G. Stasyk[1], Tim van Zutphen[2], Huyn Ah Kang[3], Oleh V. Stasyk[1], Marten Veenhuis[2], and Andriy A. Sibirny[1,4]

[1]Institute of Cell Biology, National Academy of Sciences of Ukraine, Drahomanov Street 14/16, Lviv 79005, Ukraine;
[2] Molecular Cell Biology, Groningen Biomolecular Sciences and Biotechnology Institute (GBB), University of Groningen, Biological Centre, P. O. Box 14, 9750 AA Haren, The Netherlands;
[3] Protein Therapeutics Research Center, Korea Research Institute of Bioscience and Biotechnology, 52 Eoeun-dong, Yuseong-gu, 305-333 Deajeon, Korea; [4] Department of Metabolic Engineering, Rzeszów University, Cwiklinskiej 2, 35-601, Rzeszów, Poland.

Published in *FEMS YEAST RESEARCH 2007; 7:1103-1113.*

Summary

In the methanol-utilizing yeast *Hansenula polymorpha* glucose and ethanol trigger the repression of peroxisomal enzymes at the transcriptional level and rapid and selective degradation of methanol-induced peroxisomes via a process termed pexophagy. In this report we demonstrate that deficiency in the putative *H. polymorpha* homologues of transcriptional repressors Mig1 (HpMig1 and HpMig2), as well as HpTup1, partially and differentially affects the repression of peroxisomal alcohol oxidase by sugars and ethanol. As reported earlier, deficiency in HpTup1 leads to impairment of glucose- or ethanol-induced macropexophagy. In *H. polymorpha mig1mig2* double deletion cells, macropexophagy was also largely impaired, whereas micropexophagy became a dominant mode of autophagic degradation. Our findings suggest that homologues of the elements of the *Saccharomyces cerevisiae* main repression pathway have pleiotropic functions in *H. polymorpha*.

Introduction

It is well established that intact peroxisomes are indispensable for methylotrophic growth in yeasts. These organelles harbour key enzymes that catalyze the first steps of methanol utilization (as alcohol oxidase (AO), catalase, dihydroxyacetone synthase) and provide compartmentalization of toxic methanol catabolites, formaldehyde and hydrogen peroxide (Veenhuis *et al.,* 1983a; van der Klei *et al.,* 2006). Peroxisomes, however, are redundant for growth on rich carbon sources such as hexoses and disaccharides. When methanol-grown cells are shifted to sugar carbon substrates or ethanol, peroxisomes are rapidly and selectively degraded in vacuoles (Veenhuis *et al.,* 1983b), whereas genes of peroxisomal enzymes are subjected to tight transcriptional repression (Roggenkamp *et al.,* 1984). Such coordinated genetically-programmed catabolite regulation ensures a fast and efficient cellular response to environmental changes.

It was originally assumed that the molecular pathway of glucose catabolite repression in methylotrophic yeasts may mimic that of conventional yeast *S. cerevisiae* (so-called Snf1-Mig1 pathway). Its main components whose deficiency abolishes repression signaling are hexokinase II subunit, Snf1 protein kinase, and the Mig1 repressor that tethers or facilitates binding of the Tup1-Ssn6 general repressor to promoters of repressible genes in the presence of glucose (Gancedo, 1998; Papamichos-Chronakis *et al.,* 2004). Several observations support this hypothesis.

First, Mig1-Ssn6-Tup1 and the Snf1 complexes are highly conserved among different yeasts (Gancedo, 1998). Second, promoters of *H. polymorpha* alcohol oxidase (Pereira & Hollenberg, 1996) and maltase (Alamae *et al.,* 2003) genes were demonstrated to be repressed by glucose in *S. cerevisiae*, suggesting that they are targets of the host's repression pathway.

Recently, hexose phosphorylation activity was shown to be essential for repression signaling in *H. polymorpha*: hexokinase mutant was insensitive to fructose (but not glucose) repression, whereas in a double hexo- and glucokinase mutant glucose repression was also abrogated (Kramarenko *et al.,* 2000). The above findings suggested that glucose repressible genes of C-1 metabolism in *H. polymorpha* may be the target of Mig1/(Tup1-Ssn6)-mediated transcriptional repression, analogous to the case of baker's yeast. However, Oliveira et al., (2003) reported that HpTup1 is not essential for glucose repression of peroxisomal enzymes in *H. polymorpha*.

Adding to the emerging complexity of repression pathway in this yeast, we recently identified a hexose transporter homologue, HpGcr1, which is most probably involved in the first stages of glucose (but not sucrose or ethanol) signaling for repression, but may also interfere with high affinity glucose transport (Stasyk *et al.,* 2004). Its close homologues in *S. cerevisiae*, the putative glucose sensors Snf3 and Rgt2, were not implicated in the repression mechanism but instead differentially regulate induction of functional hexose transporters in response to extracellular glucose (Johnston & Kim, 2005).

It has to be emphasized that in *H. polymorpha* and other methylotrophs, disaccharides and ethanol are potent repressors of gene expression involved in C-1 metabolism (Sibirny *et al.,* 1988, Stasyk *et al.,* 2004). However, nothing is known of the specific molecular components of ethanol- or disaccharide-triggered repression, whether different carbon source-dependent pathways physically converge, and if so, at what stage they do so.

With regard to pexophagy, significant progress has been achieved in recent years in understanding its molecular mechanisms and regulation, with *H. polymorpha* being a very productive model organism, as detailed in recent reviews (Dunn *et al.,* 2005; Sakai *et al.,* 2006; Monastyrska & Klionsky, 2006). Two morphologically distinguishable pexophagy mechanisms were observed in *H. polymorpha*: selective macropexophagy–triggered by the shift in carbon source (i.e., from methanol to glucose or ethanol) (Veenhuis *et al.,* 1983b; Tuttle *et al.,* 1993), or cold shock (Komduur *et al.,* 2004), and nonselective micropexophagy triggered upon nitrogen starvation leading to bulk turnover by general autophagy (Monastyrska *et al.,* 2002).

Most *ATG* (AuTophaGy-related) genes involved in pexophagy identified so far in *H. polymorpha* and other yeasts are conserved among eukaryotes and also appear to affect general autophagy. Those essential only for pexophagy are in many cases organism-specific (Meijer *et al.,* 2007). The latter include *H. polymorpha ATG11* and *ATG25* (Monastyrska *et al*., 2005), *ATG26* (our unpublished results), and *TUP1* (Leao-Helder *et al.,* 2004).

HpTup1 is a first representative of transcriptional repressors involved in pexophagy. As macropexophagy, in contrast to nitrogen starvation-induced microautophagy, is insensitive to cycloheximide (i.e.independent of protein synthesis *de novo*) (Monastyrska *et al.,* 2005), the function of HpTup1 in pexophagy has been suggested to be indirect (Leao-Helder *et al.,* 2004).
Knowledge of the molecular mechanisms of catabolite regulation in *H. polymorpha* is of basic and practical interest. Mutants with altered catabolite regulation of the AO gene promoter may be promising hosts for expression of recombinant proteins in methanol-free media (Krasovska *et al.,* 2007) and protein products can be targeted to peroxisomes applying this organelle as a storage vesicle (van Dijk *et al.,* 2000).
The availability of the full *H. polymorpha* genome sequence (Ramezani-Rad *et al.,* 2003) opened the possibility to search for orthologues of *S. cerevisiae* genes involved in catabolite repression and study their function. In this report we analyse the possible role of two *H. polymorpha* Mig1 homologues (designated HpMig1 and HpMig2) in the processes of catabolite repression and pexophagy.

Materials and methods

Microorganisms and growth conditions

The following *H. polymorpha* strains were used in this study: NCYC495 *leu1-1* (Gleeson & Sudbery, 1988), *Δmig1* deletion mutant, *Δmig2* deletion mutant, *Δmig1Δmig2* double deletion mutant (all this study, *Δtup1 leu1-1*(Leao-Helder *et al.*, 2004), *Δgcr1* (Stasyk *et al.*, 2004). *H. polymorpha* cells were grown at 37^{o}C in rich YPD medium (1% peptone, 2% yeast extract, 1% glucose) or minimal media containing 0.67% yeast nitrogen base (YNB, Difco, Detroit, MI, USA) supplemented with 1% glucose (YND), 1% sucrose (YNS), 1% ethanol (YNE), or 1% methanol (YNM), unless stated otherwise. For auxotrophic strains, leucine (40 mg L^{-1}) was supplemented. For selection of yeast transformants via geneticine (G418) resistance, 0.4 g L^{-1} of G418 was added to YPD plates. The *Escherichia coli* DH5α strain was used as a host for propagation of plasmids and grown at 37°C in LB medium as described in Sambrook et al., (1989).

Molecular-biology techniques

Standard cloning and DNA manipulation techniques were applied (Sambrook *et al*., 1989). Genomic DNA of *H. polymorpha* was isolated using the Wizard Genomic DNA Purification Kit (Promega, Madison, WI, USA). Restriction endonucleases and DNA ligase (Fermentas, Vilnius, Lithuania) were used according to the manufacturer specifications. PCR-amplification of the fragments of interest was done with Platinum *Taq* DNA Polymerase High Fidelity (Invitrogen, Carlsbad, CA, USA) according to the manufacturer specification. The primers used in this study are listed in Table 1.

Table 1. Primers used in this study

Gene specificity	Name of primer	Sequence
HpMIG1	OL54	5'–TGTGGATCCTTTTTTGGCGTGGATGT–3'
HpMIG1	OL55	5'–GGTTCTAGATCACTCAGAAAACATGG–3'
HpMIG1	OL57	5'–TGGAAGCTTAGAAAGACCTGCTTGCTG–3'
HpMIG1	Mi12Nf	5'–CCCAAGCTTGGTGTAGTTGTCGGAG–3'
HpMIG1	Mi12Nr	5'–ATAAGAATGCGGCCGCCTACACTGTAGCTACG–3'
HpMIG1	Mi12Cf	5'–CGAGACCTGCATACATG–3'
HpMIG1	Mi12Cr	5'–CCGGAATTCGCATCCCAGAGTACTC–3'
HpMIG2	OL91	5'–AAACTAAAACAGGGATCG–3'
HpMIG2	OL92	5'–AAAATACGACTGCAGCGA–3'
HpMIG2	OL153	5'–TGTGGATCCAAATTTTCACACCTCAGG–3'
HpMIG2	OL154	5'–CCGATATATCTAGAGACGTGCTTCCAT–3'
HpMIG2	OL155	5'– TCCATAGAAAGCTTCTGAACAGCCCCGAAGA–3'
HpMIG2	OL156	5'–GGAAGCTTGAGCTCGAAATATTTCCTTCTTTGC–3'
HpLEU2	OL143	5'–GCACAATGTTCTTACTCAT–3'
ScLEU2	CK15	5'–TGTAATTGTTGGGATTCC–3'

Transformation of *H. polymorpha* by electroporation was carried out as described previously (Faber *et al*., 1994).

Protein sequence analyses

For analysis of DNA and amino acid sequences, MacVector software (IBI, New Haven, Conn., USA) was used. Sequence alignments and phylogenetic analysis were performed using the ClustalW version 1.6 algorithm (Corpet, 1998). The BLAST Network Service of the National Center for Biotechnology Information (Bethesda, MD, USA; http://www.ncbi.nlm.nih.gov/BLAST/) was used to search for amino acid sequence similarities. For pattern and profile search, PROSCAN program at http://npsa-pbil.ibcp.fr/cgibin/ pattern_prosite.pl was used (Combet *et al*., 2000).

Construction of HpMIG1 and HpMIG2 deletion strains

A *HpMIG1* (GenBank accession number EF523343) deletion cassette was constructed as follows: a 0.93-kb fragment containing sequences of 3'-flanking region of the *HpMIG1* was amplified by PCR using genomic DNA of *H. polymorpha* as a template and the primers Mi12Cf and Mi12Cr carrying restriction sites for EcoRI and BamHI (Table 1). The 3'-flanking fragment was inserted into EcoRI/BamHI digested plasmid pBSKT (Lombo *et al.,* 1997). Next, a 0.93-kb fragment consisting of the 5'-flanking region of the *HpMIG1* was amplified by PCR with the primers Mi12Nf and Mi12Nr (Table 1) carrying restriction sites for HindIII and NotI, respectively. The 5'-flanking PCR fragment of *HpMIG1* and BamHI/NotI digested *HpLEU2* fragment were cloned into BamHI/NotI digested plasmid pBSKT-*3'MIG1*, thus generating deletion cassette for *HpMIG1* (plasmid p19-mig12::*HpLEU2*). The derivative plasmid pOH7 was constructed by replacing PstI-fragment of *HpLEU2* on p19-mig12::*HpLEU2* with PstI-fragment harboring the *APH* gene expressed under constitutive promoter of glyceraldehyde-3-phosphate dehydrogenase from plasmid pGLG578 (Sohn *et al.*, 1999) (Fig. 1).The *Δmig1*and *Δmig1leu1-1* strains were isolated by transforming recipient wild-type strain NCYC495 *leu1-1* with deletion cassettes for *HpMIG1* from p19-mig12::*HpLEU2* (EcoRI-HindIII fragment comprised of *HpLEU2* flanked by *HpMIG1* 5'- and 3'-sequences) and pOH7 (Eco32I/PaeI fragment of pOH7 comprised of *APH* flanked by the same *HpMIG1* sequences), thereby replacing the region of *HpMIG1* either with *HpLEU2* or *APH*.

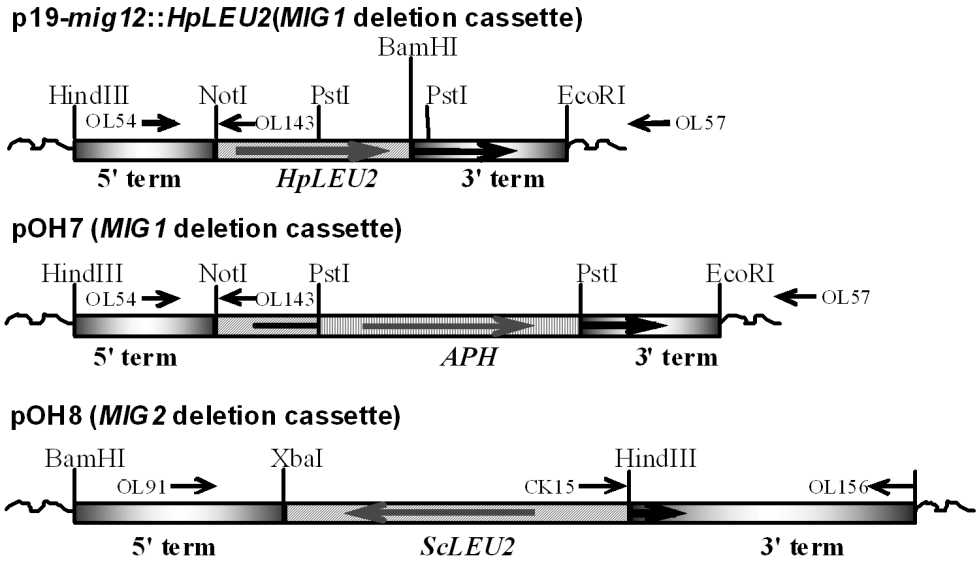

Figure 1. Scheme of construction of H. polymorpha Δmig1 and Δmig2 deletion strains. The *HpMIG1*, *HpMIG2*, *HpLEU2*, *ScLEU2* and *APH* genes and directions of transcription are indicated by arrows in plasmids p19-*mig12*::*HpLEU2*, pOH7 and pOH8. **p19-*mig12*::*HpLEU2*** consists of 943-bp fragment containing the 5' uncoding region of the *HpMIG1* gene (HindIII-NotI section); the 991-bp fragment carrying the 3' uncoding region and short terminal part of the *HpMIG1 ORF* (BamHI-EcoRI section). **pOH7** consists of 943-bp fragment containing the 5' uncoding region of the *HpMIG1* gene (HindIII-NotI section); the 897-bp fragment carrying the 3' uncoding region and short terminal part of the *HpMIG1 ORF* (PstI-EcoRI section). **pOH8** consists of 1.39-kb fragment containing the 5' uncoding region of the *HpMIG2* gene (BamHI-XbaI section); the 1.9-kb fragment carrying the 3' uncoding region and short terminal part of the *HpMIG2 ORF* (HindIII-HindIII section). Genomic DNA of the *H. polymorpha* flanking deletion cassettes upon integration into genome is represented by wavy line. Names and sequence position of the primers used in plasmid construction and PCR analysis of deletion mutants are indicated.

Prototrophic or G418 resistant transfromants were isolated and analyzed as detailed below.A *HpMIG2* (GenBank accession number EF523344) deletion cassette was constructed as follows; a 1.97-kb fragment containing sequences of 3'-flanking region of the *HpMIG2* was amplified by PCR using genomic DNA of *H. polymorpha* NCYC495*leu1-1* as a template and the primers OL155 and OL156 carrying restriction sites for HindIII (Table 1, Figure1). The 3'-flanking fragment was inserted into HindIII digested plasmid pYT1 (Tan *et al.*, 1995), carrying *ScLEU2* gene as a selection marker, to create pYT1-*3'MIG2*. Next, a 1.39-kb fragment consisting of the 5'-flanking region of the *HpMIG2* was amplified by PCR with the primers OL153 and OL154 carrying restriction sites for BamHI and XbaI respectively. The 5'-flanking PCR fragment of *HpMIG2* was cloned into BamHI/XbaI digested plasmid pYT1-*3'MIG2*, to create pOH8, generating a deletion cassette for *HpMIG2*.

The plasmid pOH8 was used as template for PCR with primers OL153 and OL156, producing a 5.56-kb fragment comprised of *ScLEU2* flanked by *MIG2* 5'- and 3'-sequences. The deletion cassette was transformed into NCYC495*leu1-1* and prototrophic transformants selected. Total genomic DNA isolated from potential *Δmig1* knock out strains (p19-mig12::*HpLEU2* and pOH7 transformants) was used as a template for PCR and Southern-blot analyses. Primer pairs OL54/OL55; OL54/OL57 and OL54/OL143 (Table 1, Fig. 1) were used to determine the presence of corresponding knock-out cassettes in *Δmig1* and *Δmig1leu1-1* genomic DNAs. PCR analysis (data not shown) indicated the presence of expected bands in the tested strains: 0.45-kb band

generated by OL54/OL55, 2.24-kb band (OL54/OL57) and absence of the band (OL54/OL143) in the control strain NCYC495*leu1-1.* The 2.91-kb band (for *Δmig1*and 3.9-kb band (for *Δmig1leu1-1*) generated by OL54/OL57 and 0.5-kb band (OL54/OL143) were present in knock out strains. Pair of primers OL54/OL55 did not generate a band in *Δmig1* and *Δmig1 leu1-1*strains. Primer pairs OL91/OL92, CK15/OL156 (Table 1, Figure 1) were used for PCR analysis of *Δmig2* strain. The 1.2-kb band generated by OL91/OL92 from genomic DNA of NCYC495*leu1-1* was absent in the deletion strain. The pair of primers CK15/OL156 was used for indication of a correctly targeted chromosomal integration of *mig2::HpLEU2* fragment. The 2.5-kb band was obtained in PCR for *Δmig2* and was absent in the control strain NCYC495 *leu1-1*. Proper integration of the single *HpMIG1* and *HpMIG2* disruption cassettes were also confirmed by Southern blot analysis (data not shown). The identified *Δmig1* was used in all biochemical and physiological experiments in this study. *Δmig1 leu1-1* was used for construction of *Δmig1Δmig2* double deletion mutant. The *Δmig1leu1-1* and *Δmig2* strains were crossed and diploid hybrids were selected on YNS medium supplemented with G418 (1.0 g L^{-1}) without leucine. After sporulation, *Δmig1Δmig2* double deletion mutant was selected among spore progeny on the same medium, and confirmed for the presence of *HpMIG1* and *HpMIG2* deletion cassettes as detailed above for single deletion mutants. Mating and sporulation techniques were performed by established procedures (Gleeson & Sudbery, 1988).

Results

Identification of *H. polymorpha* homologues of the *S. cerevisiae* Mig1 transcriptional repressor

A search in the *H. polymorpha* genome database (Ramezani-Rad *et al.,* 2003) revealed the presence of two putative homologues of *S. cerevisiae* Mig1 (ScMig1) C2H2 zinc-finger (ZnF) transcriptional repressor (Nehlin & Ronne, 1990). Similar results were obtained after probing the genome database with full-length ScMig1, or its N-terminal ZnF DNA-binding domain, which is highly conserved in all yeast Mig1 homologues (Ostling *et al.,* 1996; Cassart *et al.,* 1997; Zaragoza *et al.,* 2000; Carmona *et al.,* 2002), or the full-length sequence of the related *S.cerevisiae* Mig2 protein (Lutfiyya & Johnston, 1996). As expected, the two identified *H. polymorpha* Mig1 homologues, designated as HpMig1 and HpMig2, exhibit limited overall homology to other yeast Mig proteins: for instance, 26% identity and 41% similarity to ScMig1, 32% identity and 43% similarity to *Candida albicans* Mig1 (Zaragoza *et al.,* 2000), 34% identity and 45% similarity to *Schwanniomyces occidentalis* Mig1 (Carmona *et al.,* 2002). However, in the region of N-terminal ZnF domains, the similarity is high: 80% and 76% identity to ScMig1, for HpMig1 and HpMig2 respectively (Fig. 2A). Other predicted *H. polymorpha* proteins from the genome database exhibit < 50% identity in the ZnF region to ScMig1.

HpMig1 and HpMig2 differ in length (480 and 402 amino acid residues, respectively) and are 33% identical and 44% similar to each other. Both *H. polymorpha* proteins exhibit <69% identity in their ZnF domains to ScMig2, and <66% to the related *S. cerevisiae* Yer028c (Mig3) (Lutfiyya *et al.,* 1998). However, the DNA-binding domains of both *H. polymorpha* Mig proteins are the most similar (> 85% identity) to the corresponding regions of Mig-like CreA repressors from filamentous fungi (Ronne, 1995). Despite the low sequence conservation aside the ZnF region, yeast Mig homologues possess other semi-conserved regions (Cassart *et al.,* 1997), present also in HpMig1 and HpMig2 (Fig. 2B,C) i.e. the so-called C-terminal "effector domain" (Ostling *et al.,* 1996). In addition, the *H. polymorpha* proteins harbour an amino acid region highly similar to fungal CreA repressors that is absent in many yeast Mig proteins (Fig. 2D).

They also possess consensus phosphorylation sites for cAMP-dependent protein kinase (Fig. 2A), and Snf1 protein kinase (not shown), and therefore may potentially be the subject of corresponding regulation (Treitel *et al.,* 1998). Taken together, our analyses suggests that the identified HpMig1 and HpMig2 most probably represent potential ScMig1 orthologues of this methylotrophic yeast. The corresponding sequences were deposited in GenBank under accession numbers EF523343 (*HpMIG1*), and EF523344 (*HpMIG2*).

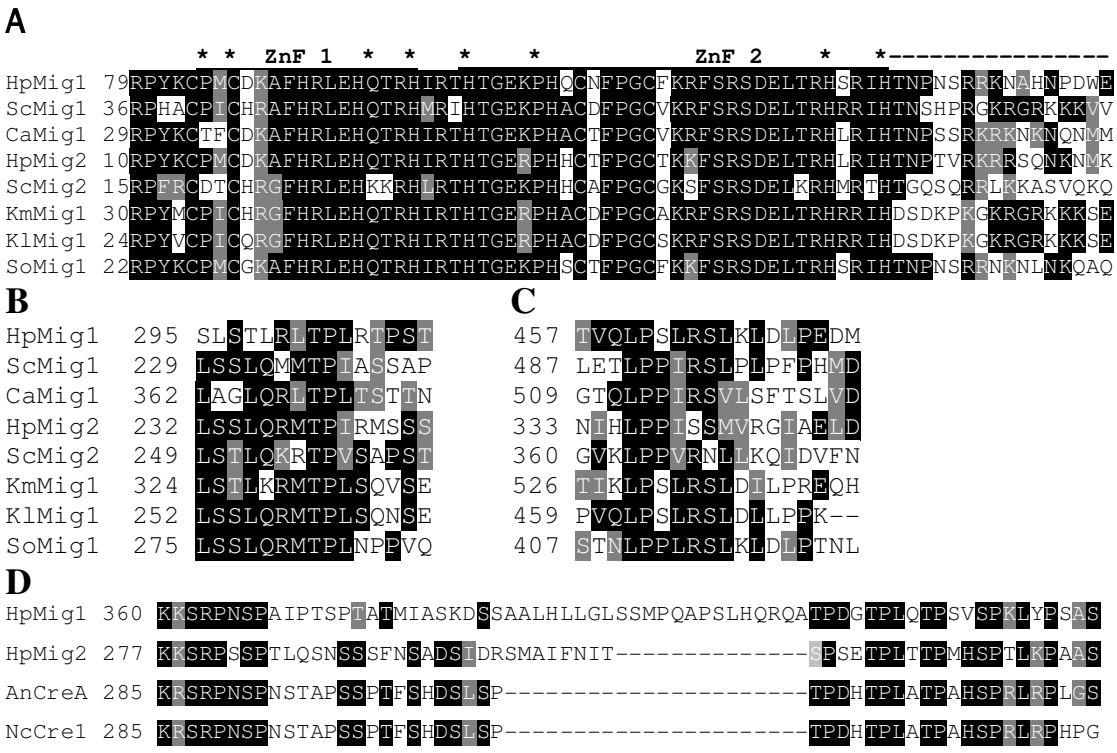

Figure 2. Multiple alignment of conserved regions of HpMIg1 and HpMig2 proteins with yeast Mig1 and fungal CreA homologues. (A) N-terminal zinc finger region. Two zinc finger domains (ZnF) are overlined. Cysteine and histidine residues involved in ZnF domains are indicated with asterisks. The phosphorylation site for cAMP-dependent protein kinase is underlined. Adjacent to ZnF basic region is overlined. (B) Highly conserved region of yeast Mig proteins. (C) Putative C-terminal effector domain. (D) Highly conserved region between *H. polymorpha* Mig and fungal CreA repressors. Species abbreviations are: Hp, *Hansenula polymorpha*; Sc, *Saccharomyces cerevisiae*; Ca, *Candida albicans*; Km, *Kluyveromyces marxianus*; Kl, *Kluyveromyces lactis*; So, *Schwanniomyces occidentalis*; An, *Aspergillus nidulans*; Nc, *Neurospora crassa*. GenPept accession numbers for proteins used in the alignments: ScMig1 - P27705; ScMig2 - P53035; CaMig1 - Q9Y7G2; KmMig1 - P52288; KlMig1 - P50898; SoMig1 - CAD10675; AnCreA - AAR02858; NcCre1 - O59958.

Isolation and physiological characterization of the *H. polymorpha* Δ*mig1*, Δ*mig2* and Δ*mig1*Δ*mig2* double mutant strains

To analyze the physiological significance of the HpMig1 and HpMig2 repressors, we constructed *H. polymorpha* deletion strains in the corresponding genes by gene replacement (Fig. 1; for details see M&M section). Several *Δmig1* and *Δmig2* null mutants were isolated and all were identical with respect to their phenotype (see below). Because HpMig1 and HpMig2 may have a redundant function in transcriptional regulation as observed in *S. cerevisiae* (Lutfiyya *et al.,* 1998), a double deletion *Δmig1Δmig2* mutant strain was isolated from spore progeny of the diploid, resulting from crossing *Δmig1* and *Δmig2* null mutants.

We observed that *Δmig1*and *Δmig2* mutants did not differ from the wild-type strain in growth on solid media supplemented with various carbon sources: glucose, sucrose (glycolytic substrates), ethanol and methanol, whereas the double deletion mutant exhibited retarded growth on sugar substrates (Fig. 3A). The mutants behaved similarly on plates with low sugar concentrations (0.1% w/v) (not shown). However, *Δmig1* and *Δmig1Δmig2* mutants could grow on methanol plates in the presence of 2-deoxyglucose, suggesting an impairment of glucose repression. The *H. polymorpha Δtup1* mutant which is not disturbed for glucose repression was used as a control (Oliveira *et al.,* 2003). Detailed analysis of growth kinetics in liquid cultures confirmed that *mig* mutants exhibit a wild-type growth rate on methanol and ethanol.

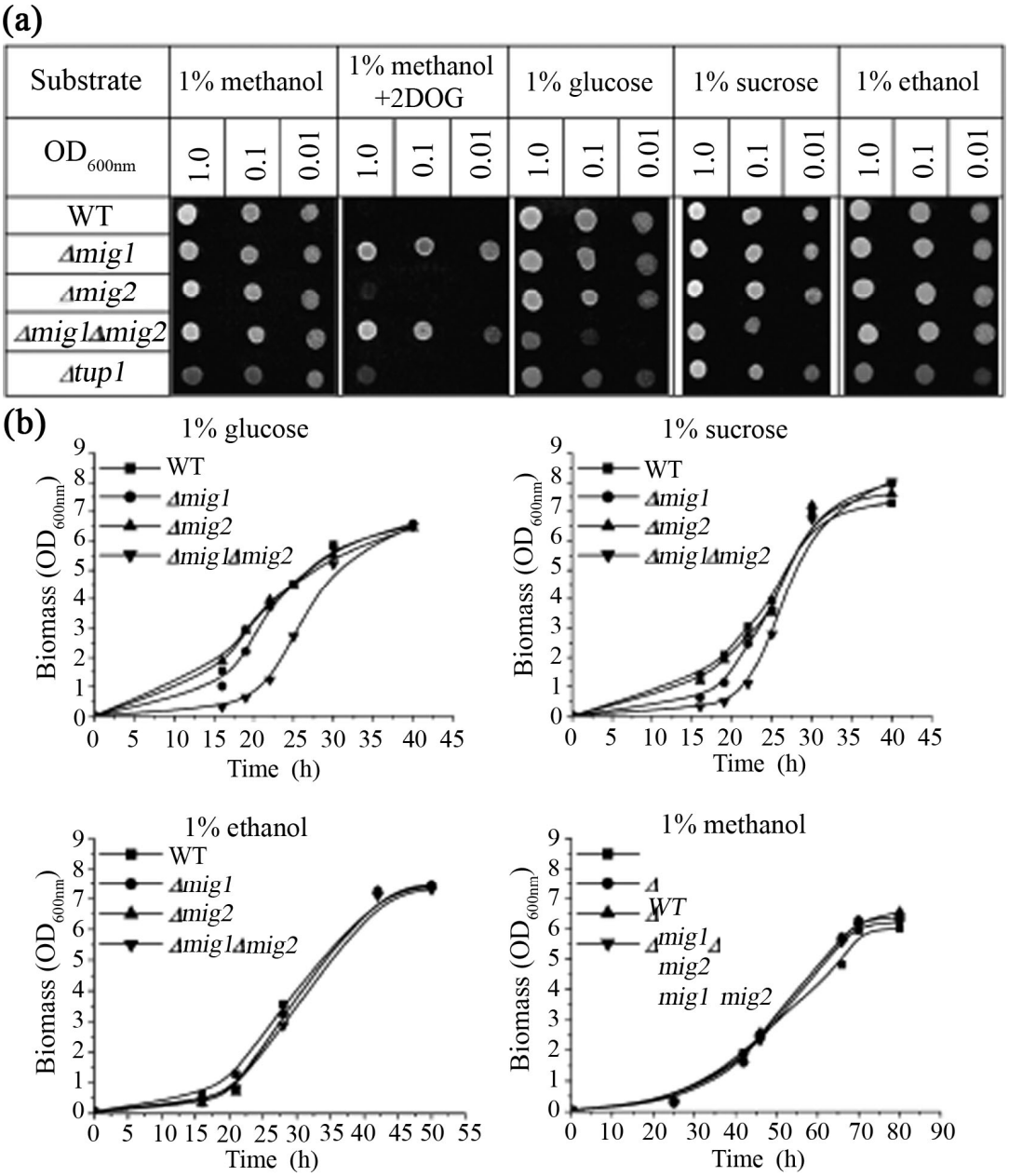

Figure 3. Growth properties of H. polymorpha mig mutants on various carbon sources. (A) Equal volumes of YPS pregrown cell suspensions were loaded in three dilutions on agarized media. Carbon substrate abbreviations: Mth, methanol; Glc,glucose; 2-DOG, 2-deoxyglucose; Sucr, sucrose; Eth, ethanol. Cells were incubated for 1 day on sugar substrates, 2 days on methanol or ethanol, and 3 days on 2-DOG containing medium (B) Kinetics of growth in the liquid culture. Cells of the indicated *H. polymorpha* strains pre-grown on rich YPS medium and shifted to the mineral media with different carbon sources. OD_{600} was measured at the indicated time points after shift.

When grown on sugar substrates, the lag phase in *Δmig1* and double *Δmig1Δmig2* mutants was extended, but growth was not affected in the exponential phase (Fig. 3B). This observation suggests that HpMig1 and HpMig2 may be involved in transient transcriptional response upon glucose adaptation.

Assessment of the role of HpMig1, HpMig2 and HpTup1 in catabolite repression

To get further insight into HpMig1, HpMig2 and HpTup1 function in repression triggered by rich carbon sources, we assayed AO protein levels in the mutants. A very moderate impairment of AO repression was observed for *Δmig1*, *Δmig1Δmig2* and *Δtup1* mutants incubated with low (0.1%) or high (1%) concentrations of glucose (Fig. 4). Previously described by us *Δgcr1* mutant strongly affected in glucose repression and constitutively synthesizing AO in glucose medium (Stasyk *et al.,* 2004) served as a positive control. Interestingly, when methanol was supplemented to glucose medium, the defect in repression in *Δmig1* and *Δmig1Δmig2*, but not in *Δtup1*, became more pronounced (Fig. 4).

This suggests that certain transcriptional induction components are induced for AO synthesis in *Δmig1* cells and may explain the mutants ability to grow on methanol in the presence of 2-deoxyglucose (Fig. 3A).

Still, AO protein level in the double *Δmig1Δmig2* mutant on carbon source mixture was considerably lower relative to glucose-grown *Δgcr1* cells or methanol-grown wild-type cells (Fig. 4 and legend).

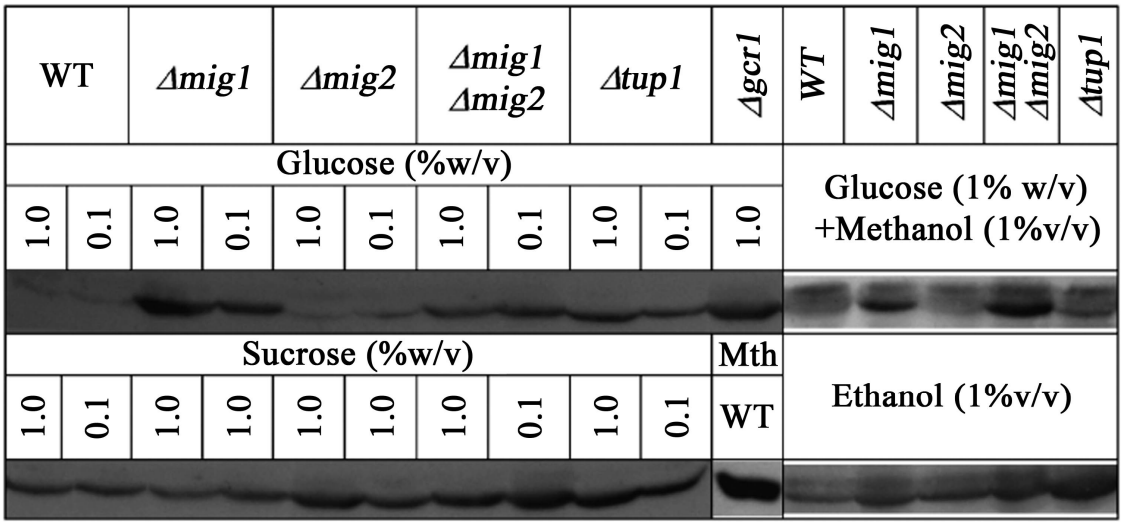

Figure 4. Analysis of AO synthesis upon incubation of wild-type and mutant strains on different carbon sources. Cells of the indicated *H. polymorpha* strains were pre-grown in the rich YPS medium and shifted to mineral media supplemented with different carbon sources (concentrations are indicated), and incubated for 6 hours. 100 μg of glucose-, sucrose- and ethanol-grown *Δmig1, Δmig2, Δmig1Δmig2, Δtup1* and 10 μg of glucose-grown *Δgcr1* TCA extracts of cultures were loaded per lane. 50 μg of methanol-with-glucose-grown cultures were loaded per lane. 5 μg of methanol-grown wild type (WT) culture was loaded per lane to serve as a control [Mth – 1% methanol (v/v)]. AO protein was visualized by Western blotting with anti-AO bodies.

Similarly, AO synthesis in *Δmig1*, *Δmig2*, *Δmig1Δmig2*, and *Δtup1* cells was only weakly derepressed in cells exposed to sucrose or ethanol (Fig. 4), suggesting a limited effect of the analysed mutations on the repression pathway(s) in *H. polymorpha*. We excluded peroxisome degradation as a principal factor influencing AO protein level in the analyzed mutants grown on multicarbon substrates, as pexophagy is blocked (in Δ*tup1*), or impaired in these strains (see next section).

Hansenula polymorpha Mig1 homologues interfere with pexophagy

H. polymorpha HpTup1 is the only transcriptional repressor demonstrated so far to be essential for macropexophagy (Leao-Helder *et al.,* 2004). We were interested in elucidating, whether its possible partners in transcriptional regulation, HpMig1 and HpMig2, also affect this process. In AO activity plate assays, upon a the shift of methanol-grown cells to glucose or ethanol, we observed that *Δmig1* and *Δmig1Δmig2,* but not *Δmig2* cells, exhibit enhanced residual AO activities relative to WT controls. However, the defect in pexophagy in *Δmig1* was less pronounced relative to *Δtup1* cells (not shown).

Similarly to the case for *Δtup1*, no *mig* mutant was significantly affected in general autophagy upon nitrogen starvation, as judged by means of the Phloxine-B plate test (Tsukada & Ohsumi, 1993) (not shown).

Detailed time-course analysis of pexophagy by following AO protein levels revealed that the rate of AO degradation differed between the wild-type strain and *mig* mutants, when methanol-grown cells were exposed to glucose or ethanol (Fig. 5A). However, Western blots demonstrated that also during growth of *Δmig1Δmig2* cells on methanol minor AO degradation bands could be observed that were absent in WT controls (Fig. 5B), indicating that peroxisomes are degraded and pexophagy is not completely blocked at these conditions in *Δmig1Δmig2* cells.

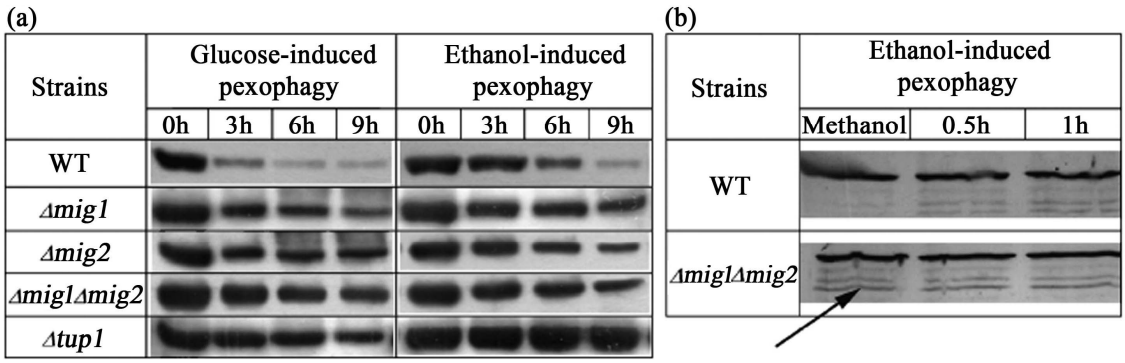

Figure 5. Kinetic analysis of pexophagy. Cells of the indicated strains were grown on methanol medium and shifted to glucose and ethanol media to induce selective peroxisome degradation. Samples were taken at the indicated time points after the shift. Equal volumes of cultures were loaded per lane and analyzed for the presence of AO protein by Western blotting using anti-AO bodies. (A) Kinetics of AO degradation induced by glucose or ethanol. (B) First stages of AO degradation induced by ethanol in WT and *Δmig1Δmig2* strains. Notice the appearance of AO degradation products in extracts of *Δmig1Δmig2* cells incubated in methanol before the shift (arrow).

Electron microscopy of methanol-grown *Δmig1Δmig2* cells exposed to ethanol revealed that peroxisomes indeed undergo degradation and AO protein can be detected in vacuolar lumen (Fig. 6C). Whereas in wild-type controls organelles were degraded via macropexophagy (not shown), unexpectedly in *Δmig1Δmig2* cells sequestration of organelles to be degraded was rarely observed (Fig. 6B). Instead, the morphological characteristics of micropexophagy, i.e. vacuolar protrusions surrounding peroxisome clusters, were prominent (Fig. 6A).

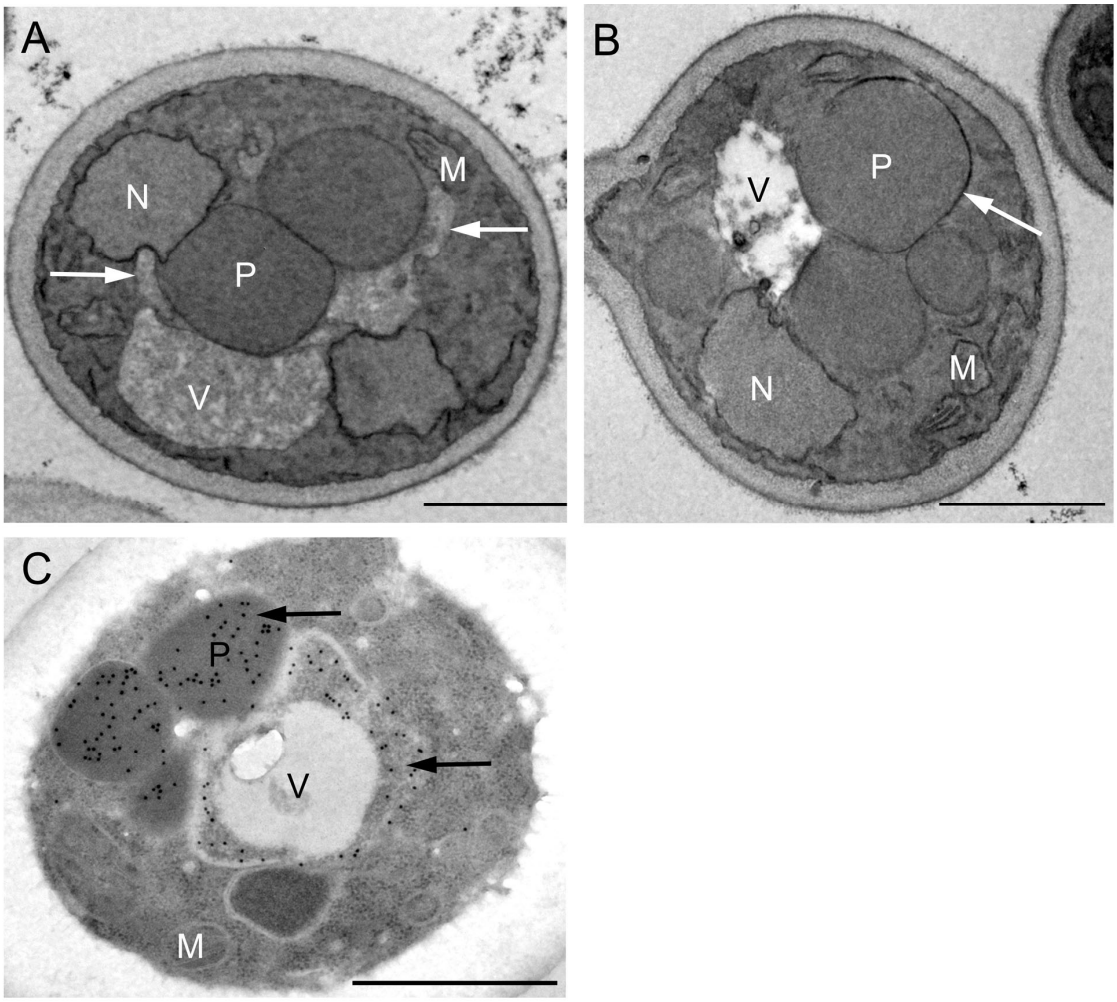

Figure 6. *H. polymorpha* Δ*mig1*Δ*mig2* cells are disturbed in macropexophagy but not in microautophagy. Methanol-grown *Δmig1Δmig2* cells were exposed for 1 hour to ethanol. (A) Peroxisomes are surrounded by vacuolar protrusions, indicative of microautophagy (arrows).

(B) A peroxisome is sequestered by additional membrane structures. However, sequestration is not completed (arrow). (C) Immunolabeling reveals that in methanol-grown *Δmig1Δmig2* cells exposed to ethanol, AO protein is localized both to peroxisomes and vacuole suggesting functional organelle degradation (arrows). Abbreviations used: M, mitochondrion; V, vacuole; P, peroxisome; N, nucleus. The bar represents 1 μm

Discussion

This paper describes the role of *H. polymorpha* transcriptional repressors in catabolite repression and peroxisome degradation (catabolite inactivation), induced by rich carbon sources. We demonstrated that the repression pathway for peroxisomal AO in this yeast apparently only partially relies on the two Mig1 homologues, irrespective of the carbon source (glucose, sucrose or ethanol). However, addition of the inducer, methanol, elevates the AO protein level in *Δmig1Δmig2* mutant incubated with glucose (Fig. 4), suggesting that it exhibits so-called "inducible" phenotype (Sibirny *et al.,* 1988).

In *S. cerevisiae* Mig1 is regulated by glucose (Ostling & Ronne, 1998) and facilitates binding of the general repressor complex Tup1-Ssn6 to the promoters of glucose repressible genes (Gancedo, 1998). However, Tup1 is involved in pleiotropic functions through interaction with specific DNA-binding proteins for each functionally related set of genes (reviewed in Malave & Dent, 2006), while the Mig1-dependent regulation is thought to be more specific, with a limited set of the target genes that include those repressed by glucose (Murad *et al.,* 2001).
Therefore, our results are in line with the previous observation that HpTup1 is not required for glucose repression of peroxisomal enzymes (Oliveira *et al.,* 2003) and suggest that, at least for alcohol oxidase, operation of the classical *S. cerevisiae* pathway with Mig1/2-mediated Tup1-Ssn6 binding to the repressible promoter is unlikely.

However, the redundant function of these repressors cannot be excluded, and the effect of combining all three mutations in one strain would be interesting to examine. An alternative explanation is the involvement of other still-unknown repressor(s). Therefore, further studies are required to obtain conclusive results on whether the effect of *mig1/2* and *tup1* mutations on catabolite repression in response to different carbon sources is direct or indirect. It also has to be investigated whether analysed mutations interfere with regulation of other glucose-repressible genes in *H. polymorpha*, for instance maltase, the regulation of which has been suggested to be Mig-dependent (Alamae *et al.,* 2003).

The pleiotropic function of Tup1 in yeast was recently extended to regulation of macropexophagy (Leao-Helder *et al.,* 2004). The finding that micropexophagy in *H. polymorpha* (Monastyrska *et al.,* 2005) and *P. pastoris* (Tuttle & Dunn, 1995) is sensitive to cycloheximide suggests that it is dependent on protein synthesis, and, consequently, on transcriptional regulation.
Our data suggest that the effect of Tup1 deletion on pexophagy is not mimicked by a similar deficiency in HpMig homologues. In *H. polymorpha Δtup1* mutant, macropexophagy is completely blocked, whereas micropexophagy occurs in the wild-type manner, i.e. only upon nitrogen starvation but not upon a shift of the carbon source (Leao-Helder *et al.,* 2004).

In the *Δmig1Δmig2* deletion strain, macropexophagy may also be impaired, whereas micropexophagy seems to be constitutively induced. This resembles the phenotype of *H. polymorpha Δatg25* mutant, which also displayed constitutive microautophagy in conjunction with a block in macropexophagy (Monastyrska *et al.,* 2005). This apparent similarity of the phenotypes of *H. polymorpha Δmig1Δmig2* and *Δatg25* mutants suggests that certain macropexophagy-specific components may be down-regulated in the absence of Mig repressors and hence, Mig repressors may be positive regulators of macropexophagy. Further research to elucidate the details of these effects is required, including the use of microarray approaches.

With regard to the control of micropexophagy, Mig1 homologues and Tup1 seem to have distinct roles depending on environmental conditions. Mig1 proteins may be a negative regulator of micropexophagy, whereas Tup1 acts as a positive regulator, but only upon a shift in the carbon source and not upon nitrogen depletion conditions. A tentative model explaining such regulations is presented in Figure 7.

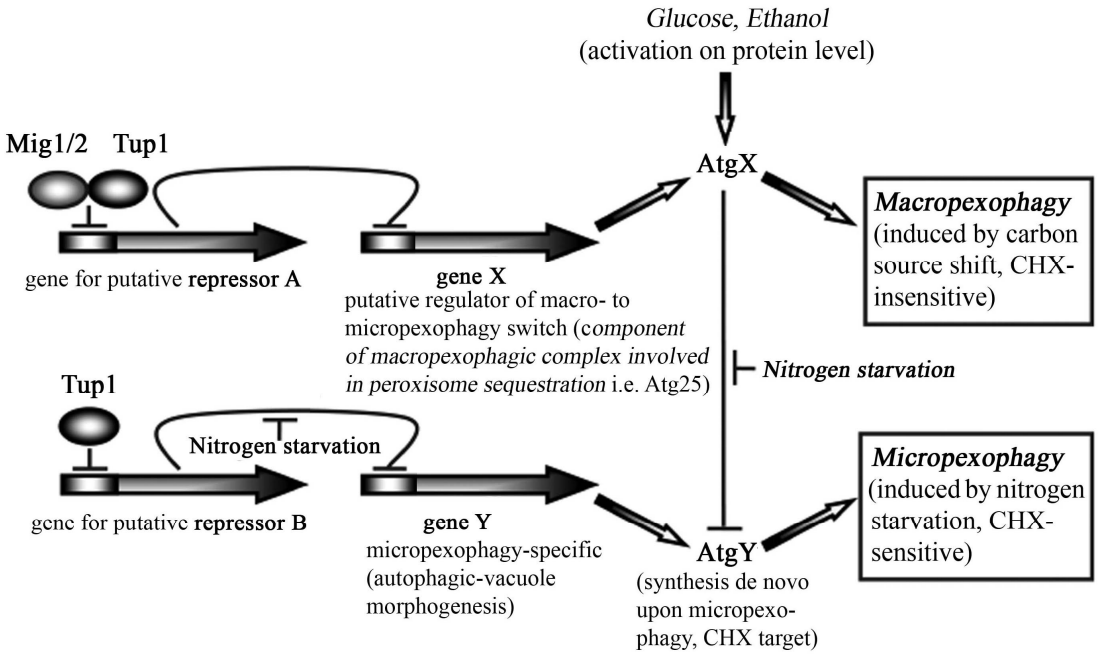

Figure 7. Tentative model of the involvement of HpMig and HpTup1-mediated transcriptional repression in regulation of pexophagy. We suggest that certain components of macropexophagy specific machinery (as HpAtg25) may be negative regulators of micropexophagy. Mig1/2 and Tup1 are indirect positive regulators of such hypothetical proteins (AtgX), which are activated posttranslationally by the effectors of macropexophagy, glucose and ethanol, and inhibit hypothetical micropexophagic component AtgY. AtgX level in the absence of either Mig1/2 or Tup1 is decreased. Nitrogen starvation confers positive regulation of AtgY by inducing its expression and repressing macropexophagy on the protein level. In the absence of Tup1, but not Mig1/2, micropexophagy occurs only upon nitrogen starvation. We suggest that AtgY may be involved in the development of microautophagic vacuoles. CHX – cycloheximide.

Acknowledgements

Authors gratefully acknowledge Rhein Biotech GmbH (Duesseldorf, Germany) for providing access to the *H. polymorpha* genome database.

References

Alamae T, Parn P, Viigand K, Karp H (2003) Regulation of the *Hansenula polymorpha* maltase gene promoter in *H. polymorpha* and *Saccharomyces cerevisiae*. *FEMS Yeast Res* **4(2)**:165–173.

Carmona TA, Barrado P, Jime´nez A & Lobato MF (2002) Molecular and functional analysis of a MIG1 homologue from the yeast *Schwanniomyces occidentalis*. *Yeast* **19**:459–465.

Cassart JP, Ostling J, Ronne H & Vandenhaute J (1997) Comparative analysis in three fungi reveals structurally and functionally conserved regions in the Mig1 repressor. *Mol Gen Genet* **255**:9–18.

Combet C, Blanchet C, Geourjon C & Deléage G (2000) NPS@: network protein sequence analysis*. TIBS* **25**:147-150

Corpet F (1988) Multiple sequence alignment with hierarchical clustering. *Nucl Acids Res* **16**:10881-10890.

Dunn WAJr, Cregg JM, Kiel JA, van der Klei IJ, Oku M, Sakai Y, Sibirny AA, Stasyk OV & Veenhuis M (2005) Pexophagy: the selective autophagy of peroxisomes. *Autophagy* **1(2)**:75-83.

Faber KN, Haima P, Harder W, Veenhuis M & Ab G (1994) Highly-efficient electrotransformation of the yeast *Hansenula polymorpha*. *Curr Genet* **25**:305–310.

Gancedo JM (1998) Yeast carbon catabolite repression. *Microbiol Mol Biol Rev* **62**: 334-361.

Gleeson MA & Sudbery PE (1988) Genetic analysis in the methylotrophic yeast *Hansenula polymorpha*. *Yeast* **4**:293-303.

Johnston M & Kim JH (2005) Glucose as a hormone: receptor-mediated glucose sensing in the yeast *Saccharomyces cerevisiae*. *Biochem Soc Trans* **33(1)**:247-252.

Komduur JA, Bellu AR, Knoops K, van der Klei IJ & Veenhuis M (2004) Cold-inducible selective degradation of peroxisomes in *Hansenula polymorpha*. *FEMS Yeast Res* **5(3)**:281-285.

Kramarenko T, Karp H, Jarviste A & Alamae T (2000) Sugar repression in the methylotrophic yeast *Hansenula polymorpha* studied by using hexokinase-negative, glucokinase-negative and double kinase-negative mutants. *Folia Microbiol (Praha)* **45(6)**:521-529.

Krasovska OS, Stasyk OG, Nahorny VO, Stasyk OV, Granovski N, Kordium VA, Vozianov OF & Sibirny AA (2007) Glucose-induced production of recombinant proteins in *Hansenula polymorpha* mutants deficient in catabolite repression. *Biotechnol Bioeng* **97(4)**:858-870.

Leao-Helder AN, Krikken AM, Lunenborg MG, Kiel JA, Veenhuis M & van der Klei IJ (2004) *Hansenula polymorpha* Tup1p is important for peroxisome degradation. *FEMS Yeast Res* **4(8)**:789-794.

Lombo F, Siems K, Brana AF, Mendez C, Bindseil K, & Salas JA (1997) Cloning and insertional inactivation of *Streptomyces argillaceus* genes involved in the earliest steps of biosynthesis of the sugar moieties of the antitumor polyketide mithramycin. *J Bacteriol* **179**:3354-3357.

Lutfiyya LL & Johnston M (1996) Two zinc-finger-containing repressors are responsible for glucose repression of *SUC2* expression. *Mol Cell Biol* **16**:4790–4797.

Lutfiyya LL, Iyer VR, DeRisi J, DeVit MJ, Brown PO & Johnston M (1998) Characterization of three related glucose repressors and genes they regulate in *Saccharomyces cerevisiae*. *Genetics* **150:**1377–1391.

Malave TM & Dent SY (2006) Transcriptional repression by Tup1-Ssn6. *Biochem Cell Biol* **84(4)**:437-443.

Meijer WH, van der Klei IJ, Veenhuis M & Kiel JA (2007) *ATG* genes involved in non-selective autophagy are conserved from yeast to man, but the selective Cvt and pexophagy pathways also require organism-specific genes. *Autophagy* **3(2)**:106-116.

Monastryska I, Sjollema K, van der Klei IJ, Kiel JA & Veenhuis M. (2002) Microautophagy and macropexophagy may occur simultaneously in *Hansenula polymorpha*. *FEBS Lett* **568**:135-138.

Monastyrska I, Kiel JA, Krikken AM, Komduur JA, Veenhuis M & van der Klei IJ. (2005) The *Hansenula polymorpha ATG25* gene encodes a novel coiled-coil protein that isrequired for macropexophagy. *Autophagy* **1(2)**:92-100.

Monastyrska I & Klionsky DJ (2006) Autophagy in organelle homeostasis: peroxisome turnover. *Mol Aspects Med* **27(5-6)**:483-494.

Murad AM, d'Enfert C, Gaillardin C, Tournu H, Tekaia F, Talibi D, Marechal D, Marchais V, Cottin J & Brown AJ (2001) Transcript profiling in *Candida albicans* reveals new cellular functions for the transcriptional repressors CaTup1, CaMig1 and CaNrg1. *Mol Microbiol* **42**:981-993

Nehlin JO & Ronne H (1990) Yeast *MIG1* repressor is related to the mammalian early growth response and Wilm's tumour finger proteins. *EMBO J* **9:**2891–2898.

Oliveira MA, Genu V, Salmazo AP, Carraro DM & Pereira GA (2003) The transcription factor Snf1p is involved in a Tup1p-independent manner in the glucose regulation of the major methanol metabolism genes of *Hansenula polymorpha*. *Genetics and Mol Biol* **26**: 521-528

Ostling J, Carlberg M & Ronne H (1996) Functional Domains in the Mig1 Repressor. *Mol and Cell Biol* **16(3)**:753–761.

Ostling J & Ronne H (1998) Negative control of the Mig1p repressor by Snf1p-dependent phosphorylation in the absence of glucose. *Eur J Biochem* **252**:162-168.

Papamichos-Chronakis M, Gligoris T & Tzamarias D. (2004) The Snf1 kinase controls glucose repression in yeast by modulating interactions between the Mig1 repressor and the Cyc8-Tup1 co-repressor. *EMBO Rep*. **5(4)**:368-372.

Pereira GG & Hollenberg CP (1996) Conserved regulation of the *Hansenula polymorpha MOX* promoter in *Saccharomyces cerevisiae* reveals insights in the transcriptional activation by Adr1p. *Eur J Biochem* **238(1)**:181-191.

Ramezani-Rad M, Hollenberg CP, Lauber J, Wedler H, Griess E, Wagner C, Albermann K, Hani J, Piontek M, Dahlems U & Gellissen G (2003) The *Hansenula polymorpha* (strain CBS4732) genome sequencing and analysis. *FEMS Yeast Res* **4**:207-215.

Roggenkamp R, Janowicz Z, Stanikowski B & Hollenberg CP (1984) Biosynthesis and regulation of the peroxisomal methanol oxidase from the methylotrophic yeast *Hansenula polymorpha*. *Mol Gen Genet* **194**:489-493.

Ronne H. (1995) Glucose repression in fungi. *Trends Genet* **11(1)**:12-17.

Sakai Y, Oku M, van der Klei IJ & Kiel JA (2006) Pexophagy: Autophagic degradation of peroxisomes. *Biochim Biophys Acta* **1763(12)**:1767-1775.

Sambrook J, Fritsh EF & Maniatis T (1989) Molecular Cloning: A Laboratory Manual. Cold Spring Harbor Laboratory, Cold Spring Harbor, New York.

Sibirny AA, Titorenko VI, Gonchar MV, Ubiyvovk VM, Ksheminskaya GP & Vitvitskaya OP (1988) Genetic control of methanol utilization in yeasts. *J Basic Microbiol* **28(5)**:293-319.

Sohn JH, Choi ES, Kang HA, Rhee JS, Agaphonov MO, Ter-Avanesyan MD & Rhee SK (1999) A dominant selection system designed for copy-number-controlled gene integration in *Hansenula polymorpha* DL-1. *Appl Microbiol Biotechnol* **51:**800–807.

Stasyk OV, Stasyk OG, Komduur J, Veenhuis M, Cregg JM & Sibirny AA (2004) A hexose transporter homologue controls glucose repression in the methylotrophic yeast *Hansenula polymorpha*. *J Biol Chem* **279(9)**:8116-8125.

Tan X, Waterham HR, Veenhuis V & Cregg JM (1995) The *Hansenula polymorpha PER1* gene encodes a novel peroxisomal integral membrane protein involved in proliferation. *J Cell Biol* **128**:307-319.

Treitel MA, Kuchin S & Carlson M (1998) Snf1 protein kinase regulates phosphorylation of the Mig1 repressor in *Saccharomyces cerevisiae*. *Mol Cell Biol* **18**:6273–6280.

Tsukada M & Ohsumi Y (1993) Isolation and characterization of autophagy-defective mutants of *Saccharomyces cerevisiae*. *FEBS Lett* **333**:169-174.

Tuttle DL, Lewin AS & Dunn WA Jr (1993) Selective autophagy of peroxisomes in methylotrophic yeasts. *Eur J Cell Biol* **60(2)**:283-290.

Tuttle DL & Dunn WA Jr (1995) Divergent modes of autophagy in the methylotrophic yeast *Pichia pastoris*. *J Cell Sci* **108(1)**:25-35.

van der Klei IJ, Yurimoto H, Sakai Y & Veenhuis M (2006) The significance of peroxisomes in methanol metabolism in methylotrophic yeast. *Biochim Biophys Acta* **1763(12)**:1453-1462.

van Dijk R, Faber KN, Kiel JA, Veenhuis M & van der Klei I (2000) The methylotrophic yeast *Hansenula polymorpha*: a versatile cell factory. *Enzyme Microb Technol* **26(9-10)**:793-800.

Veenhuis M, Van Dijken JP & Harder W (1983a) The significance of peroxisomes in the metabolism of one-carbon compounds in yeasts. *Adv Microb Physiol* **24**:1-82.

Veenhuis M, Douma A, Harder W & Osumi M **(**1983b) Degradation and turnover of peroxisomes in the yeast *Hansenula polymorpha* induced by selective inactivation of peroxisomal enzymes. *Arch Microbiol* **134**:193–203.

Waterham HR, Titorenko VI, Haima P, Cregg JM, Harder W & Veenhuis M (1994) The *Hansenula polymorpha PER1* gene is essential for peroxisome biogenesis and encodes a peroxisomal matrix protein with both carboxy and amino-terminal targeting signals. *J Cell Biol* **127:**737-749.

Zaragoza O, Rodriguez C & Gancedo C (2000) Isolation of the *MIG1* gene from *Candida albicans* and effects of its disruption on catabolite repression. *J Bacteriol* **182(2)**:320–326.

Chapter 4

Pexophagy in *Hansenula polymorpha*

Tim van Zutphen, Ida J. van der Klei and Jan A.K.W. Kiel

Molecular Cell Biology, Groningen Biomolecular Sciences Institute, University of Groningen, Haren, The Nederlands

Published in *Methods in Enzymology 2008; 451:197-215.*

Article Outline

1. Introduction

2. *Hansenula polymorpha* as model system for peroxisome degradation

3. Cultivation of *H. polymorpha* and induction of peroxisome degradation

3.1. Cultivation of *H. polymorpha* in media supplemented with methanol as the sole carbon and energy source

3.2. Glucose/ethanol induced macropexophagy

3.3. N-starvation induced microautophagy

4. Analysis of peroxisome degradation

4.1. Biochemical analysis

4.1.1. Preparation of cell extracts for biochemical analysis

4.1.2. Analysis of pexophagy by western blot analysis

4.1.3. Analysis of the levels of peroxisomal matrix proteins as marker for peroxisome degradation

4.1.4. Analysis of the levels of peroxisomal membrane proteins as marker for peroxisome degradation

4.1.5. Non-peroxisomal control proteins

4.1.6. Preparation of cell free extracts for specific enzyme activity measurements

4.1.7. Alcohol oxidase activity assay

4.2. Morphological analysis

4.2.1. Fluorescence microscopy

4.2.2. Ultrastructural analysis of pexophagy by electron microscopy

5. Concluding Remarks

Acknowledgements

References

Abstract

In the yeast *Hansenula polymorpha* the development and turnover of peroxisomes is readily achieved by manipulation of the cultivation conditions. The organelles massively develop when the cells are incubated in the presence of methanol as the sole source of carbon and energy. However, they are rapidly and selectively degraded when methanol-grown cells are placed at conditions of repression of methanol metabolism, e.g. in glucose or ethanol excess conditions, by a process termed macropexophagy. Degradation of peroxisomes is also observed when the cells are placed at nitrogen depletion conditions (microautophagy). This contribution details the methodologies that are currently in use investigating macropexophagy and microautophagy in *H. polymorpha*. Emphasis is placed on various structural (fluorescence microscopy, electron microscopy) and biochemical (specific enzyme activity measurements, western blotting) approaches.

1. Introduction

Organelle homeostasis is a requisite for optimal functioning of eukaryotic cells. One of the modes to achieve this is that specific cell organelles proliferate when required and are removed when they have become superfluous. In eukaryotes, the two major proteolytic degradation processes are the ubiquitin-proteasome pathway and autophagy. The first process is solely involved in the degradation of single protein molecules (Ciechanover, 2006), whereas the latter is capable of degrading a wide range of intracellular constituents (proteins, lipids or DNA) in the lysosome/vacuole (Klionsky, 2007). Although the process of autophagy was already described by de Duve in 1963 (de Duve, 1963; de Duve & Wattiaux, 1966), only recently has this topic gained substantial interest, mainly because of its role in a wide variety of processes, such as cell development, ageing, cell death and immunity (Mizushima *et al.,* 2008). Hence, autophagy is very important in human health and disease (Shintani & Klionsky, 2004).

The key proteins required for autophagy and autophagy related processes are encoded by *ATG* genes and most are conserved from yeast to man (Meijer *et al.,* 2007). Due to their versatility in handling, yeast species are ideal model organisms for studying the molecular mechanisms of autophagy. Indeed, most *ATG* genes were initially discovered in yeast (Klionsky *et al.,* 2003).

In particular the process of peroxisome degradation is studied in these organisms since the development and turnover of these organelles is readily manipulated by the growth conditions.

Here we describe the degradation of peroxisomes by autophagy in the methylotrophic yeast *Hansenula polymorpha* and focus on the experimental approaches that are used to monitor this process.

2. *Hansenula polymorpha* as a model system for peroxisome degradation

A limited number of micro-organisms is capable of growing on one-carbon compounds (methylotrophs). In yeast species, methylotrophy is limited to the utilization of methanol as the sole source of carbon and energy. Examples of methylotrophic yeast species are *Candida boidinii, H. polymorpha* and *Pichia pastoris*. In these organisms the initial oxidation of methanol is catalyzed by the enzyme alcohol oxidase (AO), which is a peroxisomal oxidase that generates formaldehyde and hydrogen peroxide from methanol. Formaldehyde can be assimilated via the xylulose-5-phosphate pathway, which involves the peroxisomal enzyme dihydroxyacetone synthase (DHAS), whereas hydrogen peroxide may be decomposed by peroxisomal catalase (CAT). The other enzymes involved in methanol metabolism (e.g. formaldehyde dissimilation enzymes and the other enzymes of the xylulose-5-phosphate pathway) are all localized to the cytosol (reviewed in van der Klei *et al.,* 2006).

When methylotrophic yeast species are grown on media containing glucose as the sole carbon and energy source and ammonium sulphate as nitrogen source, peroxisomal enzymes are not required for primary metabolism.

As a consequence, the cells generally contain one or only a few small peroxisomes. However, upon a shift to media containing methanol as the sole carbon source, enzymes involved in methanol metabolism are induced concomitant with an increase in the number and size of peroxisomes. Conversely, placing methanol-grown *H. polymorpha* cells into fresh glucose media leads to rapid degradation of the - now superfluous - organelles. This degradation of peroxisomes (pexophagy), is highly selective and resembles macroautophagy in mammalian cells (Leighton *et al.,* 1975) and hence is designated macropexophagy (Klionsky *et al.,* 2007). During this process individual organelles are consecutively sequestered from the cytoplasm by membranous layers forming autophagosomes. After sequestration is complete, the outer membrane layer of the autophagosome fuses with the vacuolar membrane resulting in incorporation of the sequestered peroxisome into the vacuole, where the entire organelle becomes degraded by vacuolar hydrolases (depicted in Fig. 1A).

The molecular mechanisms involved in the formation of autophagosomes and fusion of this organelle with the vacuole overlap with those involved in general macroautophagy, because various Atg proteins are involved in both processes.
Initiating macropexophagy, however, requires the function of two peroxisomal membrane proteins, Pex3 and Pex14. The function of these two peroxins, that are also essential for peroxisome biogenesis, is completely different.

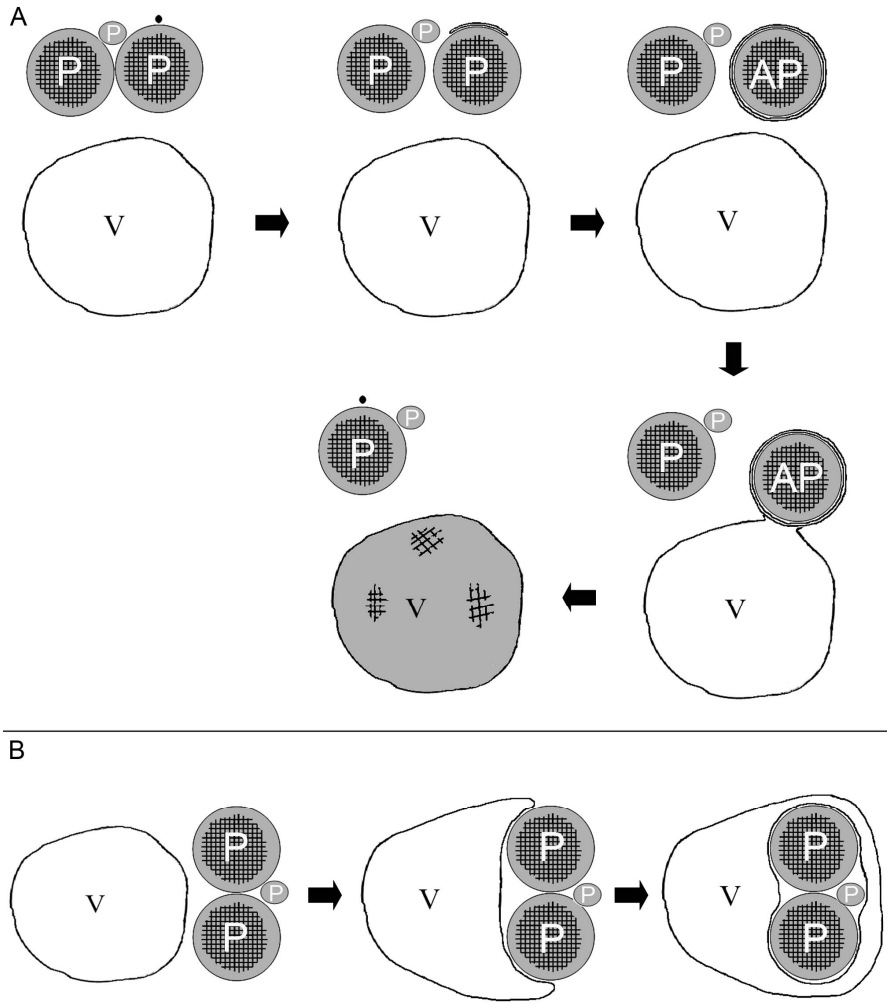

Figure 1. Methanol-grown *H. polymorpha* cells contain mature peroxisomes (P) as well as at least one immature organelle. (A) Upon induction of macropexophagy, a single mature organelle is tagged for degradation (marked by the black dot) followed by its sequestration by multi-membrane layers forming an autophagosome (AP). After sequestration is completed, the outer membrane layer of the autophagosome fuses with the vacuolar membrane resulting in the uptake of the organelle into the vacuole (V), where it is degraded by vacuolar hydrolases. Next, one by one, other mature peroxisomes are tagged and degraded. Only one (or few) immature peroxisome(s) escape(s) degradation. (B) Upon induction of microautophagy the vacuole engulfs (part of) a cluster of peroxisomes that is subsequently degraded in the vacuole lumen.

Remarkably, one of these, Pex3, has to be removed from the peroxisomal membrane to allow initiation of pexophagy, whereas Pex14 probably acts as the site of recognition of the organelle by the autophagy machinery (Bellu *et al.,* 2001a, 2002). Recognition most likely involves Atg11, a protein also functional in other selective modes of autophagy (Kiel *et al.,* 2003). Atg11 has been localized to the PAS (pre-autophagosomal structure) and autophagosomal membranes and is thought to be involved in recruiting selective cargo to the autophagosome (Yorimitsu & Klionsky, 2005).

In the related methylotrophic yeast *P. pastoris*, a peroxisomal membrane protein exclusively involved in selective peroxisome degradation was recently uncovered (designated Atg30) and may be involved in this process as well (Farre *et al.,* 2008). A putative Atg30 ortholog is present in *H. polymorpha*, but its function in pexophagy has not yet been confirmed.

In addition to macropexophagy, nitrogen limitation leads to peroxisome degradation in *H. polymorpha* by a mechanism known as microautophagy. However, this process is not considered a selective pathway, since cytosolic components are taken up concomitantly with peroxisomes (Bellu *et al.,* 2001b).

Induction of microautophagy by nitrogen starvation results in a direct engulfment and subsequent uptake of peroxisomes and cytoplasmic components by the vacuole (Fig. 1B). Microautophagy is therefore morphologically very distinct from macropexophagy. Nevertheless many components of the macroautophagy machinery function also in microautophagy (Sakai *et al.,* 2006).

Remarkably, in *H. polymorpha* microautophagic degradation of peroxisomes, but not of other cytoplasmic constituents, requires Atg11, suggesting some mode of selectivity of peroxisome degradation during nitrogen starvation (Komduur *et al.,* 2004).

3. Cultivation of *H. polymorpha* and induction of pexophagy

3.1. Cultivation of *H. polymorpha* in media supplemented with methanol as the sole carbon and energy source

For induction of pexophagy, cells from the exponential growth phase on methanol are preferably used. Care should be taken that all nutrients are present in excess and that cultures are optimally aerated. We generally use (auxotrophic derivatives of) the *H. polymorpha* strain NCYC495 and mutants generated from this strain (Gleeson & Sudbery, 1988).

For inoculation of glucose-containing batch cultures, colonies plated on a glucose-containing agar plate (e.g., YPD plate) are used. These plates can be stored at 4ºC for several weeks.

For pre-cultivation, a mineral medium (van Dijken *et al.,* 1976; Table 1) is used that contains 0.25% ammonium sulphate as nitrogen source and is supplemented with 0.5% glucose as carbon source. Optimal growth of *H. polymorpha* cells on methanol media and maximal induction of peroxisomes is only obtained when cells are extensively pre-grown on glucose prior to the shift to methanol medium. Therefore, methanol-grown cells should not be used as inoculum for these cultures.

Protocol:

1. Normally, cells from fresh glucose plates are used as inoculum. Cells are pre-cultured at 37ºC at 200 rpm in a 100 ml flask with 20 ml mineral medium containing 0.5% glucose until an optical density (OD, expressed as absorption at 660 nm) of 1.5-1.8 is reached.

2. The culture is diluted to OD_{660} = 0.1 in fresh glucose medium and grown again until the mid-exponential growth phase. This procedure is normally repeated three times until the cells continuously grow at maximal speed (doubling time of approx. 1 hour for wild-type cells).

Table 1. composition of mineral medium

Components	**g/l**	**Vishniac stock solution (1000x)**	**g/l**	**Vitamin stock solution (1000x)**	**g/l**
$(NH_4)_2SO_4$	2.5	EDTA (Titriplex-III)	10	Biotin	0.1
$MgSO_4$	0.2	$ZnSO_4.7H_2O$	4.4	Thiamin	0.2
K_2HPO_4	0.7	$MnCl_2.4H_2O$	1.01	Riboflavin	0.1
NaH_2PO_4	3.0	$CoCl_2.6H_2O$	0.32	Nicotinic acid	5
yeast extract	0.5	$CuSO_4.5H_2O$	0.315	p-Amino-benzoic acid	0.3
Vishniac stock solution	1.0 ml	$(NH_4)_6Mo_7O_{24}.4H_2O$	0.22	Pyridoxal hydrochloride	0.1
		$CaCl_2.2H_2O$	1.47	Ca-panthothenate	2
add after autoclaving:		$FeSO_4.7H_2O$	1.0	Inositol	10
Vitamin stock solution	1.0 ml			*Sterilize by filtration*	
Carbon source	0.5 %				

3. Cells from the mid-exponential growth phase (OD_{660} = 1.5-1.8) are diluted in 100 ml fresh mineral medium containing 0.5% methanol as the sole source of carbon (starting at OD_{660} = 0.1) in a 500 ml flask. After a short lag phase wild-type cells start to grow on methanol (normal doubling time is approximately 4-4.5h). Cultures at the late exponential growth phase (OD_{660} = 1.8-2.4) are used to induce peroxisome degradation.

3.2. Glucose/ethanol induced macropexophagy

In *H. polymorpha*, macropexophay is induced by exposure of methanol-grown cells to excess glucose or ethanol conditions. Both addition of glucose/ethanol to cultures growing on methanol as well as a dilution of methanol-grown cells in fresh glucose/ethanol media have been applied successfully. Although addition of glucose or ethanol to a methanol culture is experimentally easier, it must be noted that prolonged cultivation may ultimately lead to depletion of medium components (e.g. vitamins, amino acids etc.) as cultures with very high densities may be obtained.
This carries the risk of induction of non-selective autophagy due to starvation as well. Hence, a shift of cells to fresh glucose/ethanol medium is preferred.

Protocol:

1. Dilute the methanol culture in fresh, pre-warmed medium lacking a carbon source to an OD_{660} = 0.2.
2. Immediately and rapidly take a sample (T = 0 h; for OD measurement and biochemical or microscopy analysis, see below), followed by addition of inducer (glucose, ethanol) to a final concentration of 0.5%.
3. Continue to incubate the cells at 37ºC at 200 rpm.
4. Take samples of an equal culture volume as performed at step 2, at T= 1, 2 ,3 and 4 h after the addition of the inducer.

3.3. N-starvation induced microautophagy

Upon a shift of *H. polymorpha* cells from media containing excess nitrogen (generally ammonium sulphate) to media lacking any nitrogen source (i.e. also excluding amino acids), non-selective autophagy is induced.

Protocol:

1. Cells are grown on methanol (100 ml), as described above.
2. Cells are collected by centrifugation (5 min at 3,000 g at 37ºC).
3. The supernatant fraction is discarded and the cells are rapidly resuspended in an identical volume of pre-warmed mineral medium lacking any nitrogen source.
4. Samples are taken at 2 hour intervals to follow the fate of peroxisomes - and other proteins - over time.

4. Analysis of peroxisome degradation

To determine whether degradation of peroxisomes has occurred, several approaches are suitable. A combination of at least two experimental approaches is preferred.

4.1. Biochemical analysis

4.1.1. Preparation of cell extracts for biochemical analysis.

Peroxisome degradation can be demonstrated by western blot analysis of samples taken prior to, and after, the induction of autophagy, using antibodies against peroxisomal marker proteins. For western blot analysis, a culture volume corresponding to at least 3 OD_{660} (volume x OD_{660}) units is harvested. 3 OD_{660} units correspond to approximately 300 µg protein.
Upon induction of peroxisome degradation the cells may continue to grow, while peroxisome formation and the synthesis of peroxisomal proteins of methanol metabolism (AO, DHAS and CAT) is fully repressed. Thus, equal volumes of the culture before and after induction of peroxisome degradation should be studied.

Protocol:

1. Cells are pre-cultured in glucose, grown in methanol-containing medium and then shifted to glucose, ethanol or nitrogen-starvation medium as described in section 3.
2. Cultures are cooled on ice followed by collection of the cells by centrifugation (10,000 x g for 10 min at 4ºC in case of large volumes or for 1 min at 14,000 x g in a microcentrifuge when using small volumes).
3. The supernatant fractions are discarded and the cell pellets are resuspended in a solution containing 12.5% trichloroacetic acid (TCA) by vortexing, followed by freezing at -80ºC for at least 30 min.
4. For analysis, the frozen samples are thawed on ice and centrifuged at 14,000 x g at 4ºC for 5 min to collect the cells.
5. The cell pellet is washed twice (by resuspending thorougly followed by centrifugation) using 500 µl 80% ice-cold acetone (v/v) in order to remove residual TCA.
6. The pellet is dried by exposure to air and resuspended in 100 µl of a solution containing 1% SDS and 0.1 N NaOH. The high pH of this solution causes the yeast cell wall to disintegrate whereas SDS dissolves the cellular membranes. The pellet is resuspended (using a vortex) until a homogeneous cell suspension is obtained.
7. The suspension is mixed with an equal volume of concentrated SDS sample buffer (4% SDS, 10% β-mercaptoethanol, 20% glycerol, 0.002% bromophenol blue, 0.1 M Tris·HCl, pH 6.8) and boiled for 5 min.
8. Prior to loading onto an SDS-polyacrylamide gel, the sample is centrifuged for 3 min at 10,000 x g to sediment residual cell debris. The gels are used for western blotting to analyze the levels of peroxisomal marker proteins.

Cytosolic and/or mitochondrial marker proteins should be used as controls to monitor whether or not selective peroxisome degradation has occurred.

4.1.2. Analysis of pexophagy by western blot analysis

Since the synthesis of the methanol metabolism-related peroxisomal matrix proteins is fully repressed in glucose or ethanol excess conditions, the biochemical analysis of peroxisome degradation has focused on following the amount and/or specific activities of these proteins. A distinction can be made between peroxisomal matrix proteins and membrane proteins. In specific cases, in which matrix proteins cannot be used as a marker for peroxisome degradation for instance when using a mutant in which matrix protein import is strongly impaired (e.g., a *pex* mutant), the fate of peroxisomal membrane proteins should be analyzed.

4.1.3. Analysis of the levels of peroxisomal matrix proteins as a marker for peroxisome degradation

In *H. polymorpha* cells grown on methanol as the sole carbon source, AO is an abundant peroxisomal matrix protein, constituting 5-30% of the total cellular protein dependent on growth conditions.

The relatively high abundance of AO renders it an excellent marker to study the fate of peroxisomes after induction of peroxisome degradation, either by following the reduction of the level of AO protein over time (by western blotting) or by determining the decrease in AO specific enzyme activities (described below).

For analysis by western blotting, successive samples of a time series of cells that were transferred to pexophagy-inducing conditions, are loaded on 10% SDS-PAA gels.
After western blotting by standard protocols, a specific α-AO primary rabbit antiserum is used, followed by an alkaline phosphatase-conjugated secondary anti-rabbit antibody using NBT-BCIP as substrate for the detection of the immunogenic protein bands. In the protein samples taken after induction of pexophagy, the intensity of the AO band (running at ± 70 kDa) should decrease with time, which can be quantified by densitometry scanning of the blots. Additionally, degradation of AO results in the appearance of lower molecular weight degradation bands on the blot (Fig. 2). Because AO is inactivated during peroxisome degradation (Bruinenberg *et al.,* 1982), generally the kinetics of the decrease in enzyme activities is faster relative to the decrease of AO protein (see below).

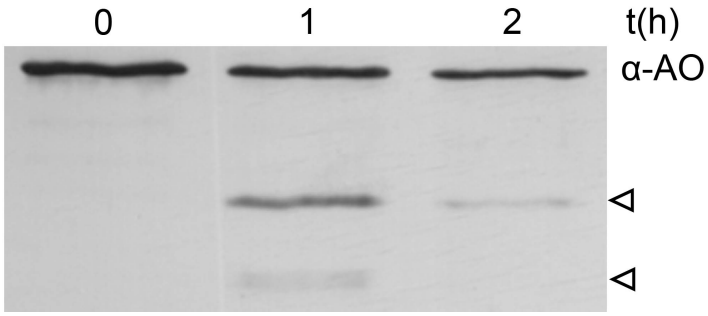

Figure 2. Western blot, prepared of crude extracts of methanol-grown *H. polymorpha* cells exposed for the indicated time points to 0.5% glucose, using an α-AO specific antiserum. AO protein levels decrease in time, while also characteristic AO degradation products (arrowheads) are observed.

4.1.4. Analysis of the levels of peroxisomal membrane proteins as a marker for peroxisome degradation

Next to monitoring the fate of a peroxisomal matrix protein by western blotting, the decrease in the level of peroxisomal membrane proteins can also be used.

However, proteins containing domains exposed to the cytosol might also be susceptible to other modes of degradation, e.g., via the ubiquitin-proteasome pathway. Before using a novel membrane protein as a tool to study pexophagy, its turnover by alternative pathways should be determined, e.g., by studying the change in levels upon induction of peroxisome degradation in an *atg1* mutant.

H. polymorpha Pex10 is a suitable peroxisomal membrane marker for degradation studies (Veenhuis *et al.,* 1996). However, because of the generally low levels of Pex10, the sensitive chemiluminescent horseradish peroxidase method is preferred (Roche BM Chemiluminescent western Blotting Kit) over the alkaline phosphatase-based method.

In addition, a constructed fusion protein consisting of the first 50 amino acids of the peroxisomal membrane protein Pex3 fused to GFP (N50.Pex3.GFP), expressed under control of the inducible *AOX* promoter, has been successfully used as a marker (van Zutphen *et al.,* 2008; see Fig. 3). The GFP portion of the fusion protein forms a rather stable barrel structure, which is relatively slowly degraded in the vacuole. The formation of cleaved N50.Pex3.GFP can also easily be monitored by western blotting or fluorescence methods (Shintani & Klionsky, 2004).

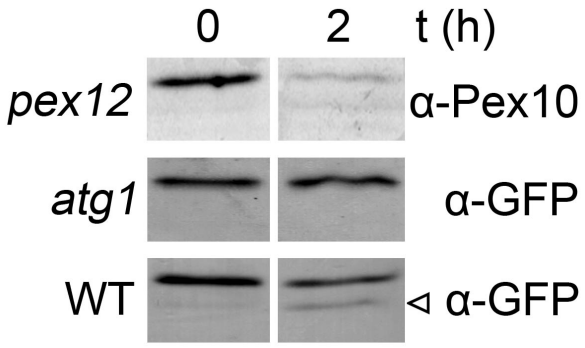

Figure 3. Glycerol/methanol-grown *pex12* cells, as well as methanol-grown *atg1* and wild-type cells that produce N50.Pex3.GFP, were exposed to excess glucose conditions to induce macropexophagy. Samples were taken prior to and 2 hours after induction and analyzed by western blotting, using α-Pex10 (for *pex12* cells) and α-GFP antisera (for *atg1* and wild-type cells). In *pex12* cells - that contain peroxisome remnants - and in wild-type cells, but not in *atg1* cells, peroxisome components decline, indicating their proteolytic turnover. In wild-type cells a second α-GFP specific protein band is observed (arrowhead) that represents free GFP accumulating in the vacuole due to its relative stability towards vacuolar hydrolases.

4.1.5. Non-peroxisomal control proteins

To determine the specificity of the peroxisome degradation process, turnover of other components in the cell should also be analysed. This has been performed mainly by western blot analysis. As markers for mitochondria, porin or malate dehydrogenase may be used, whereas as a representative of the endoplasmatic reticulum, the levels of Sec63 may be analyzed (Kiel *et al.,* 1999). As marker for the cytosol translation elongation factor 1-α (eEF1α), and Hsp70 may be applied successfully (Bellu *et al.,* 2001b).

4.1.6. Preparation of cell-free extracts for specific enzyme activity measurements

Specific enzyme activity measurements to follow peroxisome degradation are performed in crude cell free extracts which are prepared as follows.

Protocol:

1. Harvest a culture of cells - grown under the appropiate conditions as described above to induce pexophagy - with a volume corresponding to approximately 10 OD_{660} units (volume x OD_{660}) and cool on ice.
2. Centrifuge the cells for 5 min at 3,000 x g and wash the pellet twice (by resuspending and centrifugation) using 10 ml of 50 mM potassium phosphate buffer, pH 7.2.
3. Resuspend the cells in 500 µl potassium phosphate buffer and lyse the cells using a vortex or Fastprep (FP120, Bio101/Savant, Qbiogene inc, Cedex, France) after addition of 0.5 volume of acid-washed glass beads for 1 min (see chapter 1),
followed by cooling on ice for 1 min. This is repeated until the majority of the cells are broken (checked by light microscopy).
4. Remove unbroken cells and cell debris by centrifugation for 5 min at 14,000 rpm at 4ºC. The resulting supernatant can be used for enzyme activity measurements.

4.1.7. Alcohol oxidase activity assay

Alcohol oxidase catalyzes the oxidation of methanol, thereby producing formaldehyde and hydrogen peroxide. The hydrogen peroxide that is generated can be assayed via the oxidation of reduced ABTS (2.2. Azino-di-[2-ethyl benztioazolin sulfonate]) depicted in formula (I).

This reaction is catalyzed by peroxidase. The end-product, oxidized ABTS, has a green color with an absorption maximum at 420 nm (Verduyn *et al.,*1984).

(I)

$$CH_3OH + O_2 \rightarrow H_2CO + H_2O_2$$

$$H_2O_2 + 2\ ABTS_{red} \rightarrow H_2O + 2\ ATBS_{ox}$$

Protocol:

1. Add an appropriate amount of buffer A (0.5 mg/ml ABTS, 10 U/ml horseradish peroxidase, in 50 mM potassium phosphate buffer, pH 7.2) to a glass cuvette such that together with the sample the final volume will be 990 µl. Place the cuvette into the thermostated cuvette holder of a spectrophotometer (temperature set to 37ºC).

2. Add the required amount of cell free extract (as prepared in section 4.1.6).

3. Record absorbance at 420 nm (A_{420nm}) and equilibrate until the absorbance remains constant.

4. Add 10 µl of 10 M methanol (40% v/v) and mix.

5. Measure the change in absorbance at 420 nm.

6. Perform the assay in triplicate using 3 different sample volumes. All three measurements should result in similar specific activities.

7. Calculate the enzyme activity using the following equation:

$$\text{Units/mg} = \frac{V}{2.\varepsilon.d.v.c} \quad \frac{\Delta t}{\Delta E}$$

V = total volume (ml), v = sample volume (ml), ε = extinction coefficient ($cm^2/\mu mol$) = 43,2 $cm^2/\mu mol$, d = length of the light path, c = protein concentration of the sample in mg/ml

ΔE = change in absorbance, Δt = change in time (minutes)

4.2. Morphological analysis

Uptake of peroxisomes by the vacuole during autophagy can be visualized by electron microscopy or, after introduction of a fluorescent peroxisomal marker, by fluorescence microscopy.

4.2.1. Fluorescence microscopy

To visualize peroxisomes, fluorescent proteins are used that are either sorted to the peroxisomal lumen or its surrounding membrane. The use of a fluorescent matrix protein is preferred since it is not susceptible to degradation by processes other than autophagy. The most common peroxisomal matrix targeting signal is the C-terminal PTS1 (-SKL). Thus, Green Fluorescent Protein (GFP) fused to SKL localizes to the peroxisomal matrix in *H. polymorpha*. During peroxisome degradation, the matrix contents are released into the vacuolar lumen, as observed in Figure 4. A suitable peroxisomal membrane marker is the fusion protein N50.Pex3.GFP (see section 4.1.4). This marker can also be used to tag peroxisomal membranes in mutants defective in matrix protein import (Fig. 4; for details see van der Klei & Veenhuis 2007).
To demonstrate that peroxisomes have indeed been taken up by the vacuole, the vacuolar membrane can be specifically stained with the red fluorescent dye FM 4-64 (N-(3-triethylammonium-propyl)-4-(6-(4-(diethylamino) phenyl)hexatrienyl)pyridinium-dibromide, Molecular probes Invitrogen). To label with FM 4-64, 0.5 to 1 ml of culture is incubated with 1 µl of FM 4-64 solution (100 µg dissolved in 83 µl DMSO, 1µg/µl) for at least 45 minutes at 37ºC with shaking at 200 rpm, followed by washing with pre-warmed media (also see chapter 7).

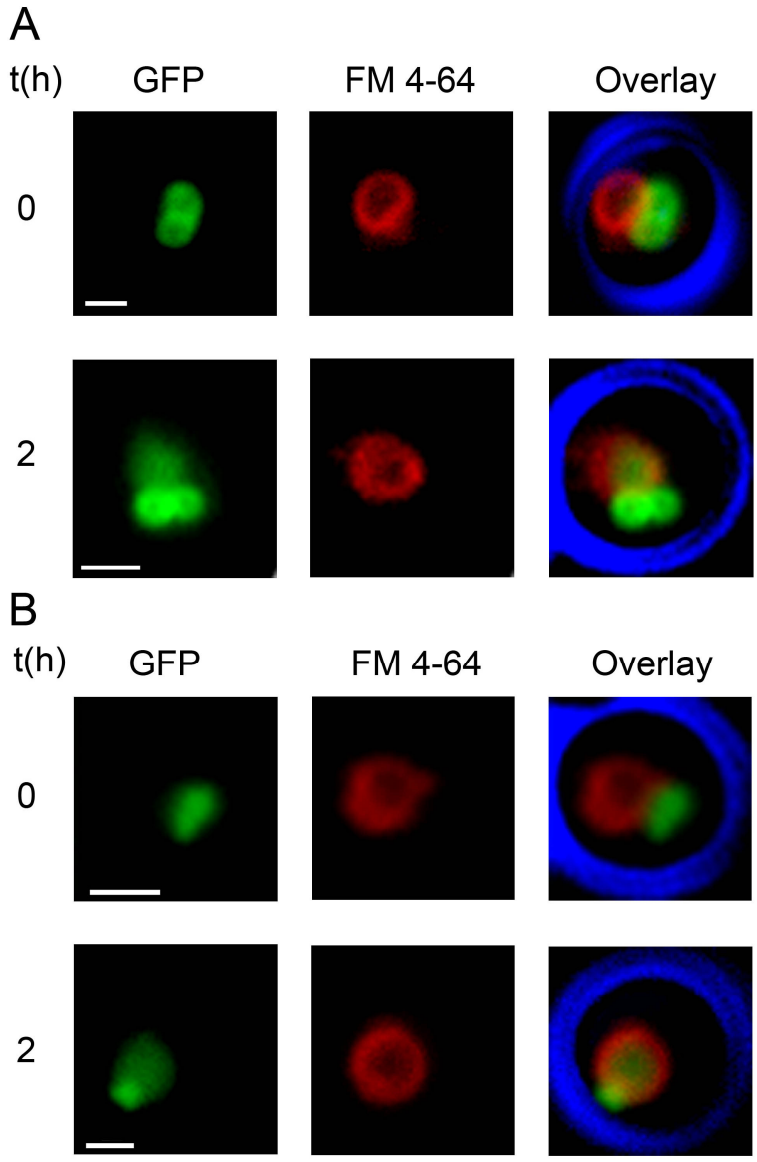

Figure 4. Fluorescence microscopy analysis of glucose-induced macropexophagy. (A) In wild-type *H. polymorpha* cells producing GFP.SKL peroxisomes are visualized by GFP fluorescence, the vacuoles by FM 4-64. At T=0 the vacuoles lack GFP fluorescence, which is evident after 2 hours of incubation in the presence of glucose, confirming that macropexophagy has occurred.
(B) In *pex13* cells peroxisome remnants are marked by N50.Pex3.GFP. Also these structures are subject to degradation at macropexophagy conditions, as is demonstrated by the presence of GFP fluorescence in the vacuole after 2 hours of incubation. The bar represents 1 μm.

Since FM 4-64 is taken up by endocytosis, the relatively slower growing methanol cells need to be incubated longer than cells cultivated on glucose.

4.2.2. Ultrastructural analysis of pexophagy by electron microscopy

Electron microscopy allows obtaining detailed morphological information on peroxisome degradation. Two types of fixation techniques are routinely used prior to embedding the cells for electron microscopy. Of these, potassium permanganate fixation is suited to visualize overall cell morphology, in particular membranes (Fig. 5A), whereas aldehyde fixations are generally used for immunocytochemistry (Fig. 5B).

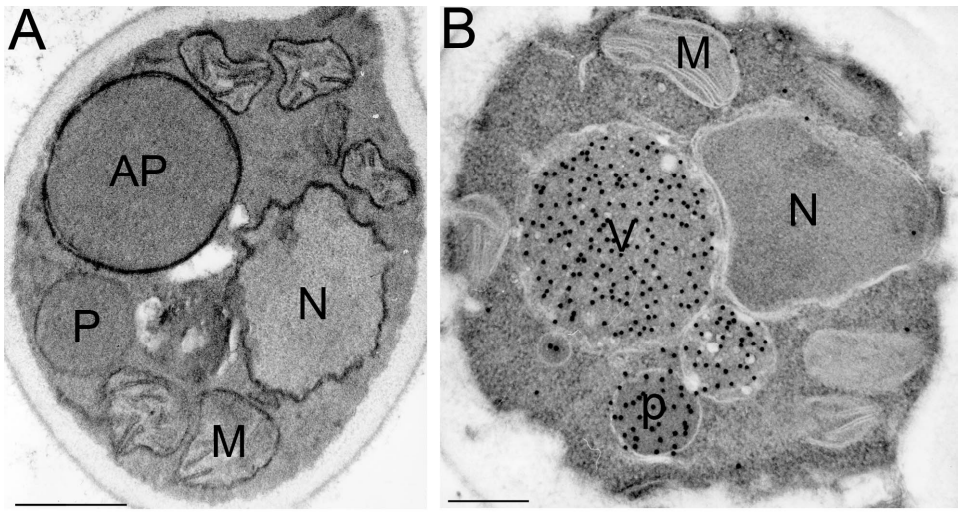

Figure 5. (A) Ultrathin section of a $KMnO_4$-fixed *H. polymorpha* cell, 30 minutes after glucose-induced macropexophagy showing sequestration of the large peroxisome (AP) in the cell leaving the smaller organelle (P) unaffected. (B) Ultrathin section of a glutaraldehyde-fixed *H. polymorpha* cell, labeled with an α-AO antiserum, showing labeling of a peroxisome (P) as well as autophagic vacuoles (V). Key: AP, autophagosome; P, peroxisome; N, nucleus; M, mitochondrion; V, vacuole. The bar represents 0.5 μm.

Protocols.

$KMnO_4$ fixation.

All incubations are performed at room temperature unless otherwise indicated.

1. Grow cells under pexophagy-inducing conditions and harvest a volume of the culture corresponding to 10-20 OD_{660} units.
2. Wash the cells three times with 5 ml demineralized water by resuspending/centrifugation (5,000 rpm, 2 min, 10 ml tubes) and subsequently resuspend the pellet in 5 ml $KMnO_4$ solution (1.5% $KMnO_4$ in water).
3. Incubate the cell suspension for 20 min at room temperature and shake gently every 5 minutes.
4. After incubation, collect the cells by centrifugation and wash with demineralized water until the supernatant is colorless (3 times with 5 ml water each, normally suffices).
5. Resuspend the pellet in 5 ml uranyl acetate solution (0.5% in water) and centrifuge for 15 minutes at 5,000 g to obtain a firm pellet. The supernatant should not be discarded, but left on top of the pellet for at least 4 h or maximally overnight at room temperature.
6. Decant the uranyl acetate supernatant from the pellet and dehydrate the cells by incubating the pellet with solutions of increasing ethanol concentrations, according to the scheme below:

- 15 min in 50% ethanol (without resuspending, the pellet remains intact)
- 15 min in 70% ethanol (the pellet is broken into small pieces, approx 1-5 mm^3, using a spatula. Incubation is performed without rotation, therefore the pieces will be lying at the bottom of the tube and the solution can be poured of directly after incubation)

- 15 min in 96% ethanol (mix carefully, do not use a vortex, the small pieces should stay intact)
- 15 min in 100% ethanol (mix carefully)
- Refresh the 100% ethanol solution and incubate for another 30 min

7. In the subsequent steps, the cells are impregnated with Epon resin. To prepare the Epon embedding resin, mix 100 g of Epon 812 (glycid ether) with 92 g of methylnadic anhydride (MNA), then add 2.3 g of 2,4,6-tri(dimethylaminomethyl) phenol (DMP-30). During the incubations with Epon/ethanol mixtures or pure Epon solutions the tubes are continuously mixed using a slowly rotating incubator. Incubate the samples (i.e. pieces of cell material) with approximately 5 ml of each of the Epon/ethanol mixtures,

according to the following scheme:

- 4 – 8 hours in a 1:1 mixture of 100% ethanol and Epon
- Overnight in a 1:3 mixture of 100% ethanol and Epon
- 1 hour in pure Epon solution
- Refresh the Epon solution and incubate for another 8 hours

8. Fill gelatin capsules ¾ full with pure Epon and load one piece of sample onto the top of the capsule; it will readily sink.

9. Polymerize the Epon by incubating the capsules for 24 hours at 80ºC.

10. Prepare sections using a diamond knife and view the sections in a transmission electron microscope.

Aldehyde fixations

All steps are performed at 4°C.

1. Harvest at least 20 OD_{660} units of a fresh culture by centrifugation (3 min at 5,000 x g).

2. Wash the cells three times with demineralized water and add 5 ml of either one of the fixation solutions:

3% glutaraldehyde in 0.1 M Na-cacodylate, pH 7.2

3% formaldehyde in 0.1 M Na-cacodylate, pH 7.2

0.5% glutaraldehyde + 2.5% formaldehyde in 0.1 M Na-cacodylate, pH 7.2 3% glutaraldehyde is the preferred fixative. However, glutaraldehyde may affect the antigenicity of specific proteins. In that case formaldehyde or a mixture of formaldehyde and glutaraldehyde mixture can be used.

3. Carefully resuspend the cells (by manual shaking) in the fixative solution and incubate for 2 h on ice. Mix the suspension every 15 min by inversion.

4. Collect the cells by centrifugation (see above) and discard the supernatant fraction. Wash the pellet using fresh Na-cacodylate buffer keeping the pellet intact.

All subsequent steps are performed at room temperature.

5. Wash the intact pellet of fixed yeast cells twice with demineralized water.

6. Add 5 ml of a freshly prepared solution of 0.4% (w/v) Na-periodate in water to the pellet (keep pellet intact).

7. After incubation for 15 min on a slowly rotating incubator, wash the pellet twice with 5 ml of demineralized water.

8. Incubate the pellet in 5 ml of a 1% (w/v) NH_4Cl solution in water for 15 min at room temperature.

9. Decant the NH_4Cl solution and wash the pellet once with demineralized water.

10. Dehydrate the cell material as indicated above for permanganate fixation. The samples are now ready for impregnation with Unicryl, the preferred plastic for immunocytochemical purposes.

11. Incubate the pieces successively as indicated below:

- 3 hours in a 5 ml of a 1:1 solution of 100% ethanol and Unicryl
- 1 hour in 5 ml of pure Unicryl
- Overnight in 5 ml of pure Unicryl
- 6-8 hours in 5 ml of pure Unicryl

12. Embed the material in BEEM capsules (Standard polyethylene embedding capsules size 00; 1x1 mm flat bottom) filled ¾ full with Unicryl. Only use carefully dried capsules! (Dried overnight in 37ºC stove).

13. Polymerize the Unicryl for 2 days using ultraviolet light at 4°C.

14. Fill the capsules completely with Unicryl and incubate for 2 more days at 30ºC.

15. Cut sections using a diamond knife and transfer sections onto nickel grids (400 mesh, formvar/carbon coated).

Immunocytochemical staining methods are performed on ultrathin sections that are collected on formvar/carbon coated nickel grids (do not use copper grids). The incubation steps are performed by floating the grids, section side down, on top of small droplets of the solution on a sheet of parafilm. All steps are performed at room temperature unless stated otherwise.

16. Incubate the grids with the following solutions: 0.5% BSA in PBS-glycine buffer for 5 min as a blocking step (PBS/Glycine/BSA buffer = 2 g/l sodium chloride, 0.05 g/l potassium chloride, 0.36 g/l disodium hydrogen phosphate, 0.055 g/l sodium dihydrogen phosphate, 0.375 g/l glycine, 0.025 g/l sodium azide and 5 g/l BSA).

Transfer grids to a droplet of appropriately diluted primary antibody in PBS-glycine buffer containing 0.5% BSA and incubate for 1 hour at room temperature (alternatively this step can be performed overnight at 4°C).

The appropriate dilution of the primary antibody is generally 10 times less than that used for western blotting (e.g. 1:100 if a 1:1,000 dilution is the optimal dilution for western blotting).

17. Rinse the grids with PBS-glycine buffer, three times 5 min each.

18. Incubate the grids with a solution of secondary antibodies conjugated to gold in PBS-glycine buffer containing 0.5% BSA (use dilution as recommended by the manufacturer). Use the appropriate secondary antibodies (i.e., Goat-anti-Rabbit (GAR)-Gold when the primary antibodies were raised in goat or Goat-anti-Mouse-Gold, when the primary antibodies were raised in mice).

19. Rinse the grids in PBS-glycine buffer, six times 5 min each.

20. Rinse grids in distilled water, four times 5 min each.

21. Remove excess water by carefully tipping one side of the grid (section side up) onto filter paper.

22. Post-stain the sections by placing the grid (section side down) onto a droplet of 1% uranyl acetate and 0.2% methylcellulose for 20 seconds.

23. Remove excess staining solution using filter paper and allow the grid to dry.

5. Concluding Remarks

The success of electron microscopy (EM) studies, much more than biochemical approaches, depends on the availability of fast growing cells that preferably are in the exponential growth phase. To avoid synthesis of storage products (e.g., glycogen) that strongly interfere with optimal cell architecture, we aim to avoid culturing cells at high concentrations of carbon sources (always < 1% glucose). Similar arguments hold for fluorescence microscopy studies aiming at live cell imaging. That is, the cellular processes are optimally visualized when the cells have not been exposed to high concentrations of the carbon source.
It should also be noted that the resolution of fluorescence techniques is still far from the resolution of electron microscopy techniques. This may in specific cases lead to overinterpretation of the data. It is therefore recommended that, wherever possible, the two methods are used in parallel.

Acknowledgements

TvZ is financially supported by a grant from the Netherlands Organisation for Scientific Research/Earth and Life Sciences (NWO/ALW). JAKWK is financially supported by the Netherlands Ministry of Economic Affairs and the B-Basic partner organizations (www.b-basic.nl) through B-Basic, a public-private NWO-ACTS program (ACTS = Advanced Chemical Technologies for Sustainability).

References

Bellu, A. R., Komori, M., van der Klei, I. J., Kiel, J. A. K. W., Veenhuis, M. (2001a). Peroxisome biogenesis and selective degradation converge at Pex14p. *J Biol Chem*. **276**, 44570-44574.

Bellu, A. R., Kram, A. M., Kiel, J. A. K. W., Veenhuis, M., van der Klei, I. J. (2001b). Glucose-induced and nitrogen-starvation induced peroxisome degradation are distinct processes in *Hansenula polymorpha* that involve both common and unique genes. *FEMS Yeast Res*. **1**, 23-31.

Bellu, A. R., Salomons, F. A., Kiel, J. A. K. W., Veenhuis, M., van der Klei, I. J. (2002). Removal of Pex3p is an important initial stage in selective peroxisome degradation in *Hansenula polymorpha*. *J Biol Chem*. **277**, 42875-42880.

Bruinenberg, P. G., Veenhuis, M., van Dijken, J. P., Duine, J. A., Harder, W. (1982). A
quantitative analysis of selective inactivation of peroxisomal enzymes in the yeast *Hansenula polymorpha* by high-performance liquid chromatography. *FEMS Microbiol Lett.* **15**, 45-50.

Ciechanover, A. (2006). The ubiquitin proteolytic system: From a vague idea, through basic mechanisms, and onto human diseases and drug targeting. *Neurology*. **66**, 7-19.

De Duve, C. (1963). *CIBA Found Symp Lysomomes*. 36.

De Duve, C., Wattiaux, R. (1966). Functions of lysosomes. *Annu Rev Physiol*. **28**, 435-492.

De Vries, B., van der Klei, I. J., Veenhuis, M., Kiel, J. A. K. W. (2008). Identification of the methylotrophic yeast-specific peroxisomal targeting signal 1 (PTS1). submitted.

Farre, J. C., Manjithaya, R., Mathewson, R. D., Subramani, S. (2008). PpAtg30 tags peroxisomes for turnover by selective autophagy. *Dev Cell*. **14**, 365-376.

Gleeson, M. A. G., Sudbery, P. E. (1988). Genetic analysis in the methylotrophic yeast *Hansenula polymorpha*. *Yeast*. **4**, 293-303.

Kaushik, S., Massey, A. C., Mizushima, N., Cuervo, A. M. (2008). Constitutive activation of chaperone-mediated autophagy in cells with impaired macroautophagy. *Mol Biol Cell.* **19**, 2179-2192

Kiel, J. A. K. W., Rechinger, K. B., van der Klei, I. J., Salomons, F. A., Titorenko, V. I., Veenhuis, M. (1999). The *Hansenula polymorpha PDD1* gene product, essential for the selective degradation of peroxisomes, is a homologue of *Saccharomyces cerevisiae* Vps34p. *Yeast*. **15**, 741-754.

Kiel, J. A. K. W., Komduur, J. A., van der Klei, I. J., Veenhuis, M. (2003). Macropexophagy in *Hansenula polymorpha*: facts and views. *FEBS Lett.* **549**, 1-6.

Kissova, I., Salin, B., Schaeffer, J., Bhatia, S., Manon, S., Camougrand, N. (2007). Selective and non-selective autophagic degradation of mitochondria in yeast. *Autophagy*. **3**, 329-336.

Klionsky, D. J., Cregg, J. M., Dunn Jr, W. A., Emr, S. D., Sakai, Y., Sandoval, I. V., Sibirny, A., Subramani, S., Thumm, M., Veenhuis, M., Ohsumi, Y. (2003). A unified nomenclature for yeast autophagy-related genes. *Dev Cell.* **5**, 539-545.

Klionsky, D. J. (2007). Autophagy: from phenomenology to molecular understanding in less than a decade. *Nat Rev Mol Cell Biol.* **8**, 931-937.

Klionsky, D. J., Cuervo, A. M., Dunn, Jr. W. A., Levine, B., van der Klei, I., Seglen, P. O. (2007). How shall I eat thee? *Autophagy.* **3**, 413-416.

Komduur, J. A. (2004). Molecular aspects of peroxisome degradation in *Hansenula polymorpha*. Phd thesis, University of Groningen, the Netherlands.

Leighton, F., Coloma, L., Koenig, C. (1975). Structure, composition, physical properties, and turnover of proliferated peroxisomes. A study of the trophic effects of Su-13437 on rat liver. *J Cell Biol.* **67**, 281-309.

Meijer, W. H., van der Klei, I. J., Veenhuis, M., Kiel, J. A. K.W. (2007). *ATG* genes involved in non-selective autophagy are conserved from yeast to man, but the selective Cvt and pexophagy pathways also require organism-specific genes. *Autophagy.* **3**, 106-116.

Mizushima, N., Levine, B., Cuervo, A. M., Klionsky, D. J. (2008). Autophagy fights disease through cellular self-digestion. *Nature.* **451**, 1069-1075.

Motley, A. M., Hettema, E. H. (2007). Yeast peroxisomes multiply by growth and division. *J Cell Biol.* **178**, 399-410.

Sakai, Y., Oku, M., van der Klei, I. J., Kiel, J. A. (2006). Pexophagy: autophagic degradation of peroxisomes. *Biochim Biophys acta*. **1763**, 1767-1775.

Shintani, T., Klionsky, D. J. (2004). Cargo proteins facilitate the formation of transport vesicles in the cytoplasm to vacuole targeting pathway*. J Biol Chem*. **279**, 29889-29894.

Van der Klei, I. J., Yorimoto, H., Sakai, Y. Veenhuis, M. (2006). The significance of peroxisomes in methanol metabolism in methylotrophic yeast. *Biochim Biophys acta.* **1763**, 1453-1462.

Van der Klei, I. J., Veenhuis, M. (2007). Protein targeting to yeast peroxisomes. *Methods Mol Biol.* **390**, 373-392.

Van Dijken, J. P., Otto, R., Harder, W. (1976). Growth of *Hansenula polymorpha* in a methanol-limited chemostat: Physiological responses due to the involvement of methanol oxidase as a key enzyme in methanol metabolism. *Arch Microbiol*. **111**, 137-144.

Van Zutphen, T., Veenhuis, M., van der Klei, I. J. (2008). Pex14 is the sole component of the peroxisomal translocon that is required for pexophagy. *Autophagy*. **4**, 63-66.

Veenhuis, M., Komori, M., Salomons, F., Hilbrands, R. E., Hut, H., Baerends, R. J. S., Kiel, J. A. K. W., van der Klei, I. J. (1996). Peroxisome remnants in peroxisome deficient mutants of the yeast *Hansenula polymorpha*. *FEBS Lett*. **383**, 114-118.

Verduyn, C., van Dijken, J. P., Scheffers, W. A. (1984). Colorimetric alcohol assays with alcohol oxidase. *J Microbiol methods*. **2**, 15-25.

Yorimitsu, T., Klionsky, D. J. (2005). Atg11 links cargo to the vesicle-forming machinery in the cytoplasm to vacuole targeting pathway. *Mol Biol Cell.* **16**, 1593-1605.

Chapter 5

Pex14 is the sole component of the peroxisomal translocon that is required for pexophagy

Tim van Zutphen, Marten Veenhuis and Ida J. van der Klei

Molecular Cell Biology, Groningen Biomolecular Sciences Institute, University of Groningen, Haren, The Nederlands

Published in *Autophagy 2008; 1:63-66.*

Abstract

Pex14 was initially identified as a peroxisomal membrane protein that is involved in docking of the soluble receptor proteins Pex5 and Pex7, which are required for import of PTS1- or PTS2-containing peroxisomal matrix proteins. However, *Hansenula polymorpha* Pex14 is also required for selective degradation of peroxisomes (pexophagy). Previously we showed that Pex1, Pex4, Pex6 and Pex8 are not required for this process. Here we show that also in the absence of various other peroxins, namely Pex2, Pex10, Pex12, Pex13 and Pex17, pexophagy can normally occur. These peroxins are, like Pex14, components of the peroxisomal translocon. Our data confirm that Pex14 is the sole peroxin that has a unique dual function in two apparent opposite processes, namely peroxisome formation and selective degradation.

Introduction

Autophagy is a highly conserved process that is responsible for the recycling of cytoplasmic components by the vacuole/lysosome.[1] Both selective and non-selective autophagic processes have been described.[2] Pexophagy involves the selective degradation of peroxisomes. In the methylotrophic yeast *Hansenula polymorpha*, pexophagy is induced upon a shift of methanol-grown cells to glucose.[3,4] This process, termed macropexophagy, initiates with the recognition and subsequent sequestration of a single peroxisome by multiple membrane layers, followed by fusion of the outer sequestering membrane layer with the vacuole membrane and finally degradation of the entire organelle by vacuolar enzymes.[5] Besides numerous autophagy-related (*ATG*)[6] genes, also the peroxisomal membrane protein Pex14 was shown to play an essential role in pexophagy, most likely in the initial recognition of the organelle to be degraded by the autophagy machinery.[3,7,8]

Initially, Pex14 was identified as a peroxin involved in matrix protein import as it is thought to recruit the PTS1 and PTS2 receptor proteins, Pex5 and Pex7, respectively, to the peroxisomal membrane.[9,10] Later studies identified two other components of the receptor docking complex, Pex13 and Pex17. A second protein complex in the peroxisomal membrane that is involved in matrix protein import is formed by three RING finger proteins, Pex2, Pex10 and Pex12. Both the docking and RING finger complexes can associate to form a super-complex.[11,12] Here we show none of the peroxins of the peroxisomal translocon besides Pex14 are essential for pexophagy.

Material & methods

Organisms & Growth

The *H. polymorpha* strains used in this study are listed in Table 1. Cells were cultivated at 37 ºC using either YPD medium (1% yeast extract, 1% peptone, 1% glucose), or mineral medium as described previously.[13] For analysis of peroxisome degradation, cells were precultivated using mineral medium containing 0.25% (w/v) ammonium sulphate and 0.25% (w/v) glucose as sole nitrogen and carbon sources respectively. Cells were subsequently shifted to 0.05% (w/v) glycerol and 0.5% (w/v) methanol as carbon sources. Exponential glycerol/methanol cultures were shifted to medium containing 0.5% (w/v) glucose to induce pexophagy.[7] When required, media were supplemented with 30 µg/ml leucine or appropriate antibiotics. For growth on plates, 2% agar was added to the media. *Escherichia coli* DH5α was used as host for propagation of plasmids using LB supplemented with appropriate antibiotics at 37º C as described.[14]

Construction of strains

Each of the *pex* strains as well as wild-type and mutant *atg1* were transformed with either SphI-linearized pHIPX4 *N50.PEX3.GFP* [15] or pHIPZ4 *N50.PEX3.GFP* [16] (as described in refs 14 and 17, Table I). Producing N_{50}.Pex3.GFP under the control of the alcohol oxidase promoter.

Table 1 Strains used in this study

Strains	**Characteristics**	**Reference**
wild-type	NCYC 495 *leu1.1* derivative	25
atg1	*ATG1* deletion strain *leu1.1*	22
pex2	*PEX2* disruption strain *leu1.1*	21
pex12	*PEX12* disruption strain *leu1.1*	26
pex13	*PEX13* disruption strain *leu1.1*	Komori M, Osaka, Japan
pex17	*PEX17* disruption strain *leu1.1*	Komori M, Osaka, Japan
WT N50.Pex3.GFP	wild-type:: pHipX4.N50.Pex3.GFP	15
atg1 N50.Pex3.GFP	atg1:: pHipZ4.N50.Pex3.GFP	This study
pex2 N50.Pex3.GFP	pex2:: pHipX4.N50.Pex3.GFP	This study
pex10 N50.Pex3.GFP	pex10 :: pHipZ4.N50.Pex3.GFP	This study
pex12 N50.Pex3.GFP	pex12:: pHipX4.N50.Pex3.GFP	This study
pex13 N50.Pex3.GFP	pex13:: pHipX4.N50.Pex3.GFP	This study
pex17 N50.Pex3.GFP	pex17:: pHipX4.N50.Pex3.GFP	This study

Microscopy

For fluorescence microscopy, 1 ml cell culture was supplemented with 2 µM FM 4-64, incubated for 45 minutes at 37 ºC and analyzed with a Zeiss Axioskop microscope (Carl Zeiss, Göttingen, Germany). Electron microscopy was performed as described previously.[18] Ultrathin sections of unicryl-embedded cells were used for immunocytochemistry, using polyclonal antiserum against GFP and gold-conjugated goat anti-rabbit antiserum.

Biochemical methods

Cell extracts were prepared as detailed previously.[15] Equal volumes of the cultures were subjected to SDS-polyacrylamide gel electrophoresis, followed by western blot analysis.[19,20] Blots were probed with rabbit polyclonal antiserum against alcohol oxidase, Pex10 or GFP followed by detection using either the Protoblot immunoblotting system (Promega Biotec) or BM Chemiluminescent Western blotting kit (Roche Molecular Biochemicals, Almere). Blots were scanned using a densitometer (Biorad GS-710, Hercules, CA, USA) and quantified using Image J (version 1.37); 3 measurements were performed on each band of 3 individual experiments per strain.

Acknowledgements. We thank Ron Booij for skillful assistance in electron microscopy and Arjen Krikken for the construction of strains. Tim van Zutphen is supported by a grant from the Netherlands Organisation for Scientific Research/Earth and Life Sciences (NWO/ALW).

Results

To investigate whether besides Pex14 other peroxins of the docking or RING finger sub-complexes are required for glucose induced pexophagy, we studied degradation of peroxisome remnants in single *PEX* deletion strains (*pex2, pex12, pex13* and *pex17*). The degradation of peroxisomal membrane remnants was monitored by the analysis of the levels of the peroxisomal membrane protein Pex10, using western blotting and anti-Pex10 antibodies.[3]

Development of various peroxisome remnants[21] was induced by growing the cells on a mixture of glycerol and methanol, followed by a shift of these cells to glucose-excess conditions. As shown in Fig. 1A, the levels of the peroxisomal membrane protein Pex10 gradually decreased in all mutants similar to the wild-type controls, although the kinetics of degradation may slightly vary. This is exemplified by the data from *pex17* cells that showed a relatively slow decrease of Pex10. As a negative control, *atg1* cells were analyzed in which pexophagy is blocked.[22] In these cells the Pex10 levels did not significantly decrease upon a shift of the cells to glucose medium.

To confirm degradation of the organelles in the vacuole, we also used an artificial marker protein, consisting of the first 50 N-terminal amino acids of Pex3 fused to enhanced Green Fluorescent Protein (eGFP; N_{50}.Pex3.GFP).

The first 50 N-terminal residues of Pex3 contain targeting information for the peroxisomal membrane and serve as specific anchor to mark the peroxisomal membrane with GFP. However, this short peptide of Pex3 is not functional in peroxisome biogenesis or degradation.[15]

Electron microscopy showed that the hybrid protein also normally sorted to the peroxisome remnants (shown for *pex13*, Fig. 1B). In fluorescence microscopy, these remnant structures are visualized as single fluorescent spots per cell.[23] We also introduced the *N_{50}.PEX3.GFP* expression cassette in two control strains, namely in wild-type and *atg1* cells. Western blot analysis revealed that upon a shift of N_{50}.Pex3.GFP-producing wild-type cells from glycerol/methanol to glucose, the levels of the hybrid protein gradually decreased (Fig 1C). The decrease of the protein levels of peroxisomal alcohol oxidase (AO) indicated that synthesis of N_{50}.Pex3.GFP did not influence degradation of a homologous marker protein.

Degradation of peroxisomal proteins was paralleled by the appearance of green fluorescence in the vacuoles as shown in Fig. 1D, in contrast to full length Pex3 which is removed from the peroxisomal membrane before uptake of the organelle by the vacuole.[24] In *H. polymorpha atg1* cells producing N_{50}.Pex3.GFP, however, N_{50}.Pex3.GFP and AO levels did not decrease (Fig. 1C) and GFP-fluorescence was not observed in the vacuoles (Fig. 1D). In addition to *pex2, pex12, pex13* and *pex17* we also studied the fate of peroxisomal ghosts in *pex10* cells.

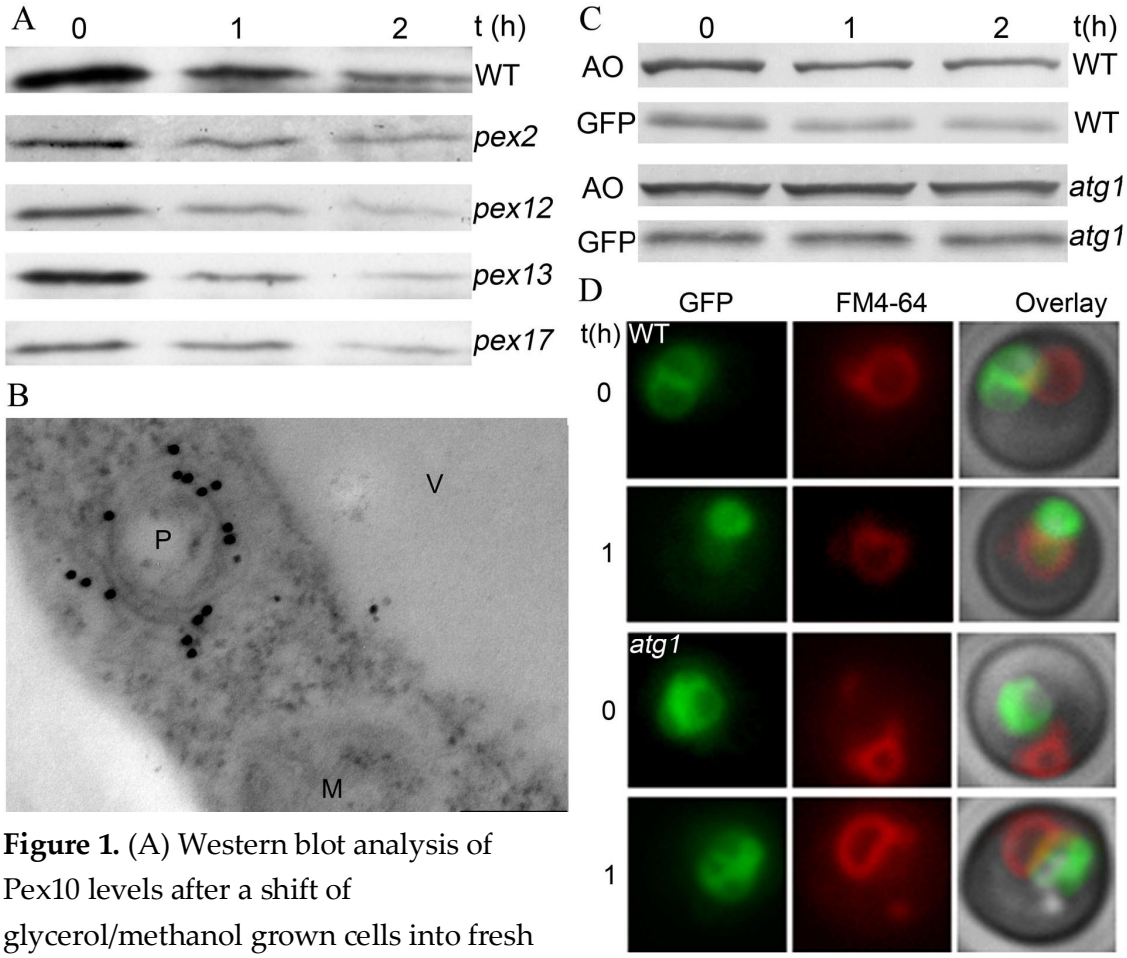

Figure 1. (A) Western blot analysis of Pex10 levels after a shift of glycerol/methanol grown cells into fresh glucose medium. As in wild-type (WT) control cells, the Pex10 levels decreased in *pex2, pex12, pex13* and *pex17* cells in the initial hours of cultivation. In *atg1* control cells the Pex10 levels did not significantly decrease. Samples were taken at the indicated time points after the shift; equal volumes of the culture were loaded per lane. The blots were decorated using α-Pex10-antibodies. (B). Immunocytochemistry to show that N_{50}.Pex3.GFP is exclusively sorted to the peroxisome membrane remnants in *pex13* cells. Ultrathin sections were incubated with α-GFP antibodies and gold-conjugated goat-anti rabbit antiserum (P, peroxisome remnant; V, vacuole; M, mitochondrion. The bar represents 0.2 μm). (C) Western blots showing the decrease of GFP or alcohol oxidase (AO) protein levels upon a shift of WT and *atg1* control cells from glycerol/methanol medium into glucose. Both strains produced N_{50}.Pex3.GFP. Blots of WT cells showed a decrease in AO and GFP protein, which was not observed in *atg1* controls. Equal volumes of the culture were loaded per lane. The blots were decorated using α-AO or α-GFP antibodies, respectively. (D) Fluorescence microscopy of WT and *atg1* cells producing N_{50}.Pex3.GFP. Cells grown on glycerol/methanol medium contain a cluster of 2-3 GFP-marked peroxisomes located adjacent to the vacuole (marked by FM 4-64). In WT cells shifted to glucose medium vacuolar GFP was detected, suggesting that peroxisome degradation had initiated. This vacuolar GFP was never observed in the *atg1* control strain.

Each of the *pex* mutants producing N_{50}.Pex3.GFP was pre-cultivated in media containing glycerol/methanol and exposed to excess glucose conditions. Western blot analysis revealed that upon the shift N_{50}.Pex3.GFP levels decreased in all mutant strains, similar to the wild-type control (Fig. 2A, shown for *pex10* cells, Fig. 2B, quantification). Also by this method, the kinetics of degradation was slowest in *pex17* cells. Fluorescence microscopy revealed that in all cases green fluorescence appeared in the vacuole (Fig. 2C; only shown for *pex13* cells).

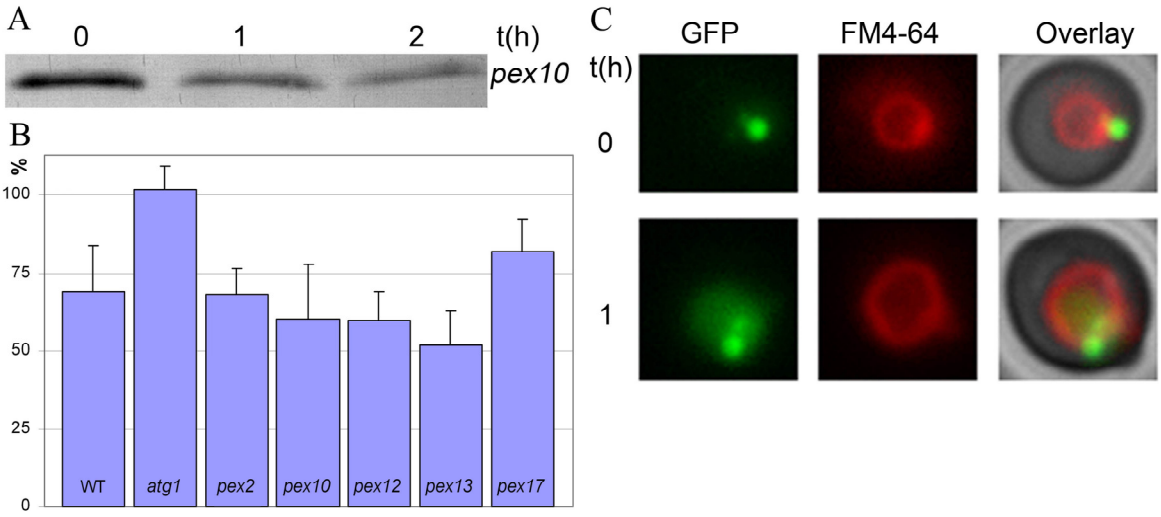

Figure 2. (A) Western blot analysis showing the decrease in N_{50}.Pex3.GFP upon a shift of *pex10* cells from glycerol/methanol to glucose media. Blot is decorated with α-GFP antibodies. (B) Quantification of N_{50}.Pex3.GFP levels in each strain, depicted here as the residual amount of N_{50}.Pex3.GFP protein levels 2 hours after the shift, adjusting the initial amount at T=0 to 100%. (C) Fluorescence microscopy of *pex13* cells producing N_{50}.Pex3.GFP. The cells contain a single fluorescent spot located adjacent to the vacuole (marked by FM 4-64). After 1 hour of cultivation on glucose, vacuolar GFP is evident, indicating degradation of (part of) these structures.

To confirm that in *pex17* cells the peroxisomal remnants were indeed subject to pexophagy, we analyzed *pex17* cells by electron microscopy upon a shift of glycerol/methanol grown cells to glucose. As shown in Fig. 3, shortly after induction of pexophagy, additional membranes were formed around the peroxisomal remnants, a typical feature of the initial stages of pexophagy.[4] Taking together these and earlier data, we conclude that of all *H. polymorpha* peroxins available yet, solely Pex14 is involved in selective peroxisome degradation.

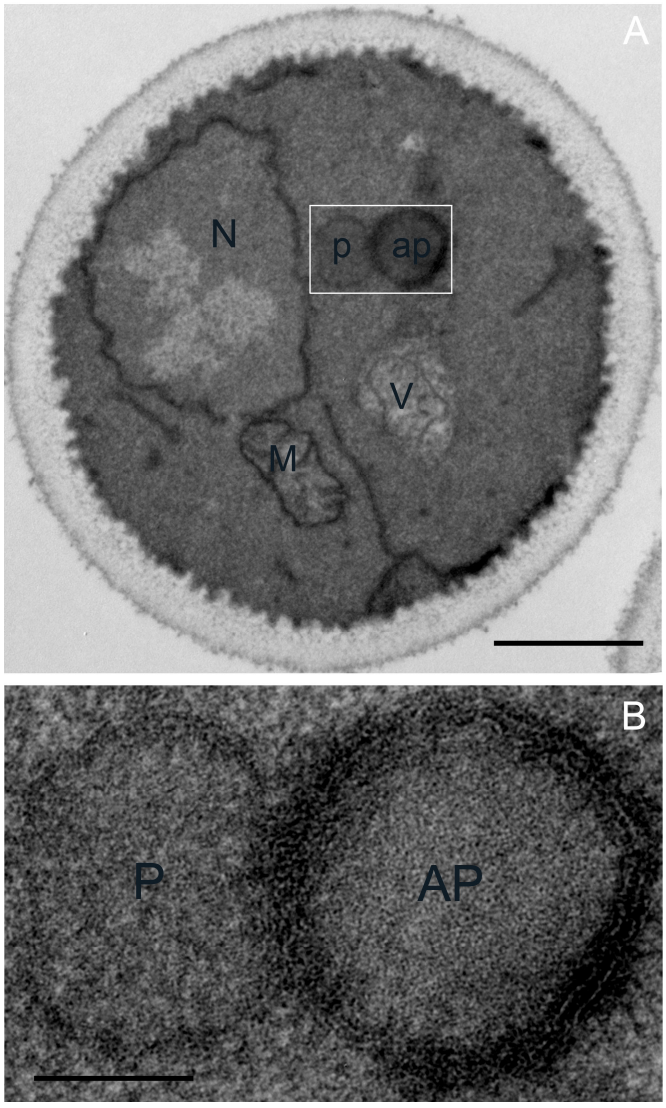

Figure 3 (A) Sequestration of a peroxisomal remnant (by an autophagosome) as observed in *pex17* cells 30 minutes after the shift from glycerol/methanol to glucose. The organelle is sequestered by multiple membrane layers. (B) shows a high magnification of the part indicated in Fig. 3A.
Abbreviations:
M, Mitochondrion; N, Nucleus; V, Vacuole; P, Peroxisome; AP, Autophagosome.
The bar represents 0.5 μm in A and 0.1 μm in B.

References

1 Levine B. Cell biology: Autophagy and Cancer. Nature 2007; 446:745-7

2 Meijer WH, van der Klei IJ, Veenhuis M, Kiel JAKW. *ATG* genes involved in non-selective autophagy are conserved from yeast to man, but the selective Cvt and pexophagy pathways also require organism-specific genes. Autophagy 2007; 3:106-16

3 Veenhuis M, Komori M, Salomons F, Hilbrands RE, Hut H, Baerends RJS, Kiel JAKW, van der Klei IJ. Peroxisome remnants in peroxisome deficient mutants of the yeast *Hansenula polymorpha*. FEBS letters 1996; 383:114-8

4 Sakai Y, Oku M, van der Klei IJ, Kiel JAKW. Pexophagy: Autophagic degradation of peroxisomes. Biochim Biophys Acta 2006; 1763:1767-75

5 Dunn WA Jr, Cregg JM, Kiel JAKW, van der Klei IJ, Oku M, Sakai Y, Sibirny AA, Stasyk OV, Veenhuis M. The selective autophagy of peroxisomes. Autophagy 2005; 1:75-83

6 Klionsky DJ, Cregg JM, Dunn WA, Emr SD, Sakai Y, Sandoval IV, Sibirny A, Subramani S, Thumm M, Veenhuis M, Ohsumi Y. A unified nomenclature for yeast autophagy-related genes. Dev Cell 2003; 5:539-45

7 Bellu AR, Komori M, van der Klei IJ, Kiel JAKW, Veenhuis M. Peroxisome biogenesis and selective degradation converge at Pex14p. J Biol Chem 2001; 276:44570-74

8 De Vries B, Todde V, Stevens P, Salomons F, van der Klei IJ, Veenhuis M. Pex14p is not required for N-starvation induced microautophagy and in catalytic amounts for macropexophagy in *Hansenula polymorpha*. Autophagy 2006; 2:183-8

9 Komori M, Rasmussen SW, Kiel JAKW, Baerends RJS, Cregg JM, van der Klei IJ, Veenhuis M. The *Hansenula polymorpha PEX14* gene encodes a novel peroxisomal membrane protein essential for peroxisome biogenesis. EMBO J 1997; 16:44-53

10 Albertini M, Rehling P, Erdmann R, Girzalsky W, Kiel JA, Veenhuis M, Kunau WH. Pex14p, a peroxisomal membrane protein binding both receptors of the two PTS-dependent import pathways. Cell 1997; 89:83-92

11 Hazra PP, Suriapranata I, Snyder WB, Subramani S. Peroxisome remnants in pex3Δ cells and the requirement of Pex3p for interactions between the peroxisomal docking and translocation complex. Traffic 2002; 3:560-74

12 Agne B, Meindl NM, Niederhoff K, Einwächter H, Rehling P, Sickmann A, Meyer HE, Girzalsky W, Kunau WH. Pex8p: an intraperoxisomal organizer of the peroxisomal import machinery. Mol Cell 2003; 11:635-46

13 Van Dijken JP, Otto R, Harder W. Growth of *Hansenula polymorpha* in a methanol-limited chemostat. Physiological responses due to the involvement of methanol oxidase as a key enzyme in methanol metabolism. Arch Microbiol 1976; 111:137-144

14 Sambrook J, Fritsch EF, Maniatis T. *Molecular cloning; A laboratory manual.* 1989; Cold Spring Harbor Laboratory Press, New York
15 Baerends RJS, Faber KN, Kram AM, Kiel JAKW, van der Klei IJ, Veenhuis M. A stretch of positively charged amino acids at the N terminus of *Hansenula polymorpha* Pex3p is involved in incorporation of the protein into the peroxisomal membrane. J Biol Chem 2000; 275:9986-95
16 Otzen M, Krikken AM, Ozimek PZ, Kurbatova E, Nagotu S, Veenhuis M, van der Klei IJ. In the yeast *Hansenula polymorpha*, peroxisome formation from the ER is independent of Pex19p, but involves the function of p24 proteins. FEMS Yeast Res 2006; 6:1157-1166
17 Faber KN, Haima P, Harder W, Veenhuis M, AB G. Highly-efficient electrotransformation of the yeast *Hansenula polymorpha*. Curr Genet 1994; 25:305-310
18 Waterham HR, Titorenko VI, Haima P, Cregg JM, Harder W, Veenhuis M. The *Hansenula polymorpha PER1* gene is essential for peroxisome biogenesis and encodes a peroxisomal matrix protein with both carboxy- and amino-terminal targeting signals. J Cell Biol 1994; 127:737-49
19 Laemmli UK. Cleavage of structural proteins during the assembly of the head of bacteriophage T4. Nature 1970; 227:680-685
20 Kyhse-Andersen J. Electroblotting of multiple gels: a simple apparatus without buffer tank for rapid transfer of proteins from polyacrylamide to nitrocellulose. Biochem Biophys Methods 1984; 10:203-9.
21 Koek A, Komori M, Veenhuis M, van der Klei IJ. A comparative study of peroxisomal structures in *Hansenula polymorpha pex* mutants. FEMS Yeast Res 2007; in Press
22 Komduur JA, Veenhuis M, Kiel JA. The *Hansenula polymorpha PDD7* gene is essential for macropexophagy and microautophagy. FEMS Yeast Res 2003; 3:27-34
23 Faber KN, Haan GJ, Baerends RJS, Kram AM, Veenhuis M. Normal peroxisome development from vesicles induced by truncated *Hansenula polymorpha* Pex3p. J Biol Chem 2002; 277:11026-33
24 Bellu AR, Salomons FA, Kiel JA, Veenhuis M, van der Klei IJ. Removal of Pex3p is an important initial stage in selective peroxisome degradation in *Hansenula*
polymorpha. J Biol Chem 2002; 277:42875-80
25 Gleeson MAG, Sudbery PE. Genetic analysis in the methylotrophic yeast *Hansenula polymorpha*. Yeast 1988; 4:293-303
26 Van Dijk R, Faber KN, Hammond AT, Glick BS, Veenhuis M, Kiel JA. Tagging Hansenula polymorpha genes by random integration of linear DNA fragments (RALF). Mol Genet Genomics 2001; 266:646-656

Chapter 6

An alternative Atg1-dependent autophagic mechanism for peroxisome degradation

Tim van Zutphen, Marten Veenhuis and Ida J. van der Klei

Molecular Cell Biology, Groningen Biomolecular Sciences and Biotechnology Institute, University of Groningen, Haren, The Netherlands

Submitted to *Autophagy*, *under revision*

Abstract

Initiation of macropexophagy in the yeast *Hansenula polymorpha* involves the degradation of the peroxisomal membrane protein Pex3 prior to sequestration of the organelle, by the autophagosome. Here we studied whether removal of Pex3 during peroxisome-inducing cultivation conditions was associated with organelle degradation. Pex3 degradation was induced by a temperature shift using *pex3Δ* cells producing a Pex3 fusion protein containing an N-terminal temperature sensitive degron sequence. Conditional degradation of Pex3 resulted in rapid peroxisome degradation by an alternative autophagic process that showed morphological characteristics of macro- and microautophagy. This mode of degradation is a very rapid process initiated by elongation of the vacuole, followed by the fusion of a vacuolar vesicle with the organelles to be degraded. Remarkably, incorporation of a vacuolar vesicle required membrane structures that share morphological properties of the autophagosomal membrane, contain Atg8 and position in between both organelles. The peroxisomal membrane first fuses with these membranes in an Ypt7-dependent manner followed by fusion of a vacuolar vesicle and subsequent degradation of the peroxisomal content. This mode of peroxisome degradation is of physiological significance as it was also observed in methanol-grown wild type cells that were exposed to methanol excess conditions.

Introduction

Autophagy is a catabolic process of eukaryotic cells and serves to degrade and recycle cytoplasmic components. This is not only required for survival during nutrient starvation, but also important for cellular housekeeping as it removes exhausted, redundant or unwanted components, also including whole organelles. In this way autophagy may act as a quality control mechanism preventing cell deterioration or supporting cell remodeling during development. The importance of autophagy in human health and disease is underscored by the findings that autophagy malfunction is linked to several serious diseases such as cancer, neurodegenerative diseases and lysosomal storage diseases.[1,2] Methylotrophic yeast species (i.e. *Hansenula polymorpha* and *Pichia pastoris*) are attractive models to study the molecular machinery of selective peroxisome autophagy (also designated pexophagy), as in these organisms peroxisome development and turnover can be readily prescribed by manipulation of the growth conditions.[3,4]

For peroxisomes, two modes of autophagic degradation have been documented namely micro- and macropexophagy.[5] In *P. pastoris* degradation of peroxisomes by micropexophagy is observed upon a shift of cells from methanol to glucose-containing media. At these conditions, clusters of peroxisomes are taken up by the vacuole for degradation and recycling.[6]

In *H. polymorpha* macropexophagy is induced upon shifting cells from methanol to glucose or ethanol media.[7] Characteristically, during glucose-induced macropexophagy in *H. polymorpha* the organelles are sequentially degraded. In particular large, mature organelles are degraded whereas at least one relatively small organelle escapes this process.[8] In addition to *ATG* genes that encode components of the general autophagy machinery, specific proteins are required for pexophagy.[9]

We previously identified two peroxisomal membrane proteins (Pex14 and Pex3) that are crucial for both peroxisome biogenesis and autophagy.[10,11] Recently in *P. pastoris* a third component, the peroxisomal membrane protein Atg30, has been identified.[12] Interestingly, Atg30 physically interacts with Pex14 and Pex3. In WT *H. polymorpha*, peroxisomes are shown to have a limited life span. During normal vegetative reproduction of cells Atg1-dependent constitutive peroxisome degradation has been observed.[13] Probably, constitutive degradation may be physiologically significant for continuous rejuvenating the peroxisome population by removing exhausted or dysfunctional organelles. As dysfunction of yeast peroxisomes may result in necrotic cell death, timely recognition and turnover of such organelles is of crucial importance, thus stressing the significance of autophagy in cell vitality.[14]

For different organelles (e.g. mitochondria and peroxisomes) it has been demonstrated that one or more proteins exposed at the surface of these organelles are essential for their turnover, suggesting that the signal for degradation may originate from the target organelle itself.[10,12,15,16,17] Interestingly, in *H. polymorpha* removal of Pex3 from the organelle membrane is suggested to act as an initial step to render the organelle susceptible for degradation.[11,18]

To further elucidate the significance of *H. polymorpha* Pex3 in initiation of peroxisome degradation, we investigated the fate of peroxisomes after removal of Pex3 from the membrane at nutrient excess conditions, using a Pex3 protein fused to a temperature sensitive degron. The data shows that at restrictive temperature, peroxisome degradation is rapidly induced by a fast and alternative degradation mechanism. This mode of organelle degradation was also observed in wild type cells, when methanol grown cells were exposed to excess methanol conditions.

Materials & Methods

Organisms and growth

The *H. polymorpha* strains that were used in this study are listed in Table I. Cultivation was performed using either YPD (1 % yeast extract, 1 % peptone, 1 % glucose) supplemented with appropriate antibiotics or mineral medium containing 0.25 % (w/v) ammonium sulphate or methylamine as nitrogen source and 0.5 % (w/v) glucose or methanol (v/v) as carbon source, supplemented with 30 mg/l leucine. *Escherichia coli* XL1 Blue was grown on LB supplemented with appropriate antibiotics.

Construction of strains

An expression cassette was constructed that encoded a part of mouse dihydrofolate reductase containing an N-terminal arginine (Arg-DHFR^{ts}, Degron)[22] fused to the N-terminus of full length Pex3. pHipZ6.*DEGRON-PEX3^{ts}* was constructed as follows; the Degron-cassette was amplified from pKL187 (Euroscarf, Frankfurt, Germany) using primer Degron-Pex3 Fw CGC GCG GCC GCG CAT GCA GAT TTT CGT CAA GAC and primer Degron-Pex3 Rv AGA TCT GGC ACC CGC TCC AGC GCC TGC A. NotI-BglII digested PCR-product was ligated into NotI-BamHI digested pHipX7-*PEX3*.[23] A SphI-SalI fragment *DEGRON-PEX3^{ts}* was ligated into SphI-SalI digested pHipZ6, generating pHipZ6.*DEGRON-PEX3^{ts}*.[24] The linearized vector (BsiWI) was integrated into *H. polymorpha pex3Δ*, resulting in strain Degron-Pex3^{ts}. Correct integration was confirmed by Southern blot analysis.[25]

Linearized (BsiWI) pHipX5-e*GFP-SKL* was integrated to label peroxisomes in Degron-Pex3^{ts}.[20]

Atg1Δ Degron-Pex3^{ts} was generated by replacing *URA3* by *NAT1* in the original *ATG1* deletion cassette and integration of an ApaI-NdeI fragment in the Degron-Pex3^{ts} strain expressing *eGFP-SKL*. PBS-*PDD7-URA* was digested with SalI, self-ligated, followed by digestion with EcoRI-HindIII and ligation of an EcoRI-HindIII fragment from pAG25 containing *NAT1*, generating pBS-*PDD7-NAT1*.[26,27] Integration was confirmed by Southern blot analysis. For Atg8 localization, *eGFP-ATG8* was isolated from pHipX6-*eGFP-ATG8* by SmaI-BamHI digestion and ligation into pHipN5.[28] Linearized (StuI) pHipX4 *eBFP2-SKL* was integrated into Degron-Pex3^{ts}, followed by integration of linearized (Bsu36I) pHipN5-*eGFP-ATG8*.[29]

YPT7 deletion was obtained by replacing the first 394 nucleotides by the *HPH* gene.[27] Primers Ypt7 Fw GAA GAA GCG ACG CCG ATC CAG TTG ATG TG and Ypt7 Rv GAA AGT ACA AAT GGC GGT GG were used to generate a PCR product which was phosphorylated and ligated into EcoRV-HpaI digested Pag32. Primers Hsp26 Fw GGC AAG CTT TAA GGA CAA GGT CAC CAT TG and Hsp26 Rv CCG GGA TCC GTA AAA TGA TGA GGC AAA GG were used to generate a second PCR product. Both vector and PCR product were digested with HindIII-BamHI and ligated. Integration of the *YPT7* deletion construct into Degron-Pex3^{ts} expressing *eBFP2-SKL* and *GFP-ATG8* was confirmed by Southern blot analysis.

Microscopy

For fluorescence microscopy, 2 µM FM4-64 was added to the culture. Upon incubation for at least 4 hours, cells were analyzed with a Zeiss Observer Z1, or confocal laser scanning microscope LSM 510 (Carl Zeiss, Göttingen, Germany). For wide-field microscopy eBFP2 was visualized using a 380 nm LED and detected with a 435-485 nm bandpass filer (BP). GFP was excited with a 470 nm LED and detected using a 500-550 nm BP filter. FM4-64 was excited with a 555 nm LED and detected using a 570-640 nm filter. For life-cell imaging, cells were transferred to an objective containing 1% agarose, incubated in the appropriate medium and kept at 37 ºC. 10% LED power was used for sequential imaging. For confocal microscopy GFP was visualized by excitation with a 488 nm argon laser (Lasos) and detected using a 500-550 nm BP filter. FM4-64 was excited with a 543 nm helium laser (Lasos) and detected using a 565-615 nm BP filter. To enhance details deconvolution was applied using the classic maximum likelihood method and a theoretical point spread function (Huygens professional v3.3, Scientific volume imaging). Electron microscopy using ultrathin sections for morphological and immunocytochemical analysis was performed as described.[30]

FACS analysis

To determine the presence of reactive oxygen species, cells were incubated with H_2DFCDA for 30 minutes and analysed by FACS using a 488 nm laser and 500-550 BP filter (FACS aria II, Becton Dickinson, Franklin Lakes USA).[14]

Biochemical methods

SDS-polyacrylamide gel electrophoresis and Western blot analysis of cell lysates were performed as detailed previously.[31,32,33] Blots were decorated using rabbit polyclonal antibodies and detected using either the Protoblot immunoblotting system (Promega, Madison, USA) or BM Chemiluminiscence Western blotting kit (Roche, Diagnostics GmBH, Almere, The Netherlands). Scanning was performed with a densitometer (Biorad GS-710, Hercules, Ca USA).

Table 1 *H. polymorpha* strains used in this study

Strain	Properties	Reference
WT	Wild type NCYC 495 *leu1.1*	19
WT. *GFP-SKL*	NCYC 495 *leu 1.1* with pHipX5-*eGFP-SKL* integration (P_{AMO})	20
pex3Δ	*PEX3* deletion strain *leu1.1*	21
Degron-Pex3^{ts}	*PEX3* deletion strain with double-copy pHipZ6-*DEGRON-PEX3^{ts}* integration *leu 1.1*(P_{PEX3})	This study
Degron-Pex3^{ts}. *GFP-SKL*	Degron-Pex3^{ts} with pHipX5-*eGFP-SKL* integration (P_{AMO})	This study
atg1Δ Degron-Pex3^{ts}	*ATG1* deletion in *pex3Δ*::*degron-pex3.* expressing *eGFP-SKL* (P_{AMO})	This study
Degron-Pex3^{ts}. *BFP-SKL. GFP-ATG8*	*pex3Δ::degron-pex3* with pHipX4-e*BFP2-SKL* (P_{aox}) and pHipN5-*eGFP-ATG8* (P_{amo}) integration	This study
ypt7Δ Degron-Pex3^{ts}	*YPT7* deletion in Degron-Pex3^{ts}. *BFP-SKL.GFP-ATG8*	This study

Results

Temperature induced degradation of Pex3 results in peroxisome autophagy

Pex3 degradation is an initial step in glucose-induced macropexophagy in *H. polymorpha* [11] To address whether artificial degradation of Pex3 at peroxisome-inducing cultivation conditions results in the induction of peroxisome degradation, we took advantage of a temperature-sensitive (ts) degron, which consists of a ts DHFR variant containing an N-terminal Arg (Arg-DHFR^{ts}), previously described for *Saccharomyces cerevisiae*.[22] *ARG-DHFR^{ts}* was fused to full length *PEX3* and introduced in *H. polymorpha pex3Δ* cells. During growth of this strain at the permissive temperature (25 ^{o}C) the cells contained normal peroxisomes and Pex3 levels akin to WT cells (Fig. 1A). We analyzed the fate of peroxisomes upon shifting cells of the Degron-Pex3^{ts} strain from the permissive to the restrictive temperature. In order to allow specific analysis of the organelle population present prior to the shift, we introduced the peroxisomal matrix marker *GFP-SKL* under the control of the substrate-inducible amine oxidase promoter (P_{AMO});.[34] During cultivation of such cells on methanol/methylamine media, GFP-SKL is synthesized and accumulates in peroxisomes. As shown before, supplementation of these cultures with excess ammonium sulphate fully represses P_{AMO} and thus, GFP-SKL synthesis, allowing discriminating between the organelles present prior to the shift and those subsequently formed after prolonged cultivation at methanol/ammonium sulphate conditions.[35]

Degron-Pex3^{ts} cells were pre-grown on methanol/methylamine at 25 ºC, subsequently supplemented with excess ammonium sulphate, and further incubated for 30 min at 25 ºC to deplete *AMO* and *GFP-SKL* mRNA's and then shifted to 37 ºC.[35] Biochemical analysis showed that in the first hours after the shift to 37 ºC, Pex3 levels strongly decreased (Fig. 1A) in conjunction with a decrease in amine oxidase (AMO) and GFP-SKL protein levels, whereas in WT controls Pex3, GFP-SKL as well as AMO did not decreased, as expected (Fig. 1B). These data suggest that peroxisomes are subject to degradation in Degron-Pex3^{ts} cells at peroxisome-inducing conditions. This was confirmed by fluorescence microscopy analysis which revealed that in these cells increasing numbers of vacuoles, the actual sites of peroxisome degradation, were characterized by the presence of GFP fluorescence (Fig. 1C). The relatively low numbers of fluorescent vacuoles in WT were expected, since peroxisomes are subject to slow but continuous constitutive degradation during vegetative reproduction of cells.[13]

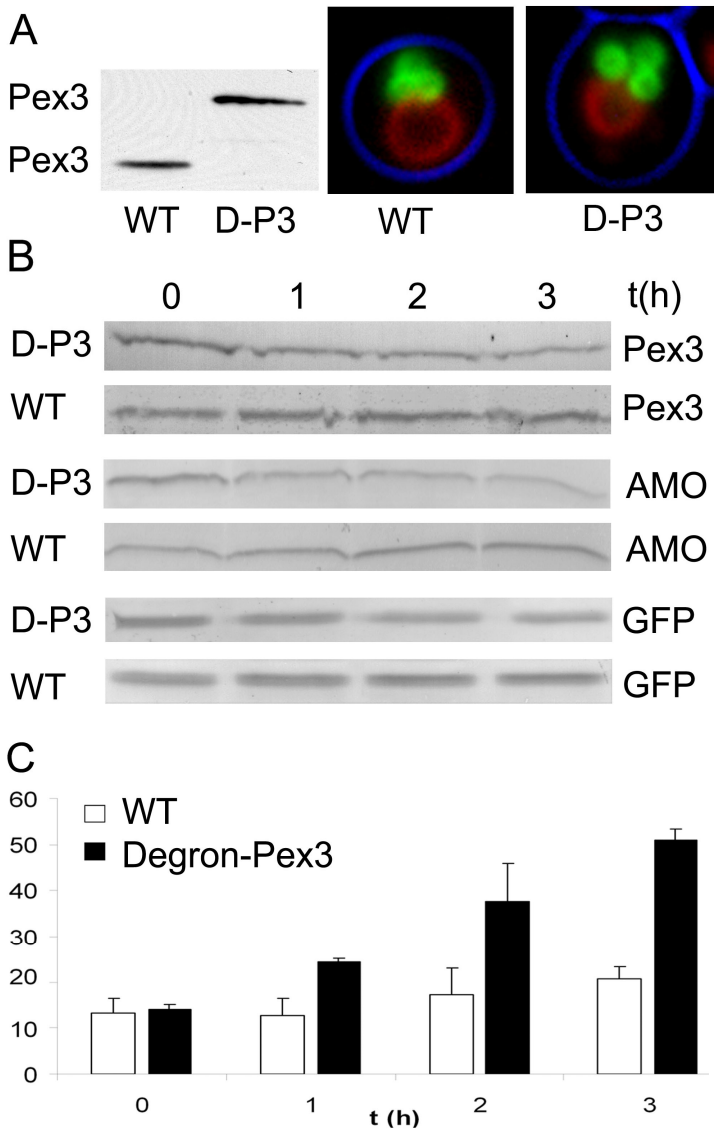

Figure 1. N-degron based Pex3 degradation induces peroxisome degradation

(A) Left: Western blot analysis of WT and Degron-Pex3^{ts} cells cultured at 25 ºC on methanol/methylamine, showing the protein level of native Pex3 or Arg-DHFR^{ts}-Pex3. Right: Merged FM images of WT and Degron-Pex3^{ts} (D-P3) cells expressing P$_{AMO}$-driven *GFP-SKL* cultured at 25 ºC on methanol/ methylamine. Cells were stained with FM4-64 to mark vacuoles (red). The brightfield image is indicated in blue. (B) Western blot analysis of Pex3, amine oxidase (AMO) and GFP levels in WT and Degron-Pex3^{ts} cells producing GFP-SKL under control of the P$_{AMO}$. Cells were pre-grown at 25 ºC on methanol/methylamine medium and shifted to 37 ºC to induce Pex3 degradation (T=0h). Samples were taken at regular time intervals after the shift. In the Degron-Pex3^{ts} cells Pex3 levels decreased rapidly; quantification of Pex3 levels from 3 individual experiments showed a reduction to 62% 2 after the shift and to 46% at 4 hours (standard deviation 9.0, 10.4 respectively) and reached a minimum of ± 10% after 8 hours. In contrast, in WT controls Pex3 levels increased. GFP-SKL and AMO levels in Degron-Pex3^{ts} cells also decreased, but slightly increased in WT cells. Blots were decorated with the indicated antibodies. D-P3: Degron-Pex3^{ts} . Equal volumes of culture were loaded per lane. (C) Quantification of cells containing vacuolar GFP before and after the shift of cells to 37 ºC as detailed in B. Vacuolar GFP was quantified in Z-stacks at different time-points after the shift of Degron-Pex3^{ts} and WT cells synthesizing GFP-SKL, stained with FM4-64 to mark vacuoles. Over 100 cells of 3 independent cultures were analysed. Bar represents SD.

Peroxisome turnover induced by Pex3 degradation is an *ATG1*-dependent process

To determine whether the observed peroxisome degradation is an autophagic process, *ATG1* was deleted in the Degron-Pex3^{ts} strain that also produces GFP-SKL. These cells were cultivated at 25 ºC on methanol/methylamine to induce GFP-SKL synthesis, followed by repression of GFP-SKL synthesis by excess ammonium sulphate and a subsequent shift of the culture to 37 ºC. Western blot analysis indicated that the GFP-SKL protein levels remained approximately constant in this strain after the shift (Fig. 2A). Moreover, vacuolar GFP was never observed (data not shown), consistent with the view that peroxisome degradation in *atg1Δ* Degron-Pex3^{ts} is inhibited and thus represents an autophagic process. As expected, the levels of Pex3 progressively reduced in these cells (Fig. 2A).

We next addressed whether peroxisome degradation in Degron-Pex3^{ts} cells is related to micro- or macroautophagy. As in *H. polymorpha* microautophagy, but not macropexophagy, is dependent of protein synthesis, we repeated the degradation experiments described above in the presence of cycloheximide (CHX).[36] The data, presented in Fig. 2B, show that peroxisome degradation is inhibited in the presence of CHX and thus may represent a microautophagy process.

Since microautophagy is considered a non-specific process in *H. polymorpha*, we also determined the levels of the cytosolic alcohol dehydrogenase (ADH) and Hsp70, as well as the mitochondrial malate dehydrogenase (MDH).

The levels of ADH, Hsp70 and MDH did however not decrease at the same conditions (Fig. 2C), consistent with the view that Pex3-degradation induced peroxisome turnover is selective for peroxisomes. In addition also Hsp70 increased in a similar manner as ADH and MDH, suggesting no heat shock response was induced by the conditions used, in agreement with the thermotolerant nature of *H. polymorpha*.[37]

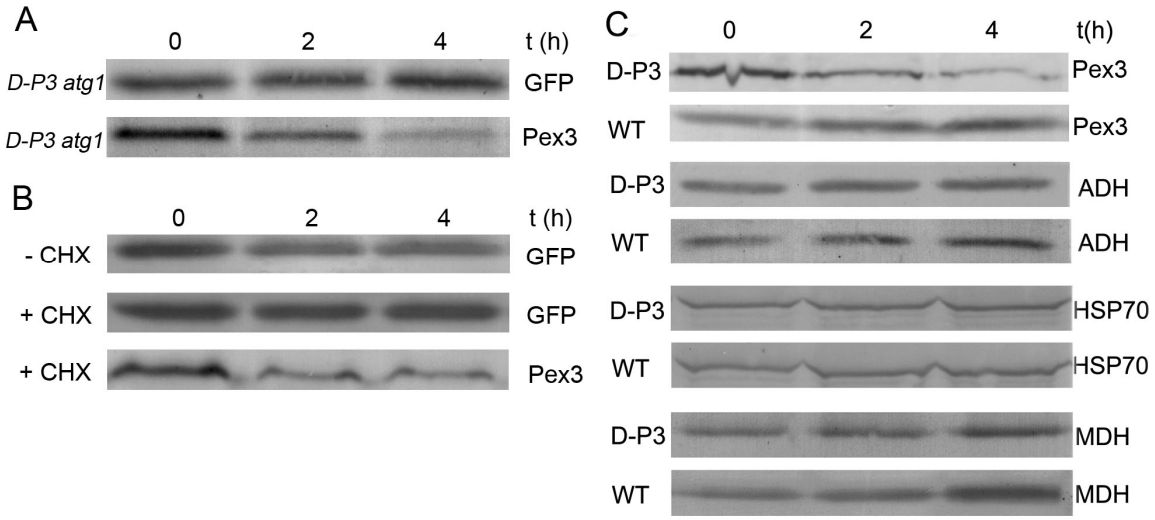

Figure 2. Pex3-degradation induced peroxisome degradation is an autophagic process

(A) Deletion of *ATG1* in Degron-Pex3^{ts} expressing P$_{AMO}$ driven *GFP-SKL* abolished the decrease of GFP-SKL after the shift to 37 ºC, as evident from Western blots (cultured as described for Fig. 1B). Pex3 levels decreased, similar to the decrease observed for Degron-Pex3^{ts} cells. (B) Addition of 6 mg/ml cycloheximide (CHX) also inhibited the degradation of GFP-SKL but not of Pex3. Cells were cultivated as described at Fig. 1B.

(C) The levels of cytosolic heat shock protein 70 (Hsp70) and alcohol dehydrogenase (ADH) as well as the mitochondrial malate dehydrogenase (MDH) increased in time after the shift to 37 ºC, whereas Pex3 levels declined rapidly, indicating that the degradation process is specific for peroxisomes. WT and the Degron-Pex3^{ts} strain producing GFP-SKL was cultivated as described at Fig. 1B. Equal volumes of culture were loaded per lane.

Pex3-degradation induced pexophagy displays novel morphological characteristics

Detailed kinetic fluorescence microscopy revealed that the intermediate stages of Pex3-degradation induced pexophagy seemed to differ from both micro- and macropexophagy. The degradation process initiated with the formation of a vacuole extension similar to micropexophagy, however instead of surrounding the peroxisome cluster, the extension seemed to protrude into the organelle (Fig. 3B). Subsequently, a weak FM4-64 fluorescent ring appeared surrounding the organelle (Fig. 3C). These rings were invariably completely surrounding the organelles (Fig. 3D). Subsequently, peroxisome degradation was observed, judged from the presence of GFP-SKL in the vacuole (Fig. 3D, E). At a later stage of cultivation, approximately 3 hours after the shift to 37 ºC, bulk of the cells contained a single enlarged peroxisome (Fig. 3F), whereas identical grown WT control cells contained several peroxisomes (Fig. 3G).

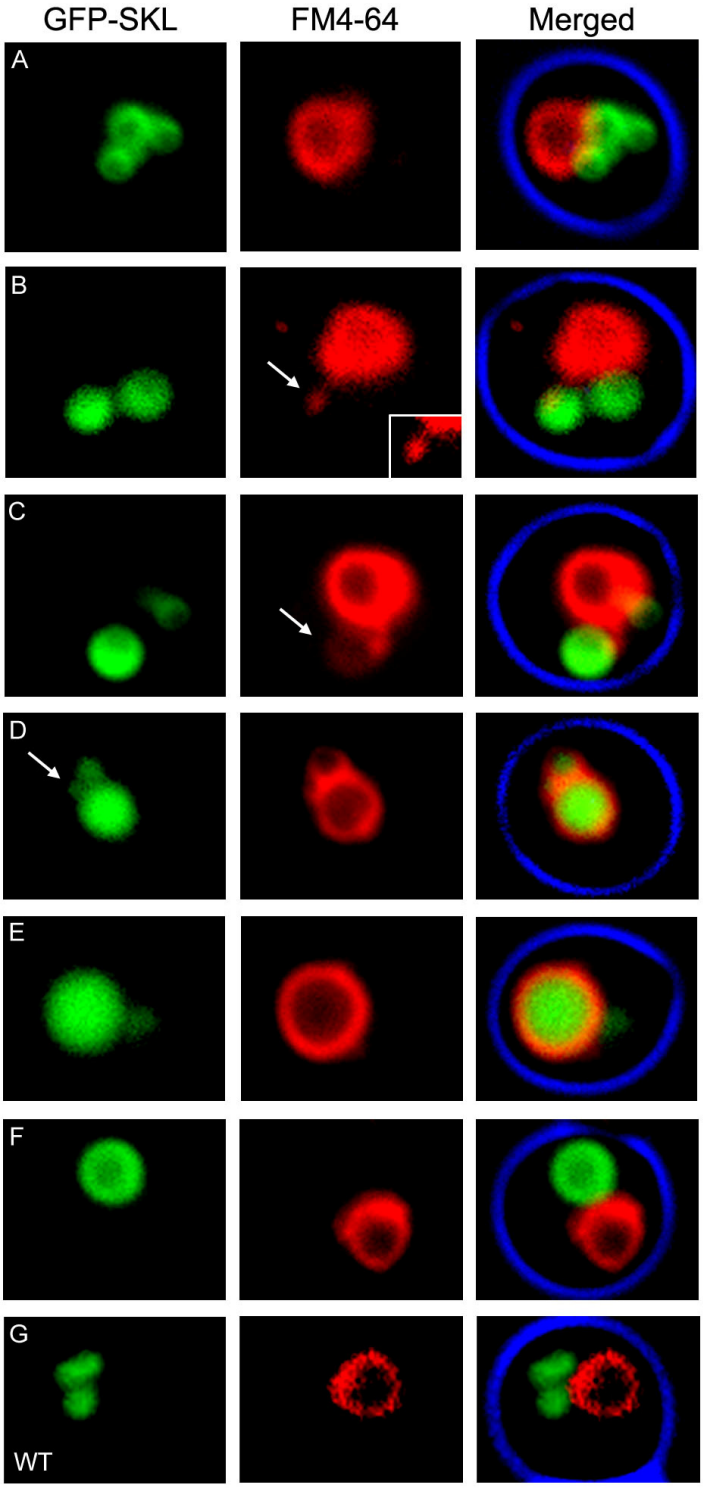

Figure 3. Fluorescence microscopy of Pex3-degradation induced peroxisome degradation

Fluorescence microscopy of Degron-Pex3^{ts} cells expressing P$_{AMO}$-driven *GFP-SKL*, shifted from 25 ºC to 37 ºC and grown as described at Fig. 1B. (A) Prior to the shift rounded vacuoles marked by FM4-64 and multiple peroxisomes are observed. (B) Approximately 30 minutes after the shift a vacuolar elongation was observed (arrow), superimposed on a peroxisome. Inset shows elongation with higher intensity (C, D). Subsequently a faint red fluorescent ring became visible surrounding a peroxisome (C, arrow). Note the small peroxisome which is not affected (D, arrow) and GFP in vacuoles (D, E, quantification shown in Fig. 1C). (F) Finally after 3-4 hours most cells contained a single enlarged peroxisome and a rounded vacuole, while WT cells still contained multiple peroxisomes (G).

To confirm that the observed morphology is distinct from both micro- and macropexophagy, sequential fluorescent images were taken at a 3-min interval of methanol-grown WT cells shifted to glucose, to induce macropexophagy. Similar to results obtained in *P. pastoris*, the rapid appearance of a transient FM4-64-stained ring around a peroxisome could be observed as a consequence of autophagosome-vacuole fusion (supplementary figure S1A).[38] In contrast to the FM4-64 related sequestration observed in Degron-Pex3^{ts} cells, the intensity of the ring surrounding the peroxisome was invariably equal to the vacuole.

Identical experiments, using cells exposed to nitrogen limitation conditions to induce microautophagy, revealed the characteristic intermediate stages of the process, namely surrounding of the organelles by the vacuole, either as extensions (S1B) or by the complete vacuole (S1C). These morphological events clearly differed from the elongation and subsequent ring formed in Degron-Pex3^{ts} cells.

As fluorescence microscopy may not resolve the details of the putative protrusion of the vacuole into peroxisomes, instead of surrounding the organelles, we carried out ultrastructural analysis of Degron-Pex3^{ts} cells upon inducing Pex3 degradation by a temperature shift.

These analyses confirmed the formation of the elongation of the vacuole towards peroxisomes upon the shift to restrictive temperatures (Fig. 4A, B). Invariably, electron dense membrane layers were observed of varying length, positioned in between the peroxisome and the vacuole extension at the site of vacuole-peroxisome tethering (Fig. 4B, C; inset). These membranes adhered but never were observed completely surrounding the organelle as in macropexophagy.[3] Instead, these membranes most likely fused with the peroxisomal membrane (Fig. 4D). This is deduced from the observation that the organelles appeared less electron dense concomitant with an increase in size in the next step of degradation (Fig. 4E, F). In the next stage the vacuole is observed invading one or even multiple organelles (Fig. 4F-H), followed by degradation of the organelle (Fig. 4I). Although direct fusion with the vacuole is never observed, we anticipate that this fusion process precedes the actual organelle degradation process. Often, small remnants of alcohol oxidase crystalloids, characteristic for peroxisomes in methanol-grown *H. polymorpha,* could be observed in these organelles confirming their peroxisomal nature (Fig. 4E). Remarkably, the membrane of the peroxisome with the membrane layers and the vacuole vesicle incorporated increased in width (from approximately 70 Å to 85 Å), which is in between the diameter of a peroxisome and vacuole membrane (110 Å). Typical examples of these membranes are shown in Fig. 4K-N. After three to four hours of cultivation at restrictive temperatures, bulk of the cells was observed containing a single enlarged peroxisome (Fig. 4J).

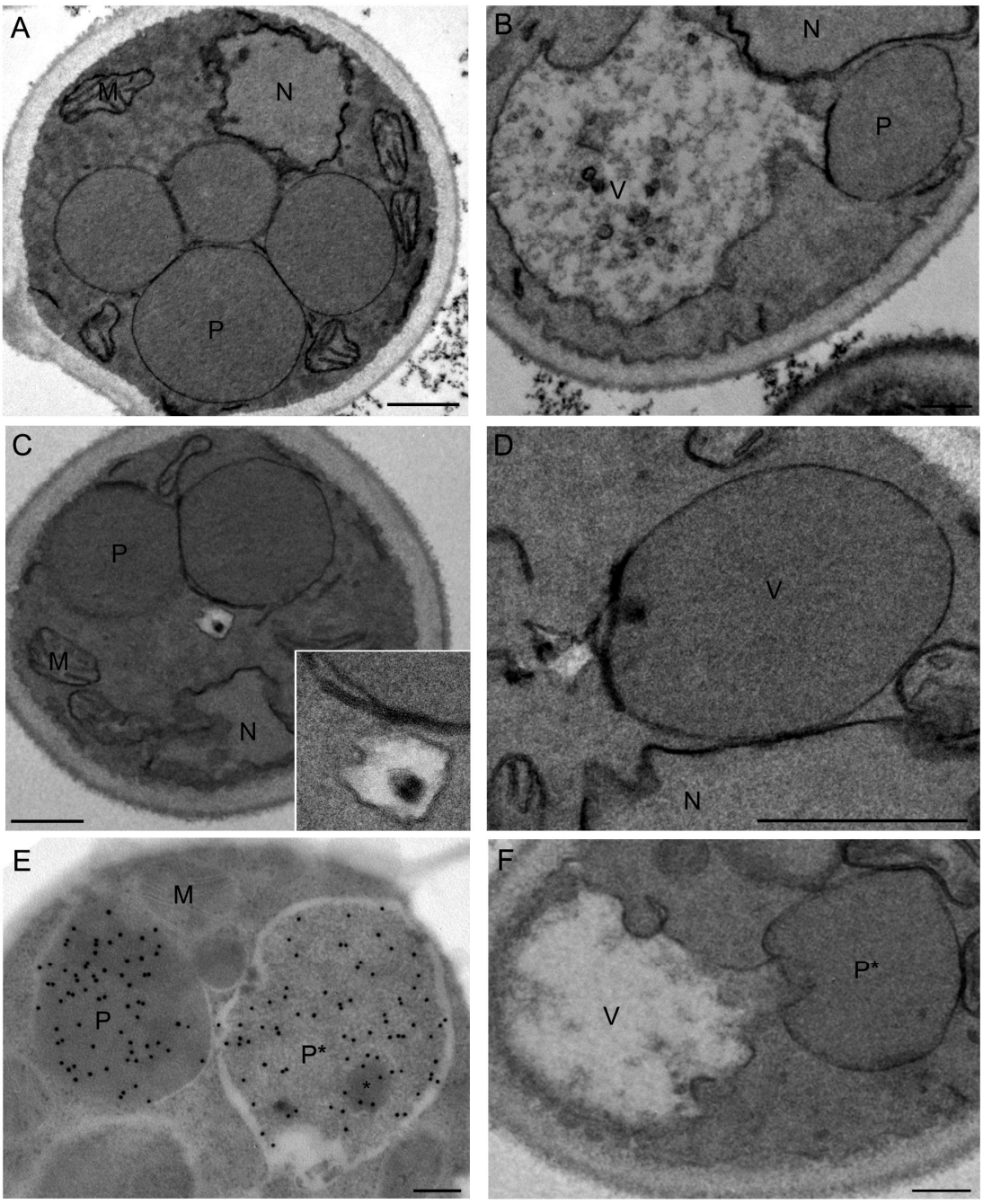

Figure 4. Electron microscopy of Pex3-degradation induced pexophagy

Ultrathin sections of $KMnO_4$-fixed Degron-Pex3^{ts} cells, grown on methanol at 25 ºC, showing the presence of multiple peroxisomes (A). (B) After the shift from 25 ºC to 37 ºC a vacuolar elongation or vesicle was observed in close proximity to a peroxisome. (C) Invariably electron dense membrane structures were observed in between the vacuole and peroxisome (enlarged in inset). (D) These membranes fused with the peroxisomal membrane, (E) resulting in a decreased electron density of the matrix. Note the remnant of the AO-crystalloid (asterisk). (F) Next, the vacuole extension invaded into one organelle, (G-N, next page).

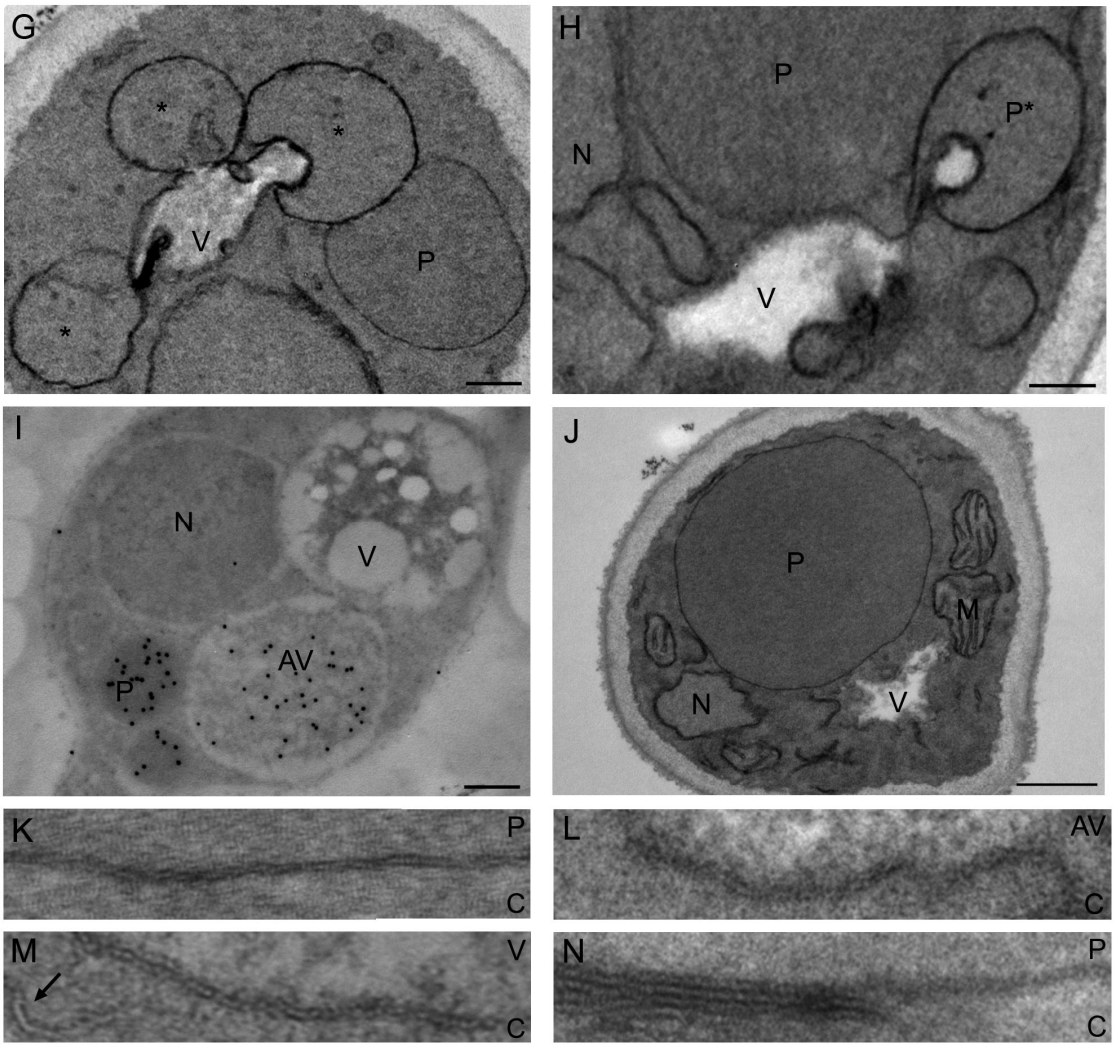

(G) or multiple peroxisomes were affected simultaneously (asterisk, note the decrease in electron density of these organelles). (H) A vacuole vesicle was next incorporated in the peroxisome, (I) leading to a further decrease in electron density, however the width of the membrane of these organelles was in between the width of the peroxisome and vacuole membrane. Finally bulk of the cells contained a single enlarged peroxisome ~3 hours after the shift (J). Measurements of the diameter of these membranes showed a width of 70 Å for a peroxisome (K), 85 Å for an autophagic vacuole (L), 110 Å for the vacuole, 130-140 Å for the cell membrane (M; arrow) and ~140 Å for the membrane patches depicted in 4C (N). Fig. 4E and 4I depict ultrathin sections of Unicryl-embedded Degron-Pex3^{ts} cells shifted to 37 ºC, labeled with α-AO antibodies. C – cytosol, AV – autophagic vacuole, M – mitochondrion, N – nucleus, P – peroxisome, V – vacuole. The bar represents 0.2 μm, except in A and J: 0.5 μm.

Characteristics of the vacuole-peroxisome fusion process

To further substantiate that the observed electron dense membranes structures at the site of vacuole-peroxisome tethering relate to the autophagic machinery, we analyzed the fate of Atg8, a component of autophagosomal membranes, in this process. To this end we introduced BFP-SKL to mark peroxisomes together with GFP-ATG8 in the Degron-Pex3^{ts} strain. When these cells were grown on methanol/methylamine at 25 ºC, bulk of the cells contained cytosolic GFP in conjunction with GFP fluorescence in the vacuole lumen (Fig. 5A).

This vacuolar GFP fluorescence is most likely related to general autophagy and the relative stability of GFP in the vacuole, which was indicated by the finding that vacuoles also displayed fluorescence when the cells were shifted to other carbon sources, i.e. ethanol instead of methanol at 25 ºC (data not shown).[39,40]

In addition, GFP-Atg8 is frequently seen as a spot, adjacent to the vacuole, that probably represents the phagophore assembly site (PAS; Fig. 5A).[41] The typical vacuole extension characteristic at the initial step of organelle turnover was associated with the presence of GFP-Atg8 fluorescence (Fig. 5B,C). In the next step a GFP-Atg8 fluorescent ring is observed surrounding the organelle, characterized by the presence of BFP-SKL, whereas the vacuole extension was still observed in close proximity of a peroxisome (Fig. 5D). Subsequently, the organelle is encompassed by a weak GFP-Atg8 fluorescent ring that also showed FM4-64 fluorescence (Fig. 5E).

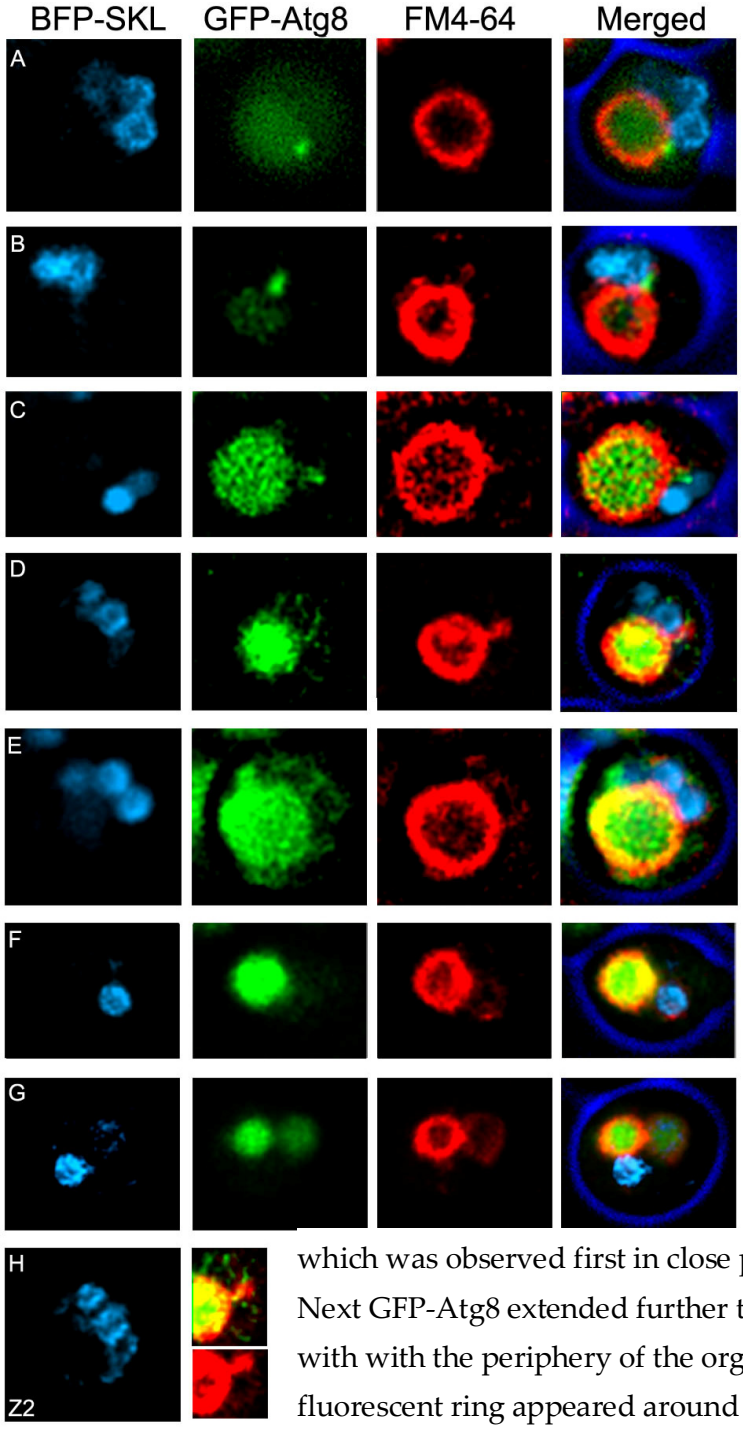

Figure 5. Atg8 is a component of the membrane layers essential for organelle fusion

Prior to the shift to restrictive temperature of methanol/methylamine-grown Degron-Pex3^{ts} cells expressing *BFP-SKL* & *GFP-ATG8*, GFP-Atg8 localized to the cytosol as well as to the vacuole. Cells characteristically contain a large, round vacuole (red, marked by FM4-64) and multiple peroxisomes (blue, labeled with BFP-SKL). (A) Shortly after the temperature shift also a peri-vacuolar spot appeared in many cells. (B)Upon formation of the vacuolar extension GFP/Atg8 was enriched at this structure, which was observed first in close proximity of a peroxisome. (C) Next GFP-Atg8 extended further then the vacuole and co-localized with with the periphery of the organelle. (D) Subsequently A GFP-fluorescent ring appeared around the peroxisomal matrix marker, followed by a GFP- & FM4-64- double-stained ring (E). Often multiple organelles were affected simultaneously; note the GFP-stained ring above the extension in D and the GPP- FM4-64- double-stained ring below the extension (details depicted with higher intensity in "H"), which is targeting a peroxisome positioned somewhat deeper in the cell (H: BFP-SKL of the next layer of the Z-stack 0.35 µm deeper). Also in E multiple peroxisomes are targeted. (F) The GFP-fluorescent ring was no longer observed shortly after formation of the autophagic vacuole, while also the peroxisome next appeared disintegrated (G). (Cultivation details,see next page).

Since sequestration of organelles during glucose-induced macropexophagy can be readily detected by electron microscopy,[3,11,42] whereas complete sequestration during extensive ultrastructural analysis in these cells was not observed, we interpret these data in that first the electron dense, Atg8-containing membranes fuse with the peroxisome to be degraded, resulting in distribution of Atg8 over the peroxisomal membrane, followed by fusion with a vacuolar vesicle, which contributes characteristics of the vacuole membrane to the surrounding membrane. After fusion with a vacuolar vesicle the organelle content is degraded (Fig. 5F,G).

Fusion of peroxisomes with the vacuole is Ypt7-dependent

To analyze the requirements of the possible multiple fusion events in the peroxisome degradation process, we analyzed the effect of deleting *YPT7* in the Degron-Pex3^{ts} strain producing BFP-SKL and GFP-ATG8. Ypt7 is known to mediate homotypic vacuole fusion and fusion of vacuoles with autophagosomes.[43,44]

Figure 5 (continued) Cells were cultivated until mid-exponential growth phase on methanol/ammonium sulphate, followed by a shift to methanol/methylamine (to induce *GFP-ATG8*) and a subsequent shift to 37 ºC to induce peroxisome degradation.

Cells grown on methanol/methylamine showed vacuole fragmentation, typical for *ypt7Δ* cells (Fig. 6A) and GFP-Atg8 fluorescence located in the cytosol. Upon a shift of such cells from permissive to restrictive temperatures, we failed to detect any GFP-Atg8 and/or FM4-64 fluorescent rings surrounding individual peroxisomes and peroxisome degradation was never observed (Fig. 6A). This was confirmed by electron microscopy analysis. These data showed that the electron dense membranes were normally formed but fusion with the peroxisome or vacuole was invariably not detected (Fig. 6B). These data led us to conclude that the membrane fusion event preceding organelle-vacuole fusion is dependent of Ypt7.

The alternative peroxisome degradation mechanism is physiologically relevant

We finally addressed whether the conditional mechanism of peroxisome degradation is of physiological significance and also occurs in *H. polymorpha* wild-type cells. To this end, we chose conditions that result in inactivation of the matrix enzyme alcohol oxidase, namely exposure of methanol-grown cells to excess methanol conditions.[45] At these conditions enhanced levels of formaldehyde and hydrogen peroxide are formed.[45]
Addition of 1% methanol to *H. polymorpha* wild type cells that were in the late-exponential growth phase on methanol resulted in a growth arrest of approximately 2 hours and a transient increase in reactive oxygen species (ROS; Fig. 7A).

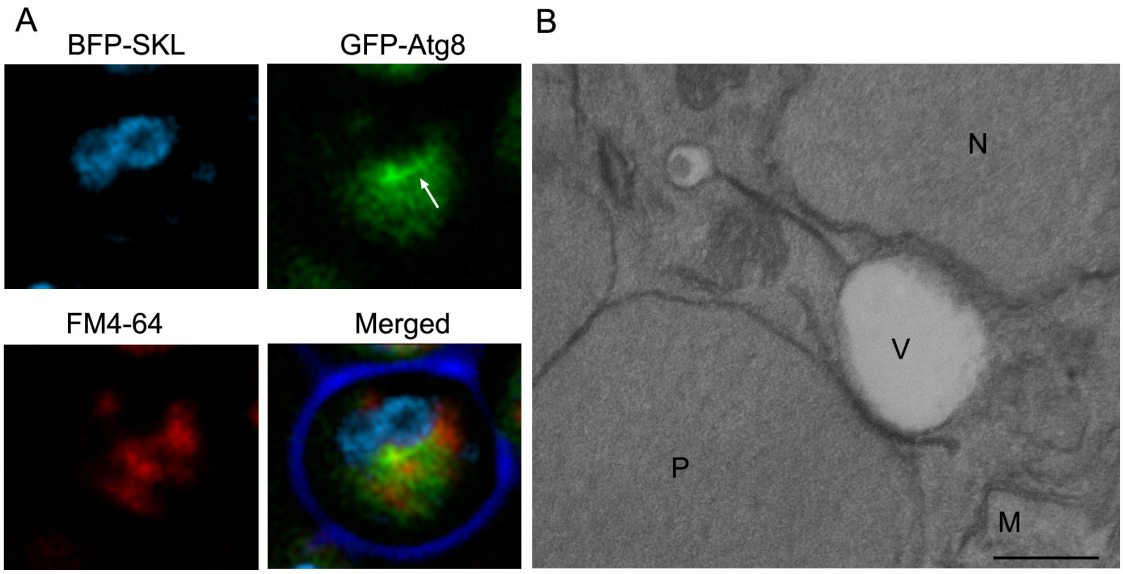

Figure 6. Ypt7 is required for organelle fusion

*Ypt7*ΔDegron-Pex3^{ts} cells expressing *BFP-SKL* and *GFP-ATG8*, often contained GFP-stretches in close proximity of peroxisomes after the shift to 37 ºC and fragmented vacuoles (A), however no GFP- or FM4-64-strained rings were observed. (B) Ultrastructural analysis showed highly fragmented vacuoles and many membrane patches in the cytosol, often close to peroxisomes, resembling the initial stages of Pex3-degradation induced pexophagy (as shown in 5D). No difference in appearance of these organelles could be observed before and after the temperature shift. M – mitochondrion, N – nucleus, P – peroxisome, Bar represents 0.2 μm.

During this phase we also observed degradation of peroxisomal marker proteins (Fig. 7B), which displayed the same structural characteristics as Pex3-degradation induced pexophagy (Fig. 7C, D). Similar observations were made during re-examination of cold shock induced peroxisome degradation (not shown).[46] From these experiments we conclude that the alternative mechanism of peroxisome degradation is a physiological important mechanism for rapidly adjusting peroxisome populations to prevailing environmental conditions.

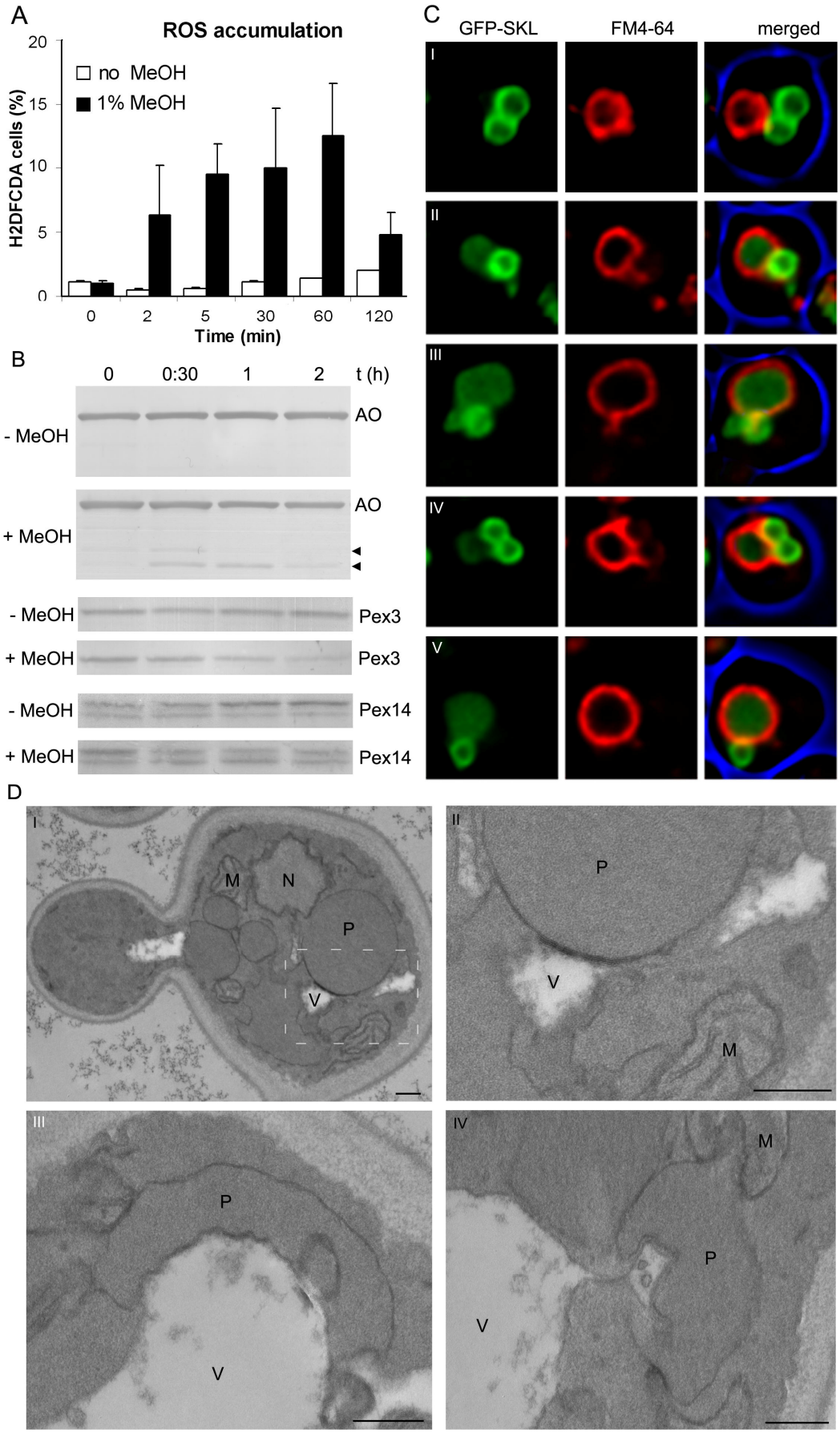
A
ROS accumulation
no MeOH
1% MeOH
H2DFCDA cells (%)
Time (min)
B
t (h)
- MeOH
+ MeOH
AO
Pex3
Pex14
C
GFP-SKL
FM4-64
merged
D
M
N
P
V

Figure 7. Peroxisomes degrade at methanol excess conditions

Shortly after addition of 1% of methanol to methanol-grown WT cells (OD 1.8), an increase in H_2DFCA-positive cells was observed, indicative for the accumulation of ROS (A). The increase remained approximately constant for 120 minutes after methanol addition and then decreased. 10.000 cells of 3 independent cultures were analyzed. The bar represents the standard deviation. (B) Western blot analysis of samples taken at various time-points after methanol addition revealed a decrease in alcohol oxidase (AO) levels (degradation products are indicated by arrowheads), indicative of peroxisome degradation. In controls not administrated with excess methanol AO levels were unchanged. Pex3 levels declined rapidly after addition of methanol, while remaining approximately unaffected in controls not supplemented with excess methanol. Pex14 levels showed a pattern reminiscent of glucose-induced macropexophagy; the phosphorylated form (upper band) declined after addition of methanol, while the non-phosphorylated form did not drastically change.[47] In the control the phosphorylated form increased, while the non-phosphorylated form did not change.(C) Prior to addition of methanol, rounded vacuoles and multiple peroxisomes were observed (I), whereas 15 minutes after addition of 1 % methanol, vacuolar extensions appeared in close proximity of peroxisomes (II). These elongations next invaded a peroxisome, after which a FM4-64 stained ring appeared around one or even multiple organelles (III, IV). One hour after methanol addition most cells contained a single peroxisome and GFP in the central vacuole (V). (D) Ultrastructural analysis of these cells also showed vacuole vesicles or elongations close to the peroxisomal membrane, with membrane patches in between both organelles (I; enlarged in II). Next peroxisomes were observed with decreased electron density, internal membrane vesicles (asterisk) and invading vacuoles (III), which were incorporated in the organelle (IV). M – mitochondrion, N – nucleus, P – peroxisome, V – vacuole. Bar represents 0.2 μm.

Discussion

In this study we present evidence that in *Hansenula polymorpha* turnover of Pex3 at peroxisome-inducing growth conditions is sufficient to induce rapid autophagic degradation of peroxisomes. This suggests that Pex3 is a key component in peroxisome maintenance and is consistent with the view that the trigger of organelle turnover is in the organelle membrane.[10,11,12,15,16,48]

The mechanism of this degradation process shares characteristics with both micro- and macroautophagy. As for microautophagy, but not macropexophagy, the process is dependent of protein synthesis.[36] As in microautophagy, different organelles can be subject to degradation at the same time. However, the morphological events also share characteristics with macropexophagy (see for a hypothetical model Fig. 8).

First, electron dense membranes are formed that resemble autophagosomes, which however have never been observed to completely enwrap a whole organelle as in macropexophagy. Our joint fluorescence and electron microscopy data suggest that these electron dense membranes contain Atg8. We speculate that fusion of these membranes with the peroxisomal membrane renders this membrane capable for a subsequent fusion step with the vacuole, similar to the autophagosome-vacuole fusion in macropexophagy.

In this view the electron dense membranes are a vehicle to allow the vacuole-peroxisome fusion that is required to expose the organelle lumen to vacuolar hydrolases thereby simultaneously protecting the surrounding membrane for degradation as it has acquired properties of the vacuole membrane as a result of the fusion. The observed increase in membrane width is consistent with this view. The finding that the process is Atg1- and Ypt7-dependent reinforces the assumption that Pex3-degradation mediated peroxisome degradation is an autophagic process and a very effective mode of organelle turnover. Additional experiments on WT *H. polymorpha* cells exposed to excess methanol or a cold shock, demonstrated that the alternative peroxisome degradation machinery is of physiological importance to rapidly adjust peroxisome numbers to specific environmental conditions.[46]

We showed before that during vegetative reproduction of WT *H. polymorpha* cells at peroxisome-inducing growth conditions, the organelles are subject to constitutive degradation.[13] Also this process is Atg1-dependent and suggested to facilitate a continuous rejuvenation of the peroxisome population present in the cells. However, we have until now never observed morphological data (e.g. autophagosome formation) supporting that this process proceeds via normal macropexophagy (van der Klei and Veenhuis, unpublished results). Therefore, the efficient organelle rejuvenation machinery also may involve turnover of redundant or exhausted organelles via this alternative process.

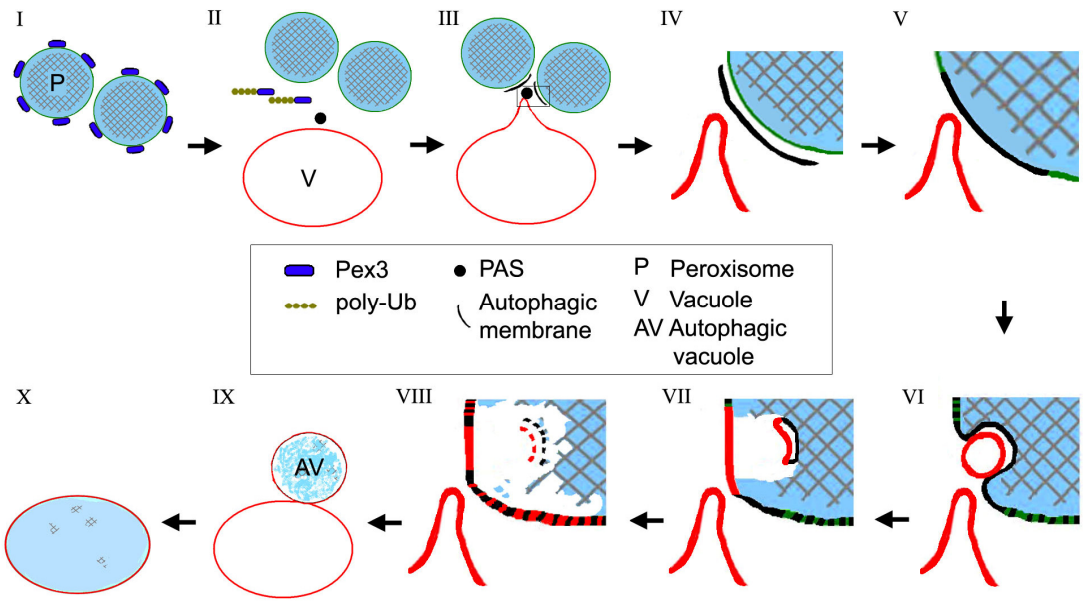

Figure 8. Hypothetical model of N-Degron-Pex3 induced pexophagy

Shortly after the shift of methanol-grown Degron-Pex3^{ts} cells to restrictive temperature (I), Pex3 is removed and degraded (II). The autophagic machinery concentrates at a peri-vacuolar location and generates a double-layered membrane, resembling autophagosome formation, while a vacuole extension is formed, which extends towards one or even multiple peroxisomes (III). The newly-formed membrane is positioned in between the extension and a peroxisome (IV), following its surface and subsequently fuses with it in an Ypt7-dependent manner; leading to swelling of the organelle, modification of the membrane and formation of internal vesicles (V). The modified membrane is now able to fuse with a vacuole vesicle, which is pinched off from the extension (VI), leading to a second modification of the membrane (VII), release of vacuolar hydrolases into the lumen of the organelle and degradation of the lumen (VIII). The uptake of membrane derived from the vacuole enables the autophagic vacuole to withstand the released hydrolases and makes the organelle capable of subsequent fusion with the central vacuole (IX). Ultimately reduced numbers of enlarged peroxisomes remain, most probably due to the low Pex3 levels in the cells (X).[23]

Earlier observations on macropexophagy in *H. polymorpha* showed that organelles sequestered by autophagosomes may incorporate vacuole vesicles at the initial stages of degradation, leading to degradation of the peroxisomal content prior to fusion of the outer autophagosomal membrane with the vacuole.[3] A shift of methanol-grown *Candida boidinii* cells to ethanol also induces selective degradation of peroxisomes, which initiated with a loss of peroxisomal integrity, prior to degradation in the vacuole, suggesting that also in these organelles the matrix content is degraded prior to vacuole uptake.[49] In higher eukaryotes autophagosomes fuse with endosomes leading to formation of an amphisome and also degradation prior to fusion with the lysosome.[50,51]

Recently it was shown that specific mitochondrial vesicles can fuse with peroxisomes and the ER can also form the template for the peroxisomal membrane, indicating that despite the differences between the membranes of these organelles, phospholipids can transfer from one to the other.[52,53] Extensive research on the origin of the autophagosomal membrane have implicated the endoplasmatic reticulum, trans-Golgi network and mitochondria as potential membrane sources.[54,55,56] Moreover, upon induction of the unfolded protein response, which was accompanied by ER-phagy, the ER was proposed to be both cargo as well as sequestering membrane at the same time.[57,58]

The alternative form of pexophagy we describe here may resemble this process by employing the membrane of the organelle itself for formation of an autophagosome-like structure, that is subsequently capable of fusing with the vacuole.
Taken together, we have identified an alternative mode of peroxisome degradation via autophagy that seems to be ideally suited to allow rapid intracellular remodeling and removal of redundant organelles during vegetative growth.

Acknowledgements

We thank Ron Booij, Arjen Krikken and Rinse de Boer for skillful assistance in microscopy and Sven Thoms & Ralf Erdmann for kindly providing us with the Degron-cassette. Tim van Zutphen is supported by the Netherlands Organisation for Scientific Research/Earth and Life Sciences (NWO/ALW). This project was carried out within the research programme of the Kluyver Centre for Genomics of Industrial Fermentation, which is part of the Netherlands Genomics Initiative / Netherlands Organization for Scientific Research.

References

1. Mizushima N, Levine B, Cuervo AM, Klionsky DJ Autophagy fights disease through cellular self-digestion. Nature 2008; 451:1069-1075.
2. Todde V, Veenhuis M, van der Klei IJ. Autophagy: Principles and significance in health and disease. Biochim Biophys Acta 2009; 1792:3-13.
3. Veenhuis M, Douma A, Harder W, Osumi M. Degradation and turnover of peroxisomes in the yeast *Hansenula polymorpha* induced by selective inactivation of peroxisomal enzymes. Arch Microbiol 1983; 134:193-203.
4. Sakai Y, Oku M, van der Klei IJ, Kiel JAKW. Pexophagy: Autophagic degradation of peroxisomes. Biochim Biophys Acta 2006; 763: 1767-1775.
5. Tuttle DL, Dunn WA Jr. Divergent modes of autophagy in the methylotrophic yeast *Pichia pastoris*. J Cell Sci 1995; 108: 25-35.
6. Sakai Y, Kooler A, Rangell LK, Keller GA, Subramani S. Peroxisome degradation by microautophagy in *Pichia pastoris*: identification of specific steps and morphological intermediates. J Cell Biol 1998; 141:625-636.
7. Veenhuis M, Zwart K, Harder W. Degradation of peroxisomes after transfer of methanol-grown *Hansenula polymorpha* into glucose-containing media. FEMS Microbiol Lett 1978a; 3:21-28.
8. Leao-Helder AN, Krikken AM, van der Klei IJ, Kiel JAKW, Veenhuis M. Transcriptional down-regulation of peroxisome numbers affects selective peroxisome degradation in *Hansenula polymorpha*. J Biol Chem 2003; 278:40749-40756.
9. Meijer WH, van der Kleij IJ, Veenhuis M, Kiel JAKW. *ATG* genes involved in non-selective autophagy are conserved from yeast to man, but the selective CVT and pexophagy pathways also require organism-specific genes. Autophagy 2007; 2:106-116.
10. Veenhuis M, Komori M, Salomons F, Hilbrands RE, Hut H, Baerends RJS, et al. Peroxisome remnants in peroxisome deficient mutants of the yeast *Hansenula polymorpha*. FEBS letters 1996; 383:114-118.
11. Bellu AR, Salomons FA, Kiel JAKW, Veenhuis M, van der Klei IJ. Removal of Pex3p is an important initial stage in selective peroxisome degradation in *Hansenula polymorpha*. J Biol Chem 2002; 277:42875-42880.
12. Farre JC, Manjithaya R, Mathewson RD, Subramani S. PpAtg30 tags peroxisomes for turnover by selective autophagy. Dev Cell 2008; 14:365-376.
13. Bener Aksam E, Koek A, Kiel JAKW, Jourdan S, Veenhuis M, van der Klei IJ. A peroxisomal Lon protease and peroxisome degradation by autophagy play key roles in vitality of *Hansenula polymorpha* cells. Autophagy 2007; 3:96-105.
14. Bener Aksam E, Jungwirth H, Kohlwein SD, Ring J, Madeo F, Veenhuis M, et al. Absence of the peroxiredoxin Pmp20 causes peroxisomal protein leakage and necrotic cell death. Free Radic Biol Med 2008; 45:1115-1124.
15. Kissova I, Salin B, Schaeffer J, Bhatia S, Manon S, Camougrand N. Selective and non-selective autophagic degradation of mitochondria in yeast. Autophagy 2007; 3:329-336.
16. Kanki T, Wang K, Cao Y, Baba M, Klionsky DJ. Atg32 is a mitochondrial protein that confers selectivity during mitophagy. Dev Cell 2009; 17:98-109.

17. Okamoto K, Kondo-Okamoto N, Ohsumi Y. Mitochondria-anchored receptor Atg32 mediates degradation of mitochondria via selective autiophagy. Dev Cell 2009; 17:87-97.
18. Bellu AR, Komori M, van der Klei IJ, Kiel JAKW, Veenhuis M. Peroxisome biogenesis and selective degradation converge at Pex14p. J Biol Chem 2001; 276:44570-44574.
19. Gleeson MAG, Sudbery PE. Genetic analysis in the methylotrophic yeast *Hansenula polymorpha*. Yeast 1988; 4:293-303.
20. Ozimek P, Lahtchev K, Kiel JAKW, Veenhuis M, van der Klei IJ. *Hansenula polymorpha* Swi1p and Snf2p are essential for methanol utilisation. FEMS Yeast Res 2004; 4:673-682.
21. Baerends RJS, Rasmussen SW, Hilbrands RE, van der Heide M, Faber KN, Reuvekamp PT, et al. The *Hansenula polymorpha PER9* gene encodes a peroxisomal membrane protein essential for peroxisome assembly and integrity. J Biol Chem 1996; 271:8887-8894.
22. Dohmen RJ, WU P, Varshavsky A. Heat-inducible degron: a method for constructing temperature-sensitive mutants. Science 1994; 263:1273-1276.
23. Baerends RJS, Salomons FA, Faber KN, Kiel JAKW, van der Klei IJ, Veenhuis M. Deviant Pex3p levels effect normal peroxisome formation in *Hansenula polymorpha*: high steady-state levels of the protein fully abolish matrix protein import. Yeast 1997; 13:1437-1448.
24. Haan GJ, Baerends RJS, Krikken AM, Otzen M, Veenhuis M, van der Klei IJ. Reassembly of peroxisomes in *Hansenula polymorpha* pex3 cells on reintroduction of Pex3p involves the nuclear envelope. FEMS Yeast Res 2006; 6:186-194.
25. Faber KN, Haima P, Harder W, Veenhuis M, AB G. Highly-efficient electrotransformation of the yeast *Hansenula polymorpha*. Curr Genet 1994; 25:305-310.
26. Komduur JA, Veenhuis M, Kiel JAKW. The *Hansenula polymorpha PDD7* gene is essential for macropexophagy and microautophagy. FEMS Yeast Res 2003; 3:27-34.
27. Goldstein AL, McCusker JH. Three new dominant drug resistance cassettes for gene disruption in *Saccharomyces cerevisiae*. Yeast 1999; 15:1541-1553.
28. Monastyrska I, van der Heide M, Krikken AM, Kiel JAKW, van der Klei IJ, Veenhuis M. Atg8 is essential for Macropexophagy in *Hansenula polymorpha*. Traffic 2005a; 6:66-74.
29. Nagotu S, Krikken AM, Otzen M, Kiel JAKW, Veenhuis M, van der Klei IJ. Peroxisome fission in *Hansenula polymorpha* requires Mdv1 and Fis1, two proteins also involved in mitochondrial fission. Traffic 2008; 9:1471-1484.
30. Van Zutphen T, van der Klei IJ, Kiel JAKW. Pexophagy in *Hansenula polymorpha*. Methods Enzymol 2008; 451:197-215.
31. Laemmli UK. Cleavage of structural proteins during the assembly of the head of bacteriophage T4. Nature 1970; 227:680-685.
32. Kyhse-Andersen J. Electroblotting of multiple gels: a simple apparatus without buffer tank for rapid transfer of proteins from polyacrylamide to nitrocellulose. Biochem Biophys Methods 1984; 10:203-209.

33. Baerends RJS, Faber KN, Kram AM, Kiel JAKW, van der Klei IJ, Veenhuis M. A stretch of positively charged amino acids at the N terminus of *Hansenula polymorpha* Pex3p is involved in incorporation of the protein into the peroxisomal membrane. J Biol Chem 2000; 275:9986-9995.
34. Zwart K, Veenhuis M, van Dijken JP, Harder W. Development of amine oxidase-containing peroxisomes in yeasts during growth on glucose in the presence of methylamine as the sole source of nitrogen.Arch Microbiol 1980; 126:117-126.
35. Waterham HR, Titorenko VI, Swaving GJ, Harder W, Veenhuis M. Peroxisomes in the methylotrophic yeast *Hansenula polymorpha* do not necessarily derive from pre-existing organelles. EMBO 1993; 12:4785-4794.
36. Monastyrska I, Kiel JAKW, Krikken AM, Komduur JA, Veenhuis M, van der Klei IJ. The *Hansenula polymorpha ATG25* gene enocodes a novel coiled-coil protein that is required for macropexophagy. Autophagy 2005b; 1:92-100.
37. Reinders A, Romano I, Wiemken A, de Virgilio C. The thermophilic yeast *Hansenula polymorpha* does not require trehalose synthesis for growth at high temperatures but does for normal acquisition of thermotolerance. J Bacteriol 1999; 181:4665-4668.
38. Ano Y, Hattori T, Oku M, Mukaiyama H, Baba M, Ohsumi Y, et al. A sorting nexin PpAtg24 regulates vacuolar membrane dynamics during pexophagy via binding to phosphatidylinositol-3-phosphate. Mol Biol Cell 2005; 16:446-57.
39. Shintani T, Klionsky DJ. Cargo proteins facilitate the formation of transport vesicles in the cytoplasm to vacuole targeting pathway. J Biol Chem 2004; 279:29889-29894.
40. Hara T, Nakamura K, Matsui M, Yamamoto A, Nakahara Y, Suzuki-Migishima R, et al. Supression of basal autophagy in neural cells causes neurodegenerative disease in mice. Nature 2006; 441:885-889.
41. Suzuki K, Kirisako T, Kamada Y, Mizushima N, Noda T, Ohsumi Y. The pre-autophagosomal structure organized by concerted functions of *APG* genes is essential for autophagosome formation. EMBO 2001; 20:5971-5981.
42. Dunn WA Jr, Cregg JM, Kiel JAKW, van der Klei IJ, Oku M, Sakai Y, et al. Pexophagy: the selective autophagy of peroxisomes. Autophagy 2005; 1:75-83.
43. Haas A, Scheglmann D, Lazar T, Gallwitz D, Wickner W. The GTPase Ypt7 of *Saccharomyces cerevisiae* is required on both partner vacuoles for the homotypic fusion step of vacuole inheritance. EMBO 1995; 14:5258-5270.
44. Kirisako T, Baba M, Ishihara N, Miyazawa K, Ohsumi M, Yoshimori T, et al. Formation process of autophagosome is traced with Apg8/Aut7p in yeast. J Cell Biol 1999; 147:435-446.
45. Veenhuis M, van Dijken JP, Pilon SAF, Harder W. Development of crystalline peroxisomes in methanol-grown cells of the yeast *Hansenula polymorpha* and its relation to environmental conditions. Arch Microbiol 1978b; 117:153-163.
46. Komduur JA, Bellu AR, Knoops K, van der Klei IJ, Veenhuis, M. Cold-inducible selective degradation of peroxisomes in *Hansenula polymorpha*. FEMS Yeast Res 2004; 5:281-285.

47. De Vries B, Todde V, Stevens P, Salomons F, van der Klei IJ, Veenhuis M. Pex14p is not required for N-starvation induced microautophagy and in catalytic amounts for macropexophagy in *Hansenula polymorpha*. Autophagy 2006; 2:183-188.
48. Kiel JAKW, Komduur JA, van der Klei IJ, Veenhuis M. Macropexophagy in *Hansenula polymorpha*: facts and views. FEBS Lett 2003; 549:1-6.
49. Hill DJ, Hann AC, Lloyd D. Degradative inactivation of the peroxisomal enzyme, alcohol oxidase, during adaptation of methanol-grown *Candida boidinii* to ethanol. Biochem J 1985; 232:743-50.
50. Dunn WA Jr. Studies on the mechanisms of autophagy: maturation of the autophagic vacuole. J Cell Biol 1990; 110:1935-1945.
51. Eskelinen E-L. Maturation of autophagic vacuoles in mammalian cells. Autophagy 2005; 1:1-10.
52. Hoepfner D, Schildknegt D, Braakman I, Philippsen P, Tabak HF. Contribution of the endoplasmic reticulum to peroxisome formation. Cell. 2005; 122:85-95.
53. Neuspiel M, Schauss AC, Braschi E, Zunino R, Rippstein P, Rachubinski RA, et al. Cargo-selected transport from the mitochondria to peroxisomes is mediated by vesicular carriers. Curr Biol 2008; 18:102-108.
54. Young AR, Chan EY, Hu XW, Köchl R, Crawshaw SG, High S, et al. Starvation and ULK1-dependent cycling of mammalian Atg9 between the TGN and endosomes. J Cell Sci 2006; 119:3888-3900.
55. Hayashi-Nishino M, Fujita N, Noda T, Yamaguchi A, Yoshimori T, Yamamoto A. A subdomain of the endoplasmic reticulum forms a cradle for autophagosome formation. Nat Cell Biol 2009; 11:1433-7.
56. Hailey DW, Rambold AS, Satpute-Krishnan P, Mitra K, Sougrat R, Kim PK, et al. Mitochondria supply membranes for autophagosome biogenesis during starvation. Cell. 2010; 141:656-67.
57. Bernales S, McDonald KL, Walter P. Autophagy counterbalances endoplasmic reticulum expansion during the unfolded protein response. PLoS Biol. 2006;4:e423.
58. Reggiori F, Tooze SA. The EmERgence of autophagosomes. Dev Cell 2009; 17:747-8.
59. Mukaiyama H, Oku M, Baba M, Samizo T, Hammond AT, Glick BS, et al. Paz2 and 13 other PAZ gene products regulate vacuolar engulfment of peroxisomes during micropexophagy. Genes Cells 2002; 7:75-90.

Supplemental figure S1

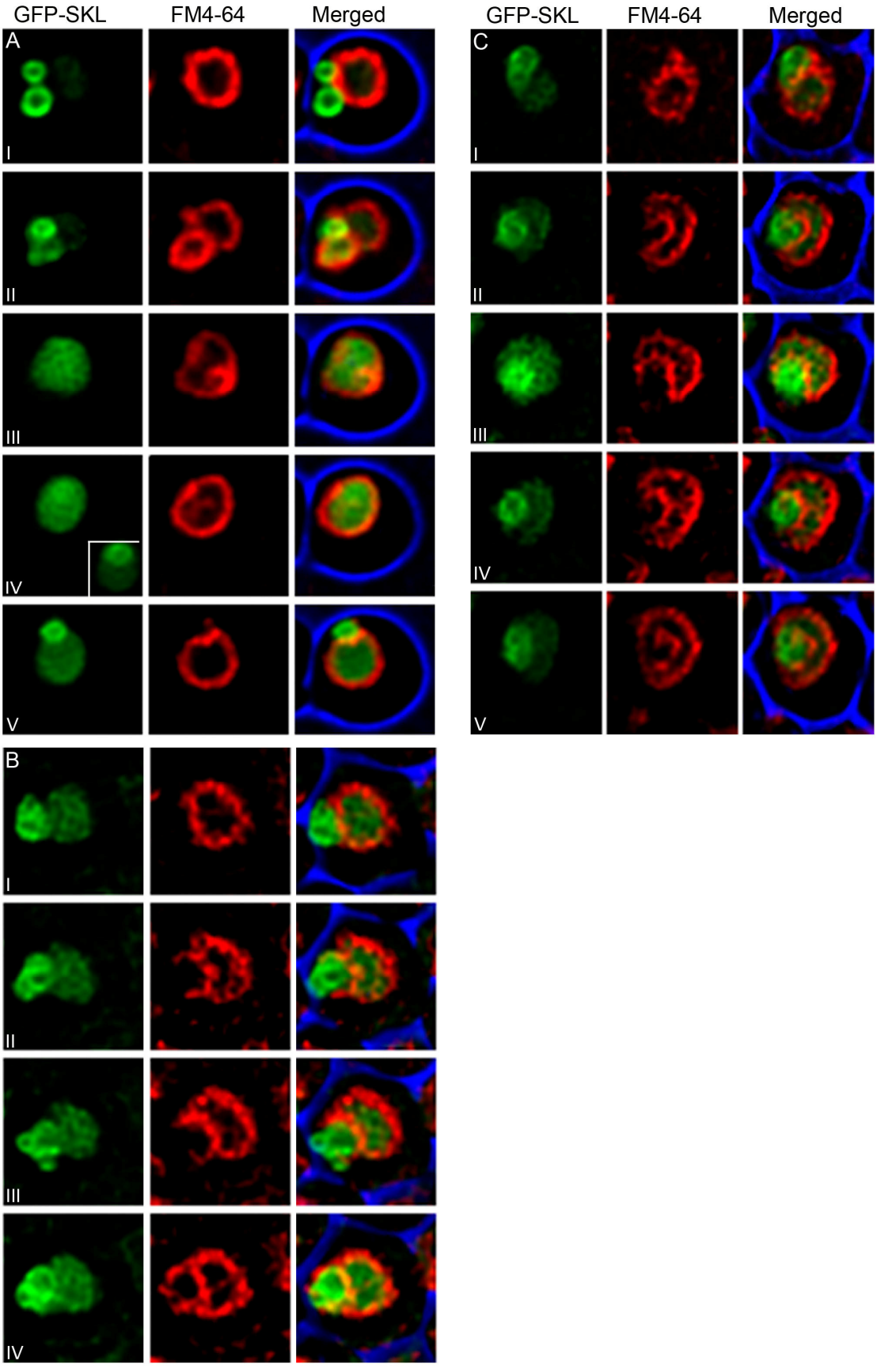

Figure S1 Sequential fluorescent images with 3 minute interval of methanol-grown wild type cells shift to fresh medium containing 0.5% glucose for 15 minutes (A). During macropexophagy, the outer layer of the autophagosome fuses with the central vacuole, stained with FM4-64 (II), leading to diffusion of FM4-64 and the transient appearance of a FM4-64-stained ring around a single peroxisome. Subsequently, the peroxisomal GFP-SKL is dispersed troughout the vacuole (III), in which also membrane is internalized (IV). The inset shows part of the cell 0.3μm lower, in which the single peroxisome can be observed, which is observed adjacent to the vacuole again 3 minutes later (V).
(B) Sequential images of methanol-grown cells at 5 minute interval shifted to fresh medium lacking nitrogen, showing either vacuolar arms (B), or the complete vacuole (C), slowly surrounding the peroxisome cluster, with much slower kinetics then glucose-induced degradation. Still, the N-starvation induced degradation observed on agar-slides generally proceeds faster than glucose-induced micropexophagy in *P. pastoris* on glass slides.[59] Also upon completion of microautophagy, internal membranes can be observed in the vacuole (C:V).

7. Summary

Eukaryotic cells contain membrane bound compartments, or organelles, that are dedicated to perform specific cellular processes. For instance, the nucleus harbours the genomic DNA, mitochondria generate energy and contain the enzymes of the citric acid cycle, whereas the vacuole is involved in several degradation processes as well as osmoregulation. A less well-known organelle is the peroxisome, first observed in 1954 by Rhodin and subsequently characterized by de Duve & Baudhuin in 1966, who named the organelle peroxisome, because of its capacity to generate as well as degrade hydrogen peroxide.
The peroxisome consists of a single membrane and a protein rich core and is involved in many metabolic processes, of which β-oxidation of fatty acids is the most widespread. Yet peroxisomes are involved in many more pathways like bile acid production in man, photorespiration in plants, bioluminescence in firefly and penicillin production in the filamentous fungus *Penicillium chrysogenum*.
In yeast species peroxisomes are involved in the metabolism of uncommon carbon sources like methanol, alkanes or fatty acids, or of organic nitrogen sources like primary amines, urate and D-amino acids. Many of these substrates are initially oxidized by hydrogen peroxide producing peroxisomal oxidases and induce proliferation of peroxisomes. Basic cell biology processes like peroxisome proliferation and their degradation by autophagy are extensively studied in yeast, because of the ease of genetic manipulation and cultivation of these single cell eukaryotes.

Moreover the genes involved in basic cellular processes are remarkably conserved throughout the eukaryotic kingdom. Therefore findings obtained in yeast can generally be translated to higher eukaryotes, including man.

Peroxisomes are not involved in the metabolism of glucose and this carbon source represses most genes coding for peroxisomal enzymes. Hence, when yeast cells are grown on glucose, peroxisome proliferation is repressed.

However, in the absence of glucose and the presence of a peroxisome-inducing substrate the appearance of the cell completely transforms.

For instance, glucose-grown cells of the methylotrophic yeast *Hansenula polymorpha* contain a single peroxisome that occupies just a few percent of the cell, yet a shift to media containing methanol as sole carbon source leads to an enormous increase in size and number of peroxisomes, occupying up to 80 percent of the cell volume. The opposite process may also occur; if peroxisomes become redundant for growth, e.g. upon addition of glucose to methanol-grown yeast cultures, all but one organelle are rapidly degraded by a selective autophagic process (also designated pexophagy). Autophagy literally means "self-eating" and this pathway is involved in degradation of virtually any component in the cell.

The shift from methanol to glucose in *H. polymorpha* induces enwrapping of a single peroxisome by multiple membrane layers, which after completion is termed an autophagosome, the hallmark of autophagy.

The outer layer of this structure fuses with the vacuole, leading to degradation of its content by vacuolar hydrolases. This type of autophagy is designated macroautophagy. The process of glucose induced selective degradation of peroxisomes in *H. polymorpha* is also called macropexophagy.
PEX genes code for proteins involved in peroxisome biogenesis and proliferation (peroxins). The peroxins can be subdivided in three major groups: proteins involved in the formation of the peroxisomal membrane, proteins involved in matrix protein import and proteins involved in regulating peroxisome abundance (e.g. organelle fission, formation from the ER).

Interestingly, some peroxins are multifunctional and also involved in pexophagy. One example is Pex3, a peroxisomal membrane protein that is involved in maintaining peroxisomal membrane integrity, regulating organelle proliferation, formation of peroxisomes from the endoplasmatic reticulum, peroxisome retention (in yeast) but also plays a role in pexophagy.
Another example is Pex14, a peroxin involved in translocation of proteins across the peroxisomal membrane into the matrix. In this process the receptors Pex5 and Pex7 recognize newly synthesized peroxisomal matrix proteins in the cytosol and sort their cargo to the importomer at the peroxisomal membrane.
The importomer is proposed to consist of the receptors, a membrane bound receptor docking complex and proteins involved in receptor recycling. Pex14 is a component of the receptor docking complex, but also important for selective autophagic turnover of peroxisomes.

In *H. polymorpha* peroxisomes can also be degraded by a second autophagic mechanism designated microautophagy, a process that is not selective for peroxisomes. This process involves uptake of cytoplasm – including organelles - by direct vacuolar engulfment and is induced in *H. polymorpha* by nitrogen starvation. This process does not involve the function of Pex14.
In addition to these highly inducible autophagic processes, organelles and cytosol are also constitutively degraded by autophagy at a low basal level by an unknown mechanism.

In **chapter 1** a general outline of the current knowledge on peroxisome homeostasis (proliferation and autophagic degradation) is described.

Chapter 2 describes a transcriptome study in which the adaptation of *H. polymorpha* upon a shift from glucose to methanol medium, i.e. from peroxisome repressing to peroxisome inducing conditions, is analysed. This analysis showed that ±1200 genes out of ±6000 were significantly up- or downregulated. Many of the downregulated genes are involved in general transcription and translation processes, which can be explained by the reduction in growth rate observed upon the shift. As expected genes involved in methanol metabolism were upregulated, whereas glycolytic enzymes were downregulated.The methanol-specific transcription factor Mpp1 was the highest upregulated gene (394-fold). Yet also genes involved in peroxisomal β-oxidation were upregulated. This may be due to the activation of mutual transcription factors, in line with a 24-fold upregulation of the central peroxisomal regulator Adr1.

However, the shift may also result in an increase in β-oxidation substrates, because upregulation of autophagy genes was observed as well as morphological evidence for an increase in vacuolar degradation. As turnover of organelles results in degradation of their membranes in vacuoles, this may be responsible for generation of fatty acids that induce peroxisomal β-oxidation enzymes. Most *PEX* genes were also upregulated, yet only to a limited extend (up to 5-fold).

In **chapter 3** a role for *H. polymorpha* Mig1 and Mig2 in glucose repression and pexophagy was analysed. In *Saccharomyces cerevisiae* Mig1 binds to the promoter of many target genes and suppresses their expression in conjunction with a second central repressor Tup1-Ssn6. *H. polymorpha* Tup1 was shown not to be essential for glucose repression of genes coding for peroxisomal enzymes. However in Δ*mig1* and *Δmig1Δmig2* cells repression of the gene coding for alcohol oxidase (AO), the first enzyme of the methanol utilization pathway, was impaired. In *Δtup1* cells sequestration of peroxisomes was observed upon induction of macropexophagy, but subsequent degradation was blocked.
In the double as well as the single *MIG* deletion strains, glucose-induced macropexophagy was severely impaired, but not blocked like in *Δtup1* cells, as judged from a reduction in AO protein levels. Morphological analysis showed a block in macropexophagy, but microautophagy was induced.

From these results *H. polymorpha* Mig1 and Mig2 were concluded to repress the induction of peroxisomal genes mainly in the presence of an inducer like methanol. Both proteins may also be involved in activation of macropexophagy and repression of microautophagy.

In **chapter 4** different approaches used to study pexophagy in *H. polymorpha* are summarized with emphasis on biochemical methods and structural analysis.

Chapter 5 describes the analysis of glucose-induced macropexophagy in *H. polymorpha* strains lacking one of the *PEX* genes coding for proteins of the peroxisomal importomer. Since these strains are unable to grow on methanol, cells were pre-cultivated on glycerol/methanol media, which induces peroxisomal genes and results in the formation of peroxisomal remnants that lack a matrix protein content, since protein import is blocked. The data show that in all mutants, except for *pex14Δ* these membrane remnants are degraded by macropexophagy upon a shift to glucose medium, as deduced from a decrease in Pex10 protein levels. This was confirmed by fluorescence microscopy using a fluorescent reporter protein consisting of the Pex3 targeting signal and green fluorescent protein (GFP; N_{50}Pex3-GFP). Both Pex10 and N_{50}Pex3-GFP protein levels decreased in time after induction of pexophagy and GFP fluorescence was observed in the vacuole. These data indicate that Pex14 is the sole member of the importomer involved in macropexophagy.

Deletion of the genes coding for the two direct binding partners of Pex14, Pex13 and Pex17, had a positive and a negative effect on the kinetics of macropexophagy respectively.

The significance of Pex3 removal from the organelle upon induction of macropexophagy is addressed in studies described in **chapter 6**. For this purpose a temperature-sensitive form of Pex3 containing an N-terminal "degron" was synthesized in cells lacking the native *PEX3* gene. As anticipated, a shift of these cells to the non-permissive temperature (37 ºC), resulted in a rapid decrease in Pex3 levels. This induced selective degradation of peroxisomes that required the key autophagy regulator Atg1. Unlike macropexophagy protein synthesis was required for this autophagic process. Surprisingly, morphologically the process differed from both micro- and macropexophagy; similar to microautophagy a vacuolar elongation was observed, yet instead of surrounding the organelles, the elongation protruded into one or several organelles and delivered a vacuole vesicle into peroxisomes, leading to degradation of the content.
Additional patches of membrane were always observed at the site where the organelles adhered. The marker for autophagosomal membrane, Atg8, also localized to this site, suggesting that these membranes were indeed autophagic membranes. These membranes may accomodate fusion between the vacuole and the peroxisome by first fusing with peroxisomal membrane. This membrane would thereby obtain autophagosomal characteristics and become capable of fusing with the vacuole.

To confirm this model, the gene coding for a regulator of vacuole-autophagosome fusion, *YPT7*, was deleted. This resulted indeed in a block in peroxisome degradation.
Since an artificial system was used to degrade Pex3, we analysed the significance of this alternative autophagic process in wild type cells and observed a similar mode of pexophagy when methanol-grown cells were exposed to excess of methanol, conditions that may cause oxidative damage.

Perspectives

The studies presented in this thesis clearly show intimate relations between the opposite processes of peroxisome homeostasis; proliferation and turnover, that goes well beyond the fact that any target of autophagy first needs be formed prior to its degradation. Previous studies indicated that peroxisomes have a limited life span and are constitutively degraded at normal growth conditions. How older organelles are distinguished from newly formed ones is still an enigma. Possibly phosphorylation and dephosphorylation processes are involved. Likely targets are Pex3, Pex14 and perhaps Atg30, a peroxisomal membrane protein important for pexophagy.
Although the core machinery of autophagy is highly conserved, also several differences between yeast species and higher eukaryotes exist. For instance how the interplay of Atg11 and Atg8 in connecting an organelle to the autophagic machinery seems to be solely executed by Atg8 in higher eukaryotes is an important issue to be solved.

One explanation might be the difference between the relatively stable conditions in mammalian tissues compared to the fluctuating availability of nutrients for yeast species, which thus need to be able to quickly adapt to environmental changes. As a consequence a more specialized system for rapid organelle turnover may have evolved.
Also, the molecular mechanisms of constitutive organelle turnover during vegetative growth is a very challenging topic for future research.

Finally, the mechanism that protects a single nascent organelle upon glucose-induced macropexophagy in yeast is still enigmatic. The link with an active importomer present in nascent organelles and inactive ones in mature organelles has been suggested. However upon induction of macropexophagy, most genes coding for peroxisomal enzymes will be repressed and import might decline rapidly. A possible role for the fission machinery during degradation might also exist, to generate a nascent organelle devoid of the enzymes involved in methanol metabolism, while the alcohol oxidase-containing peroxisomes are rapidly degraded.

8. Samenvatting

Eukaryote cellen bevatten compartimenten genaamd organellen, die door een membraan worden omsloten en specifieke processen uitvoeren. De kern bevat bijvoorbeeld het genomisch DNA, mitochondriën genereren energie en herbergen de enzymen van de citroenzuurcyclus, terwijl de vacuole betrokken is bij afbraakprocessen en osmoregulatie. Een wat minder bekend organel is de peroxisoom, voor het eerst opgemerkt door Rodin in 1954 en vervolgens door de Duve & Baudhuin in 1966 gekarakteriseerd en als peroxisoom benoemd, vanwege zijn capaciteit om zowel waterstofperoxide te genereren als af te breken.

Een peroxisoom bestaat uit een enkel membraan en een eiwitrijke kern en is betrokken bij een groot aantal metabole processen, waarvan β-oxidatie van vetzuren de meest wijdverbreide is. Daarnaast is dit organel betrokken bij een scala aan andere processen zoals galproductie in de mens, fotosynthese in planten, lichtvorming in vuurvliegjes en penicillineproductie in de schimmel *Penicillium chrysogenum*.

In gist zijn peroxisomen betrokken bij het metabolisme van zowel ongebruikelijke koolstofbronnen zoals methanol, alkanen of vetzuren en stikstofbronnen zoals amines, uraat en D-aminozuren. In veel gevallen komt er waterstofperoxide vrij bij de door peroxisomale oxidases uitgevoerde oxidatie-stap van bovenstaande substraten. Daarnaast stimuleren veel van deze substraten proliferatie van peroxisomen.

Er wordt uitgebreid onderzoek gedaan naar fundamentele celbiologische processen zoals peroxisoom-proliferatie en autofagie in gisten. Dit vanwege het gemak van zowel genetische manipulatie als het kweken van deze ééncellige eukaryoten. Bovendien zijn de cellulaire architectuur en de genen betrokken bij deze processen zeer geconserveerd in het gehele eukaryote domein. Bevindingen in gist kunnen daarom over het algemeen eenvoudig vertaald worden naar hogere eukaryoten, inclusief de mens.

Peroxisomen spelen geen rol in gluocse-metabolisme. Glucose als koolstofbron onderdrukt dan ook de meeste genen die voor peroxisomale enzymen coderen en daarmee ook peroxisoom-proliferatie. Het uiterlijk van een cel veranderd echter compleet in een omgeving zonder glucose maar met een peroxisoom-inducerend substraat. Cellen van de methylotrofe gist *Hansenula polymorpha* bijvoorbeeld, bevatten slechts één enkele peroxisoom wanneer ze op glucose gegroeid worden, peroxisomen nemen dan ook slechts een klein percentage van het celvolume in. Wanneer echter methanol i.p.v glucose als enige koolstofbron tijdens het kweken wordt aangeboden leidt dit tot een enorme groei van zowel de grootte als het aantal peroxisomen, tot wel 80 procent van het totale volume van de cel.

Het tegenovergestelde kan echter ook gebeuren, op het moment dat peroxisomen niet meer vereist zijn voor celgroei, wanneer bijvoorbeeld glucose wordt toegevoegd aan een op methanol gekweekte gistcultuur.

Hierdoor worden op één na alle organellen snel afgebroken door selectieve autofagie van peroxisomen (pexofagie). Letterlijk betekend autofagie "zelf-eten" en dit proces is in staat vrijwel alle componenten in de cel af te breken. De omslag van methanol naar glucose als koolstofbron in *H. polymorpha* induceert het omsluiten van een individiueel peroxisoom door meerdere membraan-lagen (sequestratie). Na voltooiing van sequestratie wordt de nieuwe structuur een autofagosoom genoemd, vaak omschreven als de meest kenmerkende eigenschap van autofagie. De buitenste membraanlaag fuseert vervolgens met de vacuole, waardoor de inhoud van de autofagosoom blootgesteld wordt aan vacuolaire hydrolases, hetgeen resulteert in afbraak van de inhoud. Dit type autofagie wordt ook wel macroautofagie genoemd.

PEX genen zijn zeer geconserveerd in het eukaryote domein en coderen voor eiwitten betrokken bij peroxisoom-biogenese en proliferatie (peroxines). De peroxines kunnen onderverdeeld worden in 3 groepen: eiwitten betrokken bij vorming van het membraan, eiwitten betrokken bij de import van matrix-eiwitten en eiwitten betrokken bij de regulatie van het aantal peroxisomen (bijvoorbeeld deling, of vorming vanaf het endoplasmatisch reticulum).

Opvallend aan sommige peroxines is hun multifunctionaliteit. Pex3 bijvoorbeeld, een peroxisomaal membraaneiwit, is betrokken bij het in stand houden van het peroxisomaal membraan, het reguleren van het aantal peroxisomen per cel, peroxisoom-vorming vanaf het endoplasmatisch reticulum, peroxisoom-retentie (in gist) en pexofagie.

Nog een voorbeeld is Pex14, een peroxine betrokken bij de transport van eiwitten over het membraan naar de peroxisomale matrix. De receptoren Pex5 en Pex7 herkennen deze in het cytosol gesynthetiseerde eiwitten en transporteren hun lading vervolgens naar de importomeer in het peroxisomaal membraan.
De importomeer bestaat uit de receptoren, een zogenoemd membraangebonden ”docking-complex” en eiwitten betrokken by de recycling van de receptoren. Pex14 is onderdeel van het docking-complex, maar is daarnaast ook betrokken bij de selectieve afbraak van peroxisomen door autofagie.

In *H. polymorpha* kunnen peroxisomen ook worden afgebroken door een tweede proces, aangeduid als microautofagie, dit proces is echter niet specifiek voor peroxisomen. Tijdens dit proces wordt het cytoplasma, inclusief organellen, door directe vacuolaire inkapseling opgenomen. Microautofagie wordt in *H. polymorpha* geïnduceerd door de afwezigheid van stikstof. Pex14 is niet betrokken bij dit proces.
Naast deze induceerbare afbraakprocessen, worden zowel organellen als cytosol ook continu afgebroken op een laag tempo door autofagie, echter het verantwoordelijke mechanisme is vooralsnog onbekend.

In **hoofdstuk 1** wordt een algemene omschrijving gegeven van peroxisoom-homeostase; van zowel proliferatie als afbraak.

Hoofdstuk 2 beschrijft een studie van het transcriptoom van *H. polymorpha* gegroeid op glucose vergeleken met cellen die zijn aangepast aan methanol; dus van een conditie waarbij peroxisoom-vorming geremd is naar peroxisoom-geïnduceerde condities. Deze analyse van ±6000 genen resulteerde in zowel ±1200 geïnduceerde als ±1200 geremde genen. Deze laatste groep bevatte veel genen betrokken bij algemene transcriptie en translatie. Dit kan verklaard worden door de lagere groeisnelheid na de omslag naar methanol. Zoals verwacht waren genen betrokken bij methanol metabolisme geïnduceerd, terwijl glycolytische genen werden onderdrukt. Het gen coderend voor de methanol-specifieke transcriptiefactor Mpp1 was het hoogst geïnduceerd (394x). Genen betrokken bij β-oxidatie van vetzuren waren echter ook geïnduceerd, mogelijk door activatie van gemeenschappelijke transcriptiefactoren. Dit was inderdaad het geval voor de centrale peroxisomale transcriptiefactor Adr1 (24x).

De omslag zou echter ook voor meer substraat kunnen zorgen voor de β-oxidatie, omdat ook de genen van de autofagie geïnduceerd waren en er tevens inductie van vacuolaire afbraak werd waargenomen. Afbraak van organellen leidt ook tot afbraak van membranen in de vacuole, wat vervolgens via recycling een bron van vetzuren kan opleveren, die β-oxidatie enzymen induceren. Het merendeel van de *PEX*-genen was ook geïnduceerd, evenwel tot een betrekkelijk niveau (tot 5x).

In **hoofdstuk 3** werd de rol van Mig1 en Mig2 in de onderdrukking van transcriptie door glucose van een grote groep genen in *H. polymorpha* geanalyseerd. In *Saccharomyces cerevisiae* bindt Mig1 in samenwerking met een tweede centrale repressor Tup1-Ssn6 aan de promotor van genen om de expressie te onderdrukken. Tup1 bleek in *H. polymorpha* niet essentieel te zijn voor glucose onderdrukking van genen coderend voor peroxisomale enzymen.
In Δ*mig1* en *Δ mig1Δmig2* cellen daarentegen, was de onderdrukking van het gen coderend voor alcohol oxidase (AO) het eerste enzym in het methanol metabolisme, wel verstoord.

Daarnaast werd de sequestratie van een peroxisoom wel waargenomen *Δtup1* cellen tijdens macropexofagie, maar de uiteindelijke afbraak was geblokkeerd, terwijl in zowel de dubbele als de enkele *MIG* deletiestammen macropexofagie alleen geremd was na de omschakeling naar glucose, op basis van een reductie van het AO eiwitniveau. Structurele analyse liet vervolgens zien dat macropexofagie geblokkeerd was in *Δmig1Δmig2* cellen, maar microautofagie juist geïnduceerd. Op basis van deze resultaten werd geconcludeerd dat Mig1 en Mig2 in *H. polymorpha* peroxisomale genen met name onderdrukt als er ook methanol aanwezig is en mogelijk ook macropexofagie activeert, terwijl microautofagie juist wordt onderdrukt.

In **hoofdstuk 4** worden de methoden beschreven die gebruikt worden voor onderzoek aan pexofagie in *H. polymorpha*, met name de biochemische en structurele analyse.

Hoofdstuk 5 betreft de analyse van glucose-geïnduceerde macropexofagie in stammen waarin één van de *PEX* genen coderend voor eiwitten van de importomeer ontbreekt. Omdat deze stammen geen eiwitten kunnen importeren, ontbreekt de peroxisomale matrix en bevatten deze cellen alleen peroxisomale membranen en kunnen dan ook niet groeien op methanol. Daarom werden deze cellen gekweekt op glycerol/methanol, wat leidt tot inductie van peroxisomale genen en vorming van peroxisomale membranen.
Vervolgens werden deze cellen omgeschakeld naar glucose. Uit de resultaten blijkt dat op *pex14Δ* na de peroxisomale membranen afgebroken worden via macropexofagie in alle mutanten, gebaseerd op de reductie van Pex10 eiwitniveau na de omschakeling. Dit werd bevestigd door fluorescentie-microscopie met behulp van een fluorescente label voor het peroxisomen bestaande uit het deel van Pex3 dat het "adres" bevat voor het peroxisoom en het groen fluorescerend eiwit (GFP; N_{50}Pex3-GFP). Zowel het Pex10 als N_{50}Pex3-GFP eiwitniveau verminderde na de inductie van pexofagie en de GFP fluorescentie werd waargenomen in de vacuole. Deze data geeft aan dat van de importomeer Pex14 de enige is met een rol in macropexofagie. Deletie van *PEX13*, het gen coderend voor de directe bindingspartners van Pex14, had een verhoogd effect op de kinetiek van afbraak. In tegenstelling tot Pex13, leidde afwezigheid van Pex17, de andere bindingspartner van Pex14, juist tot vertraagde afbraak.

Het belang van Pex3-verwijdering van de peroxisoom tijdens de initiële fase van macropexofagie wordt beschreven in **hoofdstuk 6**. Een temperatuur-afhankelijke vorm van Pex3 met een N-terminale "degron" werd hiervoor geïntroduceerd in cellen waarin de oorspronkelijke *PEX3* gedeleteerd was. Naar verwachting bracht een omschakeling van deze cellen naar de restrictieve temperatuur (37 ºC) een snelle afbraak van het eiwit teweeg. Pex3 afbraak leidde vervolgens tot selectieve afbraak van peroxisomen.

Deze afbraak was afhankelijk van de essentiële regulator van autofagie, Atg1, maar in tegenstelling tot macropexofagie ook van eiwitsynthese.

Onverwachts bleek het verloop van het proces af te wijken van zowel micro- als macropexofagie. Analoog aan microautofagie werd er een elongatie van de vacuole waargenomen, deze omringde echter niet het organel, maar bleek één of meer peroxisomen binnen te dringen, waardoor er een deel van de vacuole in de peroxisoom terechtkwam en de matrix werd afgebroken. Extra membranen werden altijd waargenomen op de plaats waar beide organellen in eerste instantie contact maakten. Atg8, een indicator voor het autofagosomaal membraan werd ook op deze lokatie waargenomen. Dit suggereert dat deze membranen autofage membranen zijn. Deze membranen zouden de fusie tussen de peroxisoom en de vacuole mogelijk maken door eerst zelf met de peroxisoom te fuseren. Het peroxisomaal membraan zou daardoor autofagosomale eigenschappen krijgen en daarmee vervolgens in staat zijn om met de vacuole te fuseren.

Om dit model te bevestigen werd het gen coderend voor de regulator van vacuole fusie, *YPT7* gedeleteerd. Dit resulteerde inderdaad in blokkering van de afbraak. In dit onderzoek werd echter een kunstmatige methode gebruikt om Pex3 af te breken, daarom werd geanalyseerd of deze alternative vorm van afbraak ook een rol speelt in wild-type cellen.
De alternatieve Pex3-degradatie geïnduceerde pexofagie werd vervolgens ook waargenomen wanneer wild-type cellen gekweekt op methanol een overdosering methanol kregen, mogelijk als gevolg van oxidatieve schade.

Perspectieven

Het gepresenteerde onderzoek in dit proefschrift geeft de duidelijke verhouding tussen de tegenovergestelde aspecten van peroxisoom-homeostase weer; proliferatie en afbraak. Deze relatie gaat veel verder dan dat voorafgaand aan afbraak door autofagie simpelweg eerst vorming plaats heeft moeten vinden.
Onderzoek heeft aangetoond dat peroxisomen een eindige levensduur hebben en continu worden afgebroken tijdens normale groeicondities. Hoe echter de oude organellen van de nieuwe worden onderscheiden, blijft vooralsnog onopgehelderd. Fosforylatie en defosforylatie zijn hier mogelijk bij betrokken, waarbij Pex3, Pex14 en wellicht ook Atg30 een peroxisomaal membraan eiwit betrokken bij pexofagie mogelijke kandidaten zijn.
Hoewel de fundamentele autofagie-machinerie zeer geconserveeerd is, bestaan er tussen gist en hogere eukaryoten toch ook verschillen.

Hoe bijvoorbeeld het samenspel tussen Atg11 en Atg8 de verbinding tussen een organel en de afbraak-machinerie in gist reguleert, terwijl in hogere eukaryoten alleen Atg8 hierbij betrokken lijkt te zijn, is een belangrijke vraag.
Mogelijk zou dit verschil ontstaan zijn doordat weefsels in hogere eukaryoten in een redelijk stabiele omgeving verkeren, terwijl gisten blootgesteld worden aan fluctuerende omstandigheden, met name wat betreft voedingsstoffen. Daardoor zal gist in staat moeten zijn om snel om te kunnen schakelen. Dit heeft mogelijk geleid tot de ontwikkeling van een speciaal mechanisme voor organel-afbraak.
Daarnaast is het moleculaire mechanisme achter de continu plaatsvindende afbraak van organellen tijdens normale groei een zeer uitdagend thema voor toekomstig onderzoek.
Tenslotte is het mechanisme betrokken bij de bescherming van een enkel organel tijdens macropexofagie in gist nog steeds grotendeels onbekend. De betrokkenheid van een actief importomeer in jonge peroxisomen, waar deze juist inactief is in volwassen organellen, is een reeds gepostuleerd mechanisme om dit verschil te bewerkstelligen. Gedurende macropexofagie worden peroxisomale genen echter geremd en zal import van eiwitten mogelijk geen grote rol meer spelen. Een connectie met de delings-machinerie tijdens degradatie zou ook kunnen bestaan. Een jong peroxisoom zou gegenereerd kunnen worden door deling, zonder de enzymen betrokken bij methanol metabolisme, terwijl de resterende organellen die alcohol oxidase bevatten snel afgebroken worden.